Max-Planck-Institut für Meteorologie
Max Planck Institute for Meteorology

The quasi-biennial oscillation: Representation in numerical models and effects on stratospheric transport and trace gases

Heinz Jürgen Punge


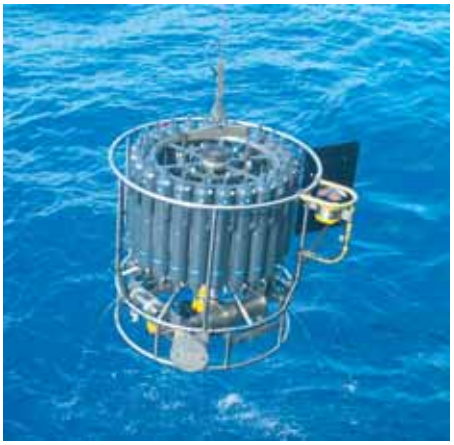


Berichte zur Erdsystemforschung 55/2008

Reports on Earth System Science

Hinweis

Die Berichte zur Erdsystemforschung werden vom Max-Planck-Institut für Meteorologie in Hamburg in unregelmäßiger Abfolge herausgegeben.

Sie enthalten wissenschaftliche und technische Beiträge, inklusive Dissertationen.

Die Beiträge geben nicht notwendigerweise die Auffassung des Instituts wieder.

Die "Berichte zur Erdsystemforschung" führen die vorherigen Reihen "Reports" und "Examensarbeiten" weiter.

Notice

The Reports on Earth System Science are published by the Max Planck Institute for Meteorology in Hamburg. They appear in irregular intervals.

They contain scientific and technical contributions, including Ph. D. theses.

The Reports do not necessarily reflect the opinion of the Institute.

The "Reports on Earth System Science" continue the former "Reports" and "Examensarbeiten" of the Max Planck Institute.

Anschrift / Address

Max-Planck-Institut für Meteorologie
Bundesstrasse 53
20146 Hamburg
Deutschland

Tel.: +49-(0)40-4 11 73-0
Fax: +49-(0)40-4 11 73-298
Web: www.mpimet.mpg.de

Layout:

Bettina Diallo, PR & Grafik

Titelfotos:
vorne:
Christian Klepp - Jochem Marotzke - Christian Klepp
hinten:
Clotilde Dubois - Christian Klepp - Katsumasa Tanaka

Berichte zur Erdsystemforschung 55/2008

The quasi-biennial oscillation: Representation in numerical models and effects on stratospheric transport and trace gases

Dissertation zur Erlangung des Doktorgrades der Naturwissenschaften
im Departement Geowissenschaften der Universität Hamburg
vorgelegt von

Heinz Jürgen Punge

aus Soest

Hamburg 2008

Reports on Earth System Science 55/2008

ISSN 1614-1199

Heinz Jürgen Punge
Max-Planck-Institut für Meteorologie
Bundesstrasse 53
20146 Hamburg
Germany

Als Dissertation angenommen
vom Department Geowissenschaften der Universität Hamburg

auf Grund der Gutachten von
Prof. Dr. Jochem Marotzke
und
Dr. Marco A. Giorgetta

Hamburg, den 9. Juli 2008
Prof. Dr. Jürgen Oßenbrügge
Leiter des Departments für Geowissenschaften

ISSN 1614-1199

The quasi-biennial oscillation: Representation in numerical models and effects on stratospheric transport and trace gases

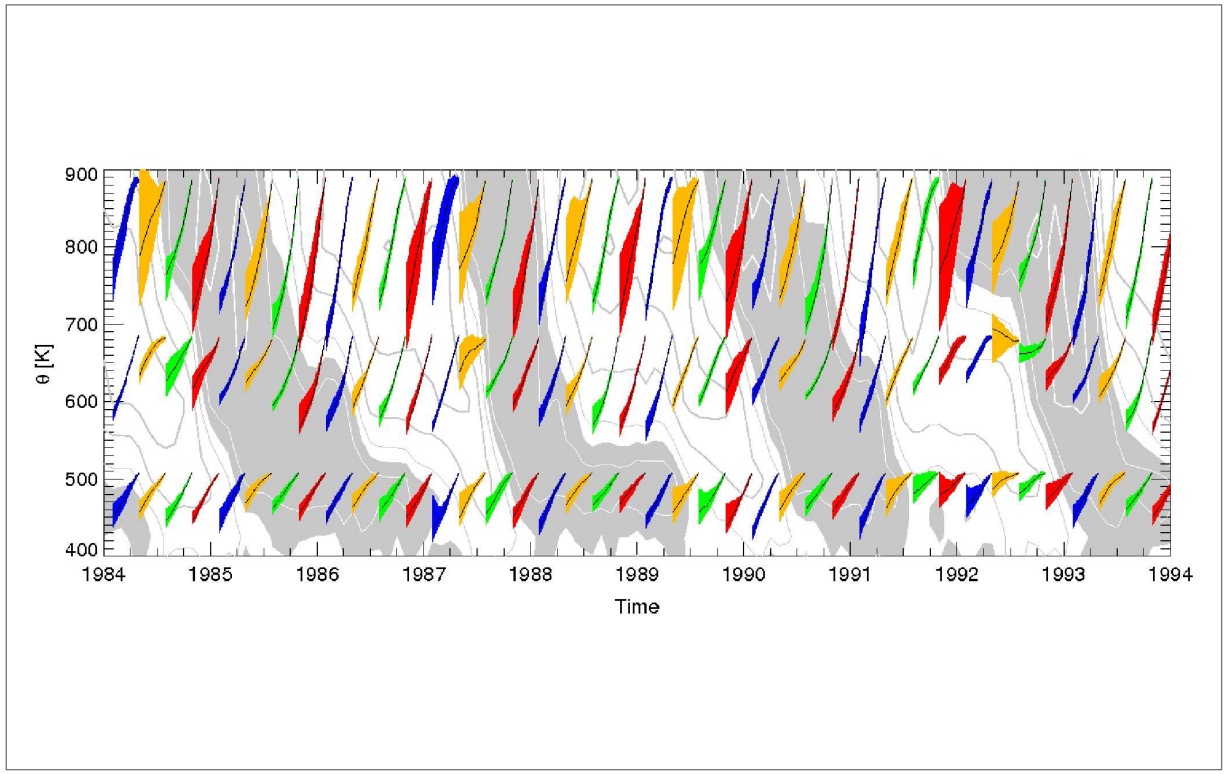

Heinz Jürgen Punge

Hamburg 2008

Cover picture source

Reprinted from Figure 4.4a in the text. It shows the variability of the ascent of air in the equatorial stratosphere caused by the QBO, which is seen in the background.

Dedication

To the memory of Hans-Jürgen Wiesmann, my longtime teacher at the
Conrad-von-Soest-Gymnasium, who led me towards a natural
scientist career by stimulating and challenging
my mathematics and physics skills.

Abstract

The quasi-biennial oscillation (QBO) of zonal wind is a prominent mode of variability in the tropical stratosphere. By a Coriolis effect on the winds it affects not only the meridional circulation and temperatures at low latitudes but also the transport and chemistry of trace gases such as ozone. Further effects on the stratospheric circulation and composition are due to the modulation of extratropcal waves propagating from the troposphere to the middle atmosphere by the QBO.

In reanalysis products, a representation of the QBO results from the assimilation of observed wind data. I show here that the wind fields in the upper stratosphere differ strongly between the first and the second half of the ERA-40 reanalysis, with a typical offset of –10 m/s in the equatorial zonal wind in the earlier part versus the later part. At the same time, the strength of the QBO remains nearly constant through the entire period. The 7-year running means of zonal wind, wind shear and temperature reveal strong anomalies, with major changes occurring in the beginning and the middle of the 1980s. Possible explanations are discussed, but no direct association to changes in the data sources or the use of data in the reanalysis is found.

In atmospheric general circulation models, the QBO can sometimes be generated internally but can also be included by assimilating zonal wind towards observations (nudging). The representation of the QBO in the nudged chemistry-climate model (CCM) MAECHAM4-CHEM, a general circulation model that extends into the middle atmosphere and has a chemistry and transport component, is discussed. The CCM can reproduce the observed QBO variations in temperature and ozone mole fractions. In particular, the CCM reproduces the phase of the observed ozone signal, which features a phase reversal in the vertical slightly below the maximum of the ozone mole fraction in the tropics due to the QBO variation in nitrogen oxides NO_x. However, the CCM underestimates the strength of the signal.

A comparison of two 20-year experiments with the MAECHAM4-CHEM model that differ by including or not including the QBO by nudging reveals differences in the 20-year mean wind fields, especially in the subtropics during summer and fall in both hemispheres. These net differences in the wind field due to the QBO lead to net differences in the meridional circulation, by the same mechanism that causes the QBO's secondary meridional circulation (SMC), and thereby affecting mean temperatures and the mean transport of tracers. In the tropics, the net effect on ozone is mostly due to net differences in upwelling and, higher up, the associated temperature change. A net surplus of up to 15% in NO_x in the tropics above 10 hPa in the experiment that includes the QBO does not lead to significantly different volume mixing ratios of ozone. Differences in the strength of the Brewer-Dobson circulation and in further trace gas concentrations are analyzed. These results underline the importance of a representation of the QBO in CCMs for realistic modelling of stratospheric conditions and constitution.

I investigate the effects of the QBO on transport in detail with the help of trajectory

calculations based on the output of the same CCM model. The evolution of groups of backward parcel trajectories over three months shows a distinct impact of the SMC and how the instantaneous circulation anomalies add up to constitute the effect on transport on a seasonal time scale. At the Equator, the time integrated effect of the QBO-induced variation of ascent rates consists in a variation of the vertical displacement of air parcels that is delayed in time with respect to that of the ascent rates. During the solstitial seasons, a large number of parcels stems from the summer hemisphere, but the effect of the QBO is still clearly seen. The calculations also show the greater variability in the regions of origin of parcels ensembles in the CCM run in which the QBO is nudged compared to the model version that does not include the QBO. A transport barrier at the edge of the tropical ascent region during summer in the easterly phase of the QBO is diagnosed from PV gradients and also studied by means of a trajectory analysis. At about 15 degrees latitude, the barrier develops due to the inability of planetary waves to penetrate into the tropics in the easterly phase, but only in summer when the horizontal circulation anomalies due to the annual and QBO cycles roughly cancel. Enhanced residence times of the parcel trajectories at their initial latitude confirm the existence of a barrier, as does the enhanced horizontal gradient of CCM simulated methane mixing ratios in the region of the barrier during the easterly compared to the westerly phase of the QBO.

Zusammenfassung

Die quasi-zweijährige Oszillation (quasi-biennial oscillation, QBO) des zonalen Windes ist eine bedeutende Art von Variabilität in der tropischen Stratosphäre. Durch den Corioliseffekt auf die Winde beeinflußt sie die Meridionalzirkulation und die Temperaturen in niederen Breiten, aber auch den Transport und die Chemie von Spurengasen wie etwa Ozon. Weitere Effekte der QBO auf die stratosphärische Zirkulation und Zusammensetzung werden durch die Modulation von extratropischer Wellen, die sich aus der Troposphäre in die mittlere Atmosphäre ausbreiten, verursacht.

In Reanalysen wird die Repräsentation der QBO durch die Assimilation beobachteter Winddaten erreicht. Es wird gezeigt, dass die Windfelder in der oberen Stratosphäre in der ersten und der zweiten Hälfte der ERA-40 Reanalyse sich deutlich unterscheiden, wobei die zonalen Winde am Äquator im früheren Teil un bis zu –10 m/s gegenüber dem späteren versetzt sind. Dabei bleibt die Stärke der QBO während des gesamten Zeitraums praktisch konstant. Die siebenjärigen laufenden Mittelwerte von zonalem Wind, vertikaler Scherung des zonalen Winds und Temperatur zeigen auffällige Strukturen und deutliche Änderungen um Anfang und Mitte der 1980er Jahre. Mögliche Erklärungen werden diskutiert, aber es wird keine direkte Verbindung zu Veränderungen in den Datenquellen oder deren Benutzung in der Reanalyse gefunden.

In Modellen der generellen Zirkulation (general circulation models, GCMs) der Atmosphäre kann teilweise eine QBO intern erzeugt werden, aber sie kann auch durch Einbindung von beobachteten zonalen Winden produziert werden (nudging, engl. für anstoßen). Die Darstellung der QBO im genudgten Chemie-Klimamodell (chemistry-climate model, CCM) MAECHAM4-CHEM, einem GCM, dass bis in die mittlere Atmosphäre reicht und auch Chemie und Transport von Spurengasen behandelt, wird untersucht. Das CCM kann beobachtete QBO-Variationen in der Temperatur und der Ozonkonzentration reproduzieren. Insbesondere das beobachtete QBO-Signal im Ozon, dessen Phase sich, bedingt durch die QBO-Variation in den Stickoxiden NO_x, in den Tropen knapp unterhalb des Ozonmaximums umkehrt, wird diskutiert. Das Signal ist schwächer als in Satellitenbeobachtungen, aber die Phase stimmt gut überein.

Ein Vergleich von 20 Jahre dauernden Simulationsexperimenten mit dem MAECHAM4-CHEM-Modell mit und ohne nudging der QBO zeigt Unterschiede auch im über den gesamten Zeitraum gemittelten zonalen Windfeld, besonders in den Subtropen in Sommer und Herbst auf beiden Hemisphären. Diese durch die QBO bedingten Nettounterschiede führen, durch den selben Mechanismus, der auch die meridionale Sekundärzirkulation (secondary meridional circulation, SMC) der QBO verursacht, auch zu Nettounterschieden in der Meridionalzirkulation, und verändern damit auch die gemittelten Temperaturen und den mittleren Transport von Spurenstoffen. In den Tropen ist der Nettoeffekt der QBO auf das Ozon haupsächlich durch einen Nettounterschied im Aufsteigen und, weiter oben, den damit ver-

bundenen Temperatureffekt bedingt. Interessanterweise führt eine um etwa 15% erhöhte NO_x-Konzentration in den Tropen oberhalb 10 hPa im Experiment mit QBO nicht zu deutlich unterschiedlichen Ozonkonzentrationen. Die Unterschiede in der Stärke der Brewer-Dobson-Zirkulation und weiteren Spurengaskonzentrationen werden untersucht. Diese Ergebnisse unterstreichen, wie wichtig die Repräsentation der QBO für eine realistische Simulation des Zustands und der Zusammensetzung der Stratosphäre in Chemie-Klima-Modellen ist.
Trajektorienrechnungen auf Basis der Ergebnisse der gleichen CCM-Simulationen wurden durchgeführt, um die Effekte der QBO auf den Transport genauer zu verstehen. Gruppen von Rückwärtstrajektorien werden bei Ihrer Ausbreitung über drei Monate deutlich von der SMC beeinflusst. Die instantanen Zirkulationsanomalien addieren sich dabei zu einem Effekt auf den Transport über saisonale Zeitskalen auf. So besteht der zeitlich integrierte Effekt der QBO-bedingten Variation der Aufstiegsraten am Äquator in einer Variation der vertikalen Bewegung von Luftpaketen, die gegenüber der der Aufstiegsraten zeitverzögert ist. Während der Sonnwendjahreszeiten stammt ein erheblicher Teil der Luftpakete aus der jeweiligen Sommerhemisphäre, doch der Effekt der QBO ist auch dann deutlich zu sehen. Die Berechnungen zeigen auch die größere Variabilität der Ursprungsregion der Luftpakete im genudgten Lauf gegenüber dem Lauf des Modells ohne QBO-Repräsentation. Eine Transportbarriere am Rand der tropischen Aufstiegsregion wird aus Gradienten der potentiellen Vortizität (PV) diagnostiziert und auch anhand von Trajektorienrechnungen untersucht. Die Barriere bildet sich bei einer Breite von etwa 15 Grad, weil während der QBO-Ostphase planetare Wellen nicht in die Tropen vordringen können. Dies geschieht jedoch nur im Sommer, wenn sich die horizontalen Zirkulationsanomalien durch die SMC der QBO und den Jahresgang etwa ausgleichen. Die Trajektorien von Luftpaketen verbleiben in dieser Situation lange im Breitenbereich ihrer Initialisierung, was ebenso das Vorhandensein einer Transportbarriere belegt. Ein stärkerer horizontaler Gradient der im CCM simulierten sommerlichen Methanverteilung in der Ostphase im Vergleich zur Westphase der QBO resultiert auch aus der Barriere während der Ostphase.

Contents

Chapter 1

Role of the quasi-biennial oscillation in the tropical stratosphere—an introduction

1.1 Historic perspective

In August 1883, during the eruption of Mt. Krakatoa in Indonesia, ashes from the volcano where ejected high into the atmosphere, to altitudes hardly accessible to contemporary in-situ observations. Aerosols stemming from the eruption remained in the stratosphere and moved westward, thereby indicating the presence of easterly winds in the tropical stratosphere. This finding was in contradiction to the observations of Lord Benson, who in 1908 found his balloons launched at Lake Victoria (1°S, 33°E) moving eastward in the lower stratosphere.

The apparent paradox was first explained by postulating permanent easterly and westerly jets in the upper and lower stratosphere, respectively, but later was resolved in 1961, when Reed et al. (1961) and Veryard and Ebdon (1961) analyzed the first continuous observations of zonal winds at equatorial latitudes by radiosondes launched at Canton Island, Nairobi and Christmas Island from the mid 1950s on, and were surprised to find synchronous variation on a close to biennial time scale, as shown in Figure 1.1. The phenomenon was termed quasi-biennial oscillation (QBO, see `http://ugamp.nerc.ac.uk/hot/ajh/qbo.htm` for an introduction to the QBO and Hastenrath (2007) for more detailed historical reflections) and has since been subject to extensive studies. Many of these, including the theory of the generation of the QBO by the damping of tropospheric waves (Lindzen and Holton, 1968; Holton and Lindzen, 1972), are summarized and referenced in the review of Baldwin et al. (2001).

Besides an evaluation of the long-term evolution of stratospheric winds and a study of the long-term mean effect of the QBO on the stratosphere, it comprises a detailed study of the QBOs effects on transport with foci on the vertical and latitudinal directions.

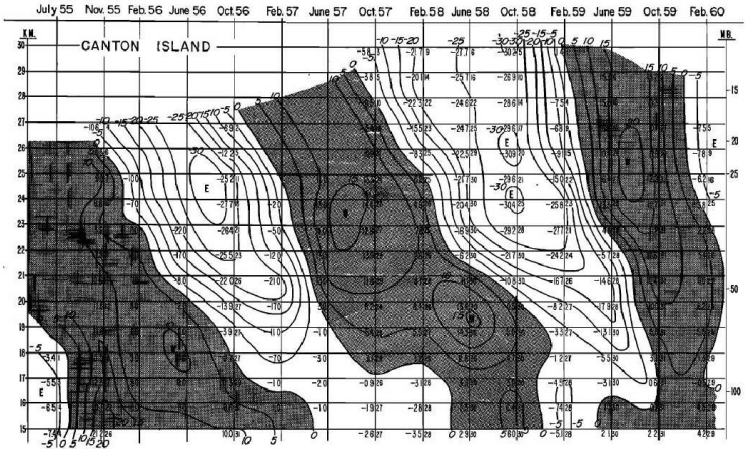

Figure 1.1— Zonal wind measurements by radiosondes at Canton Island, reprinted from Reed et al. (1961).

1.2 Motivation

The quasi-biennial oscillation of zonal wind in the equatorial stratosphere is a prominent mode of atmospheric variability, and both its dynamic generation and effects on the meridional circulation, transport and chemistry are topics of high scientific interest.

Understanding of the variability of the stratosphere on the interannual time scale is a prerequisite for identification of trends and prediction of the future evolution of stratospheric dynamics and constitution under varying forcings, of which anthropogenic chlorofluorocarbon (CFC) and carbon dioxide (CO_2) emissions are the most prominent examples. There is growing evidence for connections between stratospheric conditions and tropospheric weather systems, as, e.g., between the stratospheric polar vortex and the North Atlantic oscillation(NAO) (Ambaum and Hoskins, 2002) or the QBO and the monsoon circulation (Chattopadhyay and Bhatla, 2002; Giorgetta et al., 1999). Hence, any changes to the stratospheric circulation can be expected to feed back on the troposphere and vice versa. In the context of climate change, it has to be noted that most of the present projections (on Climate Change , IPCC) are based on climate model calculations that fail to represent the stratosphere accurately and will therefore miss any such feedbacks.

Nonetheless, numerical models of the general circulation, when modified to resolve the stratosphere and extended to include stratospheric chemistry, are most important tools to study stratospheric processes in detail. One of the improvements over traditional models is the representation of the QBO, which is the dominant mode of variability in the tropical stratosphere and affects many of these processes.

Except for deviations in its lower part (e.g., Huesmann and Hitchman, 2004), the circulation in the tropical stratosphere is largely zonally symmetric, and so are

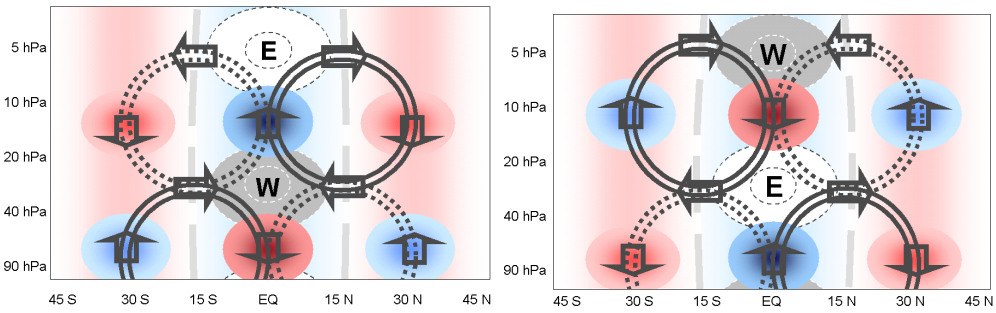

Figure 1.2— Schematic representation of the secondary meridional circulation of the QBO, in analogy to Plumb and Bell (1982). Gray and white fields denote the zonal wind jets, dashed and full arrows the circulation anomaly associated with the QBO corresponding to positive and negative anomalies of the stream function, and red and blue fields the resulting temperature anomalies. **(a)** Easterly shear phase at 10 hPa, **(b)** Westerly shear phase at 10 hPa. Red (blue) background shading shows the regions of mean subsidence (upwelling).

trace gas distributions. Hence there is little direct impact of the zonal transport of air by the QBO. However, due to the special geometry at the Equator, there is an effect of the interchanging easterly and westerly winds on the meridional circulation, termed secondary meridional circulation (SMC) (Plumb and Bell, 1982; Baldwin et al., 2001), which is illustrated in Figure 1.2. It is crucial for the generation of QBO anomalies in temperature and trace gas fields (e.g., Zawodny and McCormick, 1991; Randel et al., 1998; Schoeberl et al., 2008), and therefore plays an important role in all parts of this thesis. At low latitudes, on the equatorial β-plane (e.g., Lindzen, 1967), the Coriolis force on moving air is weak and insufficient to establish geostrophic balance. Nonetheless, the force is sufficient to drag air poleward at the flanks of the easterly QBO jet and equatorward at the flanks of the westerly QBO jet. The resulting convergence and divergence at the Equator are balanced by vertical flow anomalies in the regions between the westerly and easterly jets. The relative upwelling (downwelling) in the easterly (westerly) shear phases results in cold (warm) temperature anomalies and affects trace gas distributions, as will be discussed later in the text.

Three different approaches to achieve a representation of the QBO in models can be distinguished. A direct modelling of a QBO has been achieved recently in several GCMs (Takahashi, 1996; Scaife et al., 2000; Hamilton and Hsieh, 2002; Austin, 2002; Shibata and Deushi, 2005; Tian and Chipperfield, 2005; Giorgetta et al., 2006). It requires a realistic representation of the wave mean-flow interaction for (a) resolved waves, requiring a sufficient vertical resolution for horizontally resolved waves, and for (b) unresolved waves, as far as they are known to contribute to the QBO forcing, for which the interaction must be parameterized. A weakness of this approach is that the QBO modelled in this way, even if initialized in phase, will deviate from the observed QBO after several cycles, due to the variability of the QBO period, which is not understood in detail and can not be modelled. This complicates the comparison of results obtained by such a model to observed effects.

A solution to this problem is to provide observed QBO phase information to the model. This can be done in reanalysis projects which, as a weather forecast model, use observations to constrain the evolution of the atmosphere, but on suitably long time scales for studying the QBO. In this case, various observations are assimilated into a numerical weather prediction model. When sufficient observations of the stratosphere are included, in particular of zonal wind, a QBO will result, as in the ERA-40 and NCEP-2 reanalyses (Huesmann and Hitchman, 2004; Pascoe et al., 2005).

An alternative is to use only observations of zonal wind in the QBO core region to induce a QBO in a general circulation model. This nudging technique (Giorgetta et al., 1999) produces little interference with the models own dynamics, hence generates a realistic QBO in a mostly self-consistent framework. The technique can also be applied to GCMs that otherwise do not generate a QBO, as the MAECHAM4 used in this study. I use this opportunity to include or not include a QBO in the same model to assess the systematic biases in models without QBO representation, which have been neglected to date.

1.3 Scope of this thesis

The aim of this dissertation is to contribute to the understanding of the role of the QBO in the stratosphere.

This contribution is structured in three chapters, which have been published or are in preparation for publication in scientific journals separately. Consequently, the chapters can be studied independently of each other, but some overlap in the introduction and model description can not be avoided.

The following questions are treated in the next three chapters of this work, and an overview of the answers obtained and remaining questions is given in the final chapter:

- What is the quality of the representation of the tropical stratospheric circulation including the QBO in a current reanalysis? What are the potential weaknesses, and is there evidence for trends?

- How does the reanalysis compare to a GCM with internally generated QBO in this respect?

- Does nudging towards observed winds in the QBO region lead to a realistic QBO representation in general circulation models with extension into the stratosphere and inclusion of chemistry? Can such models help understanding observed QBO variations in trace gases?

- What are the systematic weaknesses in the circulation of models that have no QBO representation? How are trace gas concentrations affected by the net differences in the dynamics?

- How do the instantaneous QBO-induced variations of the mean meridional circulation translate to anomalies in the long-term transport of air and trace gas distributions? What is the role of seasonal variations of the Brewer-Dobson-circulation in the tropics and how do they relate to the QBO?
- How does the QBO affect transport at the tropical-subtropical edge? What is the role of the QBO effect on planetary wave propagation (Shuckburgh et al., 2001) relative to the horizontal branch of the secondary meridional circulation?

1.4 Thesis outline

Chapter 2 comprises the questions regarding the reanalyses. By including a maximum of past observations, reanalyses are extremely valuable for the analysis of past variability of the stratospheric circulation. For example, a good representation of the QBO has been noted in the ERA-40 reanalysis (Pascoe et al., 2005; Baldwin and Gray, 2005). Unfortunately, changes to the assimilation scheme are unavoidable, as most observations do not cover the entire time span of these reanalyses. Chapter 2 includes an analysis of the changes to upper stratospheric winds and temperatures identified in ERA-40 around 1986 and discusses potential causes. This part complements the analysis of Huesmann and Hitchman (2004), who performed a similar study on the NCEP/NCAR reanalysis. For a comparison to the variability in model simulations, the reader is referred to the diploma-equivalent thesis "Interdecadal variability of the QBO in the ERA-40 reanalysis and in the MAECHAM5 and HAMMONIA climate models" that is based on the same article as this chapter and was prepared by the author as a prerequisite for admission to doctoral studies at the University of Hamburg. This chapter has been published in *Atmospheric Chemistry and Physics*, **7**, 599-608, 2007, with M.A. Giorgetta as co-author.

Chapter 3 shows that the nudging technique for including a QBO in a model, when applied to the chemistry-climate model MAECHAM4-CHEM, produces realistic QBO variations in temperature and ozone concentrations. In particular, the QBO variations in ozone that has been studied in much detail in both observations and models (Tian et al., 2006; Butchart et al., 2003) are in qualitative agreement with observations, and the relevant mechanisms are identified from chemical reaction and transport rates. The climatological long term mean fields of selected quantities are considered in the model versions with and without QBO nudging, and differences are discussed. Specifically, the relation of "net" mean zonal wind differences and the differences in temperature and ozone mixing ratios is explained in the chapter using dynamic and chemical concepts. The net differences in the stream function and further trace gases are presented in Appendix A of the thesis. The magnitude of the net effects of including the QBO is put in relation to the strength of the QBO variations in these quantities. This chapter has been accepted for publication in *Atmospheric Chemistry and Physics Discussions* in 2008, with M. A. Giorgetta as co-author.

In chapter 4, the QBOs effects on transport are studied explicitly in a nudged

model using trajectory calculations. The general ascent of air in the tropical stratosphere is modulated by the secondary meridional circulation of the QBO (Plumb and Bell, 1982), which leads to variations in trace gas transport and causes many of the observed QBO variations in trace gases (e.g., Randel et al., 1998). Here it is discussed how air ascends differently in the different phases of the QBO, how it is affected by the changing QBO phase during its ascent over several months and therefore carries a memory of the past QBO evolution. The analysis of parcel trajectories illustrates this relation of the instantaneous circulation anomaly and transport on a monthly time scale. The analysis of potential vorticity (PV) and methane concentrations in the CCM shows that a transport barrier is present in the subtropics when the QBO is in the easterly phase, for which evidence was given by Shuckburgh et al. (2001), especially in summer. This is confirmed by the analysis of trajectories, and an explanation for the observed seasonal dependence is derived. This chapter is in preparation for submission to *Journal of Geophysical Research* with M. A. Giorgetta, P. Konopka and R. Müller as coauthors.

Chapter 5 chapter contains a general summary and conclusions. The main findings of the thesis are highlighted and an outlook on future challenges is given.

Chapter 2

Differences between the QBO in the first and in the second half of the ERA-40 reanalysis[1]

2.1 Introduction

Present-day reanalyses include observations over several decades in a rather consistent manner. Dynamic modes like El Nino-Southern oscillation (ENSO), North Atlantic Oscillation (NAO) or the quasi-biennial oscillation (QBO) are represented with remarkable accuracy. For the QBO of zonal wind, the present study confirms this statement for the lower stratosphere, showing a continuous signal over the course of the ERA-40 reanalysis (Uppala et al., 2005). In the upper stratosphere, however, the early and late portions of the data set differ significantly.

Unfortunately, the number of QBO cycles in the time series available from reanalysis is limited. More or less continuous observations of the QBO domain in the stratosphere exist only since the 1950s. For this reason, it is very difficult to make statistically sound statements. Also, this work does not include a detailed comparison to observational data records on the QBO, as it has already been presented in the literature (Baldwin and Gray, 2005; Uppala et al., 2004). Rather, the purpose of this work is to illustrate the change in the upper stratospheric conditions and the QBO using two 20 year sections of zonal wind data. It should be noted that there is another useful way to study the QBO and its variability by use of climate models that recently managed to simulate a realistic QBO, see Takahashi (1996) or Giorgetta et al. (2006) for instance.

The European Centre for Medium-Range Weather Forecasts (ECMWF) has used a recent version of its forecast model to prepare the long time reanalysis ERA-40. It is based on a wide range of observation data, accumulated from ground stations, aircraft measurements and satellites. However, the kind and number of observations

[1]Published in *Atmospheric Chemistry and Physics*, **7**, 599-608, 2007, with M.A. Giorgetta as co-author.

vary strongly during 1957 to 2002, the time range of the reanalysis (Uppala et al., 2004). A study on sensitivity of ERA-40 on the observing system was performed by Bengtsson et al. (2004). Their work shows that the representation of the QBO depends crucially on the assimilation of winds from radiosonde records and can not be achieved using satellite data alone. In the reanalysis system, the atmosphere is covered up to an altitude of 0.1 hPa with a good vertical resolution of 60 levels. Therefore one can expect a fair representation also of the stratosphere. However, care needs to be taken because observations are sparse at high altitudes. We want to look at variability on the interannual scale, so it is sufficient to use monthly means of the 6-hourly ERA-40 data set for our work.

A realistic representation of the QBO in ERA-40 has been reported in previous publications on this topic, e.g. in Baldwin and Gray (2005), Pascoe et al. (2005) and Randel et al. (2004a). The QBO time series of zonal wind in ERA-40 presented in the literature (Uppala et al., 2004, see Fig. 12 therein) and the remarks of Giorgetta et al. (2006) motivated a closer look at possible long term variations in the QBO amplitude. We choose a composite approach to study this question. The ERA-40 record is split to reveal a possible difference between its earlier and later years, and to still have a comparable number of cycles in each composite. Some details of the composite are highlighted and the magnitude of the difference in the QBO is compared to the one in the annual cycle.

In the second part, a more detailed picture of the underlying variability is aimed at. Possible explanations for the observed differences are sought after by studying wind and temperature fields on a time scale of 7 years in order to detect the timing of when the change occurred while the QBO signal itself is mostly eliminated. A brief discussion of implications of the findings concludes this work.

2.2 Methods

Composites are a common tool for analyzing periodic signals. Given a time series of data, one chooses a reference value and marks all points in time when the time series is rising above (or alternatively falling below) this selected reference value. The composite is then computed as the average of all partial time series centered around the identified points in time. This composite shows the typical time evolution in the selected time frame with respect to the time when the reference value occurs. Uncertainty in the evolution increases by construction from the point of reference to larger time lags before or after this point, and also with increasing spatial distance to this point.

This method is applied routinely (Giorgetta et al., 2006), for QBO signals, where usually the transition from easterlies to westerlies or vice versa is chosen as reference value. Difficulties can arise when the number of nodes varies among the levels, which is why this method is feasible only in regions where the QBO is the dominant mode of variability.

For our purposes it is adequate to neglect the latitude dependence of the QBO

amplitude, as it is approximately Gaussian around the equator where the QBO is driven (Holton and Lindzen, 1972; Baldwin et al., 2001). Thus, +/–5° latitudinal averages are used throughout this work, accounting for the core zone of the QBO. The QBO amplitudes mentioned here will therefore be slightly smaller than the amplitudes observed directly at the equator. Furthermore, for the composites, we subtract the climatological annual variability but retain the annual mean, so that the filtered data still contain the characteristic asymmetries between westerly and easterly jets.

Unfortunately the zonal wind time series are not strictly monotonic around the east-west/west-east transitions even in the QBO core region between 10 and 50 hPa where the signal is most prominent. Some cycles show delays or short reversals on the order of few months. This can lead to additional, artificial partial time series in the construction of composites which distort the result. One solution to this problem would be to compute the composites from smoothed, e.g. 5 month averaged time series. Instead, we decided to construct our composites only at one level at the upper end of the QBO core region, and to check the partial time series manually. The 10 hPa level was chosen because in this work the focus is on the upper stratosphere where observations are sparse and therefore discrepancies are likely to occur. The closer the construction level is to the region of interest, the more accurate are the composites. If there are several transitions of zero zonal wind close to each other due to a reversal as described above, we select only the first one of them for the composites as it appears to suit best for depicting the QBO evolution before and thereby above the transition, as the QBO generally propagates downward.

To estimate the evolution of the QBO amplitude we use the method presented by Baldwin and Gray (2005). In brief, they show that if a reference QBO area at the equator between 70 and 10 hPa is selected, one can compute the amplitude of the signal at any position in the atmosphere simply by taking the product of the best correlation to a level within the reference area and the variance at this position. This is valid if the QBO contribution at that position is perfectly correlated to the corresponding reference series. We apply this method to find QBO amplitudes at altitudes above 10 hPa. By defining 7-year time series within the full data set we can get the time evolution of the (7-year based) QBO amplitude. Seven year periods seem appropriate for analyzing a $\approx$ 28-month phenomenon - this way, shorter term variations are averaged over, but long term trends are retained. However, one should note that the method applied here may overestimate the actual QBO amplitude if the underlying assumptions do not apply completely, as stated by Pascoe et al. (2005).

2.3 Results

Composites of zonal wind in time and altitude, taken at the transition from easterlies to westerlies at 10 hPa, are shown in Fig. 2.1. Composites are displayed for the whole ERA-40 record (a) and partial records 1960 to 1979 (b) and 1980 to 1999 (c).

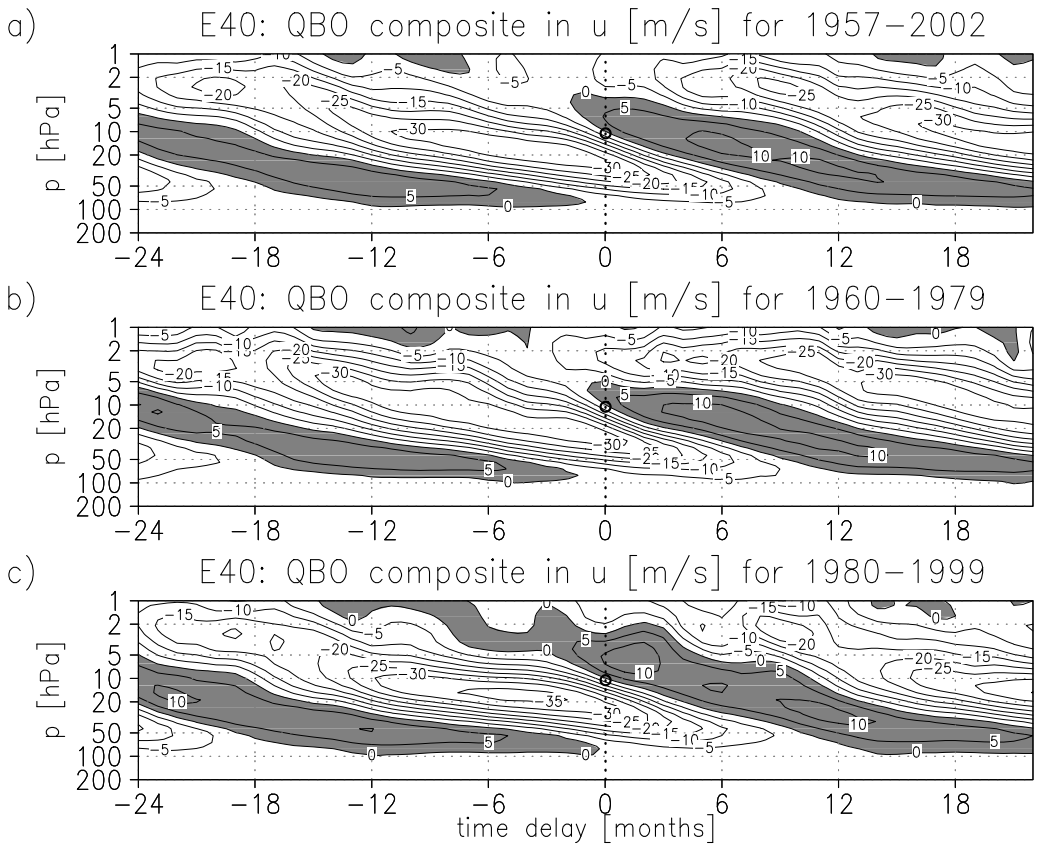

Figure 2.1— Composites of the zonal wind QBO in the equatorial stratosphere of the ERA-40 reanalysis, taken at the transition from easterlies to westerlies. The transition at the 10 hPa level takes place at 0 time delay. Composites are computed for (**a**) the full data set (September 1957–August 2002), (**b**) January 1960–December 1979 and (**c**) January 1980–December 1999.

For all three composites, the QBO period is about 27 months, the peak-to-peak amplitude reaches 45 to 50 m/s and the velocity of vertical propagation is similar. Furthermore, all composites feature some typical characteristics of the QBO, including stronger easterlies than westerlies, westerlies persisting longer in the lower part of the QBO regime, and rapid decrease of the amplitude below 70 hPa. At the top of the QBO domain, however, the composites differ from each other.

Significant differences occur for the two 20-year time frames used for Figs. 2.1b and c. Between 2 and 10 hPa in the upper stratosphere, an easterly anomaly in zonal wind is observed in the early years when compared to the later period. At lower levels, below 10 hPa, the two composites agree quite well, considering that only 7 and 6 QBO cycles were used for the construction, respectively. To further illustrate the differences we present cross sections through the composite in Figs. 2.2 and 2.3.

Figure 2.2 displays the state of the QBO at transition from easterlies to west-

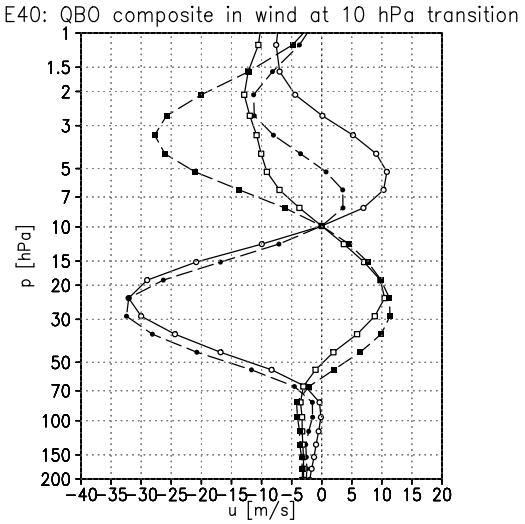

Figure 2.2— Composites of the zonal wind QBO of the ERA-40 reanalysis, at the time of east-west and west-east transitions at 10 hPa. Solid, open circles: 1980–1999 composite east to west; dashed, filled circles: 1960–1979 composite east to west; solid, open squares: 1980–1999 composite west to east; dashed, filled squares: 1960–1979 composite west to east.

erlies and from westerlies to easterlies at 10 hPa. For both composite types, the difference between the early and late periods of ERA-40 is obvious. The differences are strongest between 7 and 2 hPa. Above, it tends to reverse, but one has to keep in mind that there may be some difference in phase among the composites at these levels and that the QBO amplitude becomes small. Below 10 hPa, the differences are small for both kinds of composites, i.e. smaller than 10% of the amplitude. For the transition to easterlies, there seems to be a slight phase difference between the two composites, potentially distorting the construction of composites to a small amount.

Figure 2.3 shows the evolution of the QBO at 4.2 hPa. The difference between the two periods amounts to up to 25 m/s. Note that the signals are relatively noisy, as the semiannual oscillation is quite strong at these levels and does not cancel entirely for the 20 year periods, indicating that the removal of the annual signal was not complete. Indeed, Figure 2.1c shows some residual 6-month signal. This is related to an alignment of QBO and SAO in the second 20-year record. The transition to westerlies at 10 hPa occurs in the same month in 4 out of 9 cases there. As the SAO also changed during this time span, we see the residual signal in the composite. We conclude from this figure that the difference does not seem to depend on the phase of the QBO in a simple manner.

To confirm the difference between the two 20-year periods, the respective average zonal mean zonal wind is computed. Both profiles are shown in Fig. 2.4a, together with their difference. For both time periods, the average zonal wind is similar up to 15 hPa. It is easterly in the troposphere, approaches zero in the lower stratosphere

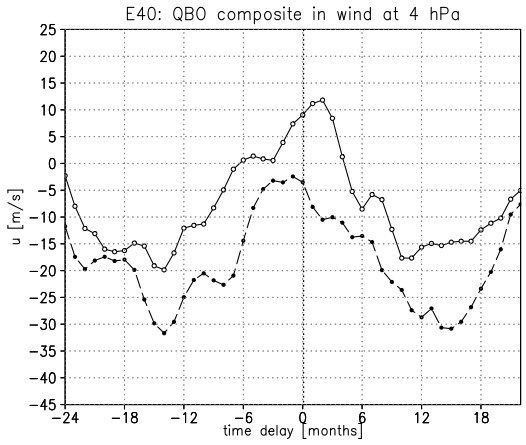

Figure 2.3— Composites of the zonal wind QBO of the ERA-40 reanalysis as in Fig. 2.1, only at the 4.2 hPa level. Solid: 1980–1999 composite, dashed: 1960–1979.

around 70 hPa and is easterly above. Above the 15 hPa level, at which the mean zonal wind is –12 m/s, the earlier period has much stronger easterly winds than the later one. At 4 hPa, the difference reaches a maximum of more than 8 m/s. At the top of the stratosphere, the averages approach each other again and are equal at 1 hPa, being easterly at about 5 m/s. A student t-test shows that the difference between the two periods is significant at the 95% confidence level between 7 and 2 hPa.

Figure 2.4b shows the peak-to-peak range of the QBO signal, i.e. the difference between the maximum easterlies and westerlies at each level, in the two 20-year composites of Fig. 2.1b and c and their difference. The figure shows that the strength of the QBO is quite similar at the beginning and the end of the ERA-40 record. In the lower stratosphere, the QBO signal in the earlier period is stronger by about 5 m/s. At about 5 hPa, this reverses and the QBO of the later time period is stronger by about the same amount. Since the composites consist of only a small number of QBO cycles, these differences are not significant in the sense of a student t test, and so they can not be distinguished from the natural variability of the cycles.

Figure 2.4 illustrates that it is the change in the climatology that causes the difference in the QBO composites, while the strength of the QBO remains almost constant.

To further investigate the timing and origin of the observed changes, we compute running means of zonal wind and temperature through the course of the reanalysis record. 7-year running means are taken to cover 7 annual and about 3 QBO cycles, and thereby mostly eliminate these two modes. Figure 2.5a shows the change in zonal mean zonal wind over the course of ERA-40 in the equatorial stratosphere. Some residual QBO is left in Figure 2.5a, e.g. in between 50 and 20 hPa around 1985. This happens at times of misrepresentation of easterly and westerly QBO phases in

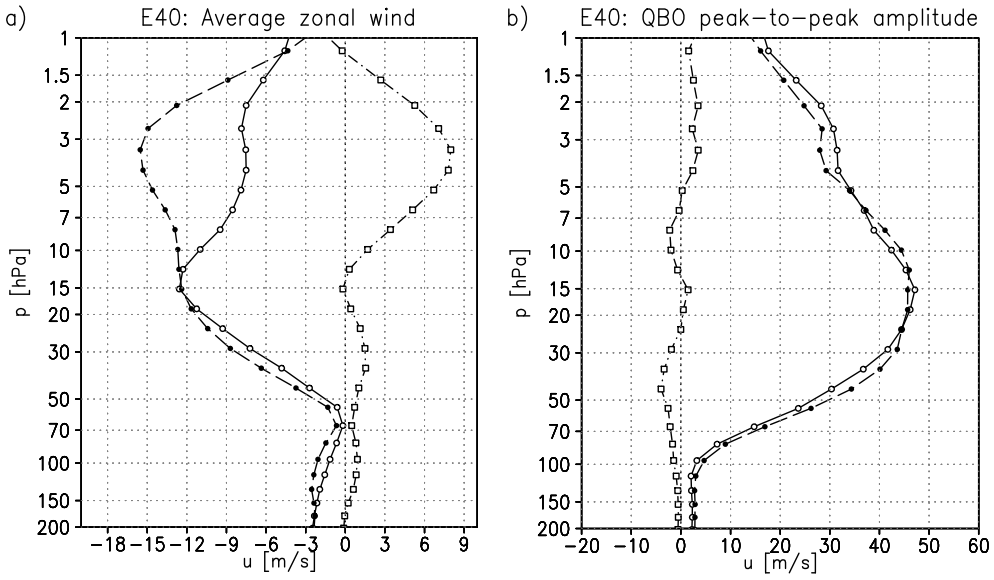

Figure 2.4— (a) Long-dashed: Annual mean equatorial zonal wind of the 1960–1979 period; solid: Same for the 1980–1999 period; dot-dashed: difference between the two periods. (b) QBO peak-to-peak range in the composites of Fig. 2.1; long-dashed: 1960–1979 period, cf. Fig. 2.1b; solid: 1980–1999 period, cf. Fig. 2.1c; dot-dashed: difference between the two periods. Note the different scales at the abscissae of the two panels.

the 7-year period, which can occur because of the variable duration of the individual QBO phases.

In the lower stratosphere, average winds are about zero and constant throughout the record. Between 10 and 20 hPa, there is a phase of stronger easterly winds between 1983 and 1989 and less easterly winds in some years like 1973, 1996 and 1970. No general trend is found, consistent with Fig. 2.4a. Higher up, between 7 and 2 hPa, average winds are strongly easterly at –16 m/s until 1979, less easterly at -12 m/s until about 1983, and show a further westerly trend towards the 1990s, where about -4 m/s are recorded between 1989 and 1995. Thereafter, winds become slightly more easterly again.

Figure 2.5b shows the QBO peak-to-peak amplitude in zonal wind. Here, the QBO peak-to-peak amplitude was estimated using the method of Baldwin and Gray (2005). Because amplitudes were computed over 7-year periods some smoothing is involved. The QBO maximum occurs between 10 and 20 hPa. Relative to the other years, it is shifted downward slightly in the years around 1980. The amplitude of the maximum is reduced during the 1970s and towards the end of the record. In the upper stratosphere, we find a maximum around 1989, where the amplitude is increased by 50% compared to its average value at 4 hPa. A similar increase appears at the very end of the record.

Figure 2.5c shows the 7-year running mean temperature, where the overall mean

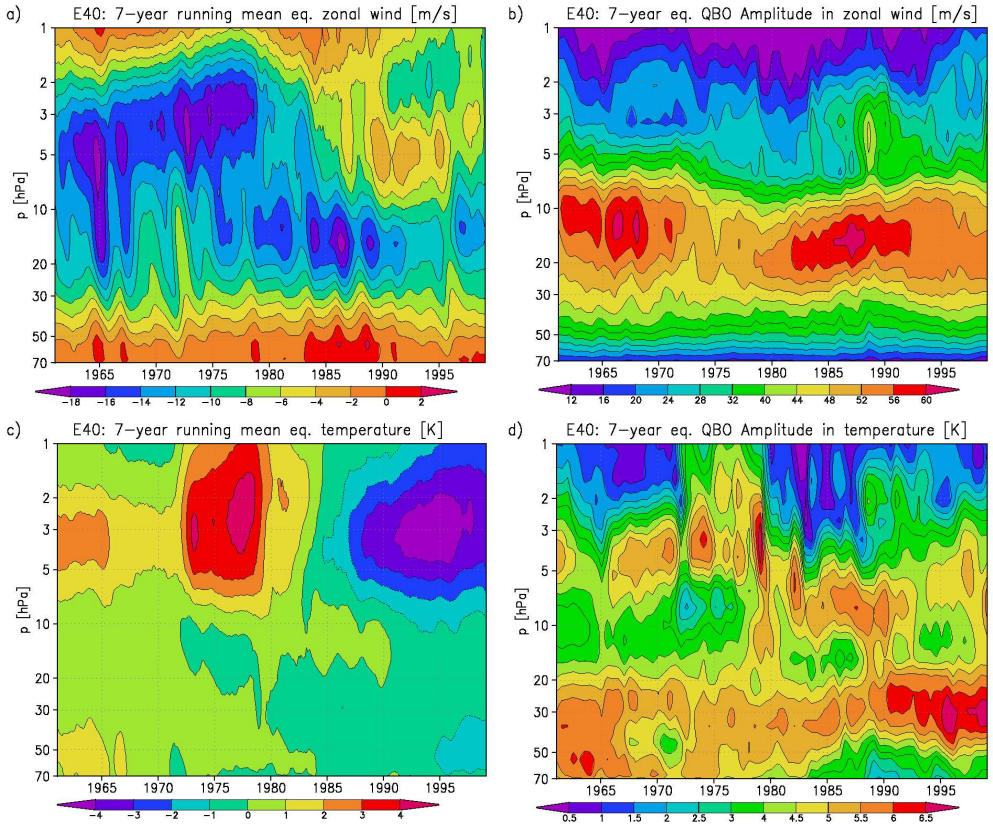

Figure 2.5— **(a)** Seven year running mean of zonal mean zonal wind at the equator, in m/s. **(b)** Seven year running mean estimate of the QBO amplitude over the course of the record, in m/s. **(c)** As in (a), but for temperature anomaly, in K. **(d)** As in (b), but for temperature, in K.

of 1957–2002 was subtracted. Above 7 hPa, there is a warm period in the mid-1970s and a cooling trend after 1983.

The QBO amplitude in temperature anomaly given in Fig. 2.5d also has some interesting aspects. At 70 hPa, there is a decrease after 1983, while at 30 hPa, the amplitude was increased in the 1990s. Between 10 and 5 hPa, the amplitude is larger in the second part of ERA-40 compared to the first one, while the reverse is true above. There is virtually no QBO signal in temperature between 2 and 3 hPa during 1983–1988.

Figure 2.6 reveals that the changes in the 7-year mean displayed in Figs. 2.5a and c did not occur uniformly in all seasons. January and June were selected because they show the most pronounced changes. 7-year averaged anomalies from the 45-year climatological mean are displayed for both zonal wind (a and c) and temperature (b and d). In June zonal wind, shown in Fig. 2.6b, two domains are clearly visible above 7 hPa, with a transition from easterly to more westerly conditions starting in about 1977 at 5 hPa and reaching 1 hPa by 1982. The difference is strongest at 2 hPa and

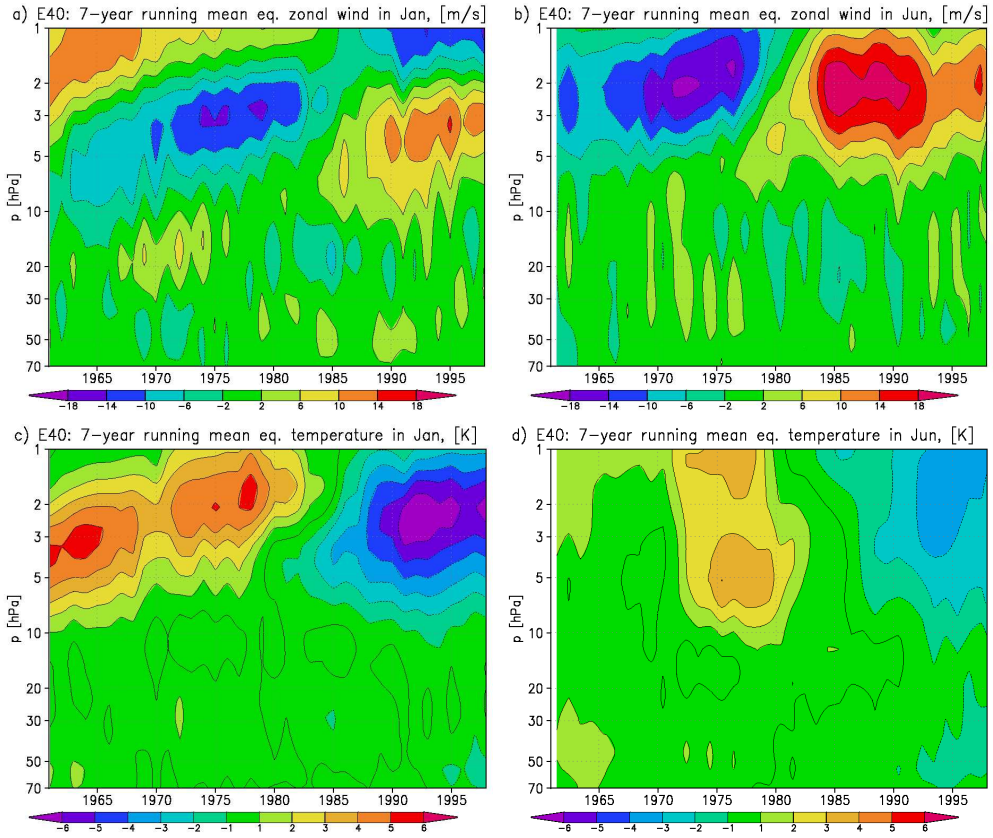

Figure 2.6— (a) 7-year running climatology of zonal mean zonal wind anomaly in January, in m/s. (b) As in (a), but for June. (c) As in (a), but for temperature anomaly, in K. (d) As in (c), but for June.

amounts to 30 m/s between the 1970–75 and 1985–90 periods. For January, shown in Fig. 62.6a, the evolution is distinctly different. Two domains are also found between 10 and 2 hPa, but the transition towards more westerly winds occurs between 1983 and 1985 here. In the earlier part, there is a trend for the anomaly to move upward from about 6 to 3 hPa and strengthen. Furthermore, there are two domains with a reversed change from westerly to easterly between 2 and 1 hPa.

The change in the temperature for June in Fig. 2.6d is a bit less distinct than in the annual running mean, but shows the same features; they extend downward a bit further. January temperatures in Fig. 2.6c, however, show a very distinct anomaly similar in shape to the corresponding zonal wind anomaly. High temperature anomalies occur at times of more westerly wind shear in the first part and cold anomalies in the more easterly wind shear later on, consistent with thermal wind balance, which shall to be discussed in the next paragraph.

An expression for the relation of vertical wind shear and meridional temperature gradient in the equatorial β-plane was given by Baldwin et al. (2001). We check

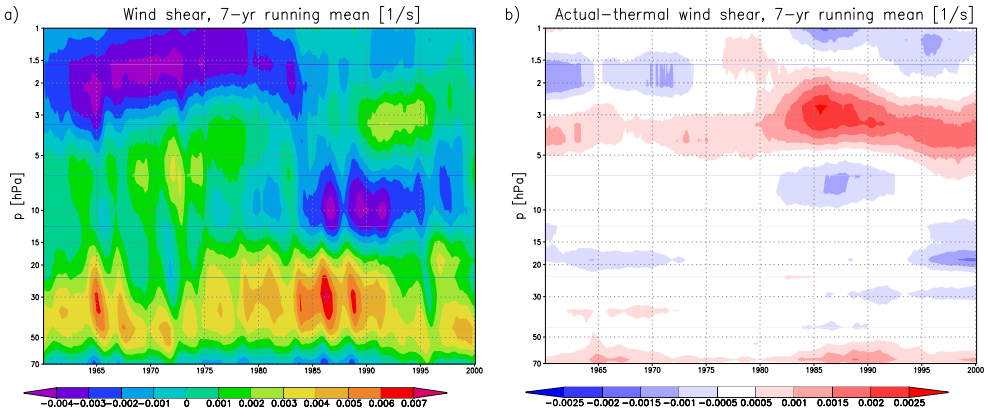

Figure 2.7— (a) 7-year running mean of vertical zonal mean zonal wind shear at the Equator, in 1/s. (b) Difference between (a) and 7-year running mean thermal wind shear, in 1/s.

for this relationship in the ERA-40 record. The result is given in Figure 2.7. The wind shear reflects the changes that were found in the wind field. As Figure 2.7a shows, negative shear dominates above 3 hPa until 1983, while mostly positive shear is found between 3 and 10 hPa. After 1983, shear is negative between 15 and 5 hPa and neutral to positive above. After the transition, during 1983–1989, wind shear between 20 and 50 hPa is also increased. Figure 2.7b illustrates that thermal wind balance generally gives a good approximation to the wind shear. However, during the period 1983–1989 and, to a lesser degree, afterwards, thermal wind balance is weaker between 5 and 2 hPa. A further analysis based on 1-year instead of 7-year means (not shown) can demonstrate that this feature does not have a QBO signal itself.

The Figures 2.5–2.7 shows a number of features especially in the region above 10 hPa, and differences between the initial and later period of the reanalysis, as expected from the composites.

2.4 Discussion of the observed trends and variations

Possible Explanations for features of interannual variability in the ERA-40 reanalysis fall in two groups:

1. Features of the real atmosphere
2. Features due to shortcomings of the observing and analysis system

In the first group, the QBO is most important in the tropical stratosphere. It is variable in period and also shows variability in amplitude, as Fig. 2.5b suggests.

Since the QBO is a dynamically driven phenomenon, it can be expected that amplitude changes are connected to other atmospheric processes, e.g. via strength

Table 2.1— Possible sources for anomalies and inconsistencies in the ERA-40 reanalysis system that are discussed in the text.

Year	Month	Event
1957	Sep	Start of ERA-40, stream No. 2
1972		Start satellite temperature assimilation from VTPR
1972	Jun	Stream No. 2.5
1973		Start station ID problem with radiosondes
1973	Apr	Stream No. 3
1977		End station ID problem with radiosondes
1978		End of VTPR temperature assimilation
1979		Start satellite observations from TOVS
1979		Start ozone assimilation from from TOMS/SBUV
1982		Start use of METEOSAT cloud motion winds
1985	May	Stream No. 5
1986	Jun	Stream No. 4
1987		Start of SSM/I satellite observations
1988		End use of METEOSAT cloud motion winds
1989	Feb	Stream No. 1
2002	Aug	End of ERA-40

of tropospheric waves and their propagation conditions. These are, however, fairly complex and likely nonlinear, and their discussion is therefore beyond the scope of this work, also considering the sparsity of early data and changes to the observing system later.

A closer investigation of the increased QBO amplitude at the end of the 1980s displayed in Figure 2.5b reveals that a strong QBO phase in 1986/7 that enters the seven year window is responsible for the increase. A more smooth decrease of the amplitude follows in the 1990s and another rapid increase occurs in the last year of the record but can not be identified very clearly in Fig. 2.5b. The similarity of the two jumps suggests that they are not due to the observing system but either a product of model dynamics (not constrained by observations) or a common property of the climate system. A potential mechanism would be the alignment of annual and quasi-biennial cycles in a certain constellation affecting the amplitudes. The data record is however too short to prove such a connection. Instead, one could argue that the 1986/87 jump is due to other explanations to be discussed below. On the other hand, increased QBO amplitudes after 1985 coincide with the colder period in the temperature field of Figure 2.5c.

The annual cycle and the semi-annual oscillation are the other two important modes of variability in the tropical stratosphere. They are not represented in Fig. 2.5a, but, clearly, changes in the annual or semiannual cycle will affect the annual mean. In fact, it is found that the monthly climatological values of zonal

wind in the earlier and later period differ.

In an earlier study, Crooks and Gray (2005) discussed the effect of ENSO and volcanic eruptions on the climate of the stratosphere in ERA-40. They found easterlyward shifts in annual mean zonal wind of up to 5 m/s per standard deviation change in stratospheric optical depth between 5 and 10 hPa after major volcanic eruptions. However, Figure 2.5 does not show more easterly winds for the years following the eruptions of Agung (1963/4), El Chichon (1984) and Mt. Pinatubo (1993). Similarly, an impact of ENSO on upper stratospheric winds can not be shown in this study, also because time resolution is too small. We do not find signatures of the 11-year solar cycle, as there are too many short term variations superimposed to a potential cycle. ERA-40 may actually not cover such effects if they originate higher up in the atmosphere, as the model top is at 0.1 hPa.

Finally, a general trend in climate conditions will also affect the conditions in the upper stratosphere. In fact, a stratospheric cooling trend in ERA-40 as it is observed in Fig. 2.5c has previously been reported by Santer et al. (2004) and been related to a global warming trend in the troposphere. On the other hand, a trend towards more westerly wind shear as found in Fig. 2.7c above 5 hPa would mean by thermal wind balance a relative warming of the tropical stratosphere with respect to the subtropics and thus support that the equatorial region is not as susceptible to the cooling effect of climate change as the subtropics are. On the other hand, shrinking of the meridional extent of the QBO as found by (Huesmann and Hitchman, 2004) in the NCEP-reanalysis, would have the same effect.

The second group of possible explanations is similarly diverse. Table 1 lists the events discussed here. First of all, the number and kind of observations varies over the course of the record. The lack of data in the assimilation in the pre-satellite era allows the model to develop its own dynamics (Sterl, 2004; Uppala et al., 2005). Satellites deliver valuable information on the state of the upper stratosphere which is not reached by radiosondes particularly after 1979, when TOVS data is assimilated. Considering our results, e.g. the monthly anomalies in Fig. 2.6b, it seems likely that the introduction of extensive satellite data around 1979 caused much of the diagnosed difference between the two halves of ERA-40. However, it is not clear why this change should be delayed by up to six years.

Furthermore, Andrae et al. (2004) discuss the corrections that were applied to the radiosonde temperature data from 1980 on. While corrections were generally small, a stronger correction at one of the relatively few equatorial stations could have a strong effect. For the period 1973–77, these authors also report problems with inconsistent station IDs that led to the same data being used twice. Besides this, their Figure 2.1 shows a drop in the number of 30 hPa radiosonde observations after 1978.

The changes can not only be due to more accurate measurements, but resolution effects can also play a role. Huesmann and Hitchman (2004) proposed that satellite measurements will underestimate the temperature QBO amplitude because of lacking vertical resolution.

The warm period observed in Figure 2.5c during the 1970s is deceiving – we found that it is due to a strong warm anomaly of up to 15 K in the years 1975 and 1976 that is smoothed by our averaging algorithm to give a 4 K anomaly lasting from 1972 to 1979. A similar anomaly also shows up as a bias in ERA-40 first guess global mean temperature versus radiosonde data as reported by Andrae et al. (2004) in their Figure 2.1, although that one, at 30 and 250 hPa, is much smaller, below 1 K in amplitude. Gleisner et al. (2005) report anomalous upper tropospheric thickness for the same period. There is reason to believe that this anomaly is due to a problem with the assimilation system during the period, that just is much more severe in the upper stratosphere as the model is not restricted by sonde observations there. The ERA-40 web-page reports an increased error rate in temperature data from the VTPR instrument on NOAA4 satellite at the end of its service in 1976, also mentioned by Santer et al. (2004) and van Noije et al. (2006) as a potential error source.

The deviation from thermal wind balance found for 1983–88 coincides with the period during which METEOSAT cloud motion winds were assimilated. While a direct effect of the tropospheric winds on those in the upper stratosphere is impossible, the wind assimilation may have affected resolved waves that were damped in the stratosphere and thereby transferred their momentum.

The ERA-40 reanalysis was computed in six streams as shown in the online documentation (`http://www.ecmwf.int/research/era/`). The transitions among streams are also potential sources for changes in the reanalysis data set. In particular, the transitions of streams 3 to 5 (May 1985), 5 to 4 (June 1986) and 4 to 1 (February 1989) coincide with some of the anomalies in Figure 2.5. During stream 4, zonal winds were particularly easterly between 10 and 20 hPa, while they became more and more westerly above 7 hPa. The start of stream 4 also marks the beginning of the cooling phase in Fig. 2.5c.

2.5 Conclusions

The variability of atmospheric conditions of the equatorial upper stratosphere can not be fully understood from the ERA-40 reanalysis record. The ERA-40 system produces a periodic pattern of the quasi-biennial oscillation which is consistent with the better-observed middle and lower stratospheric QBO from radiosonde observations. However, this study reveals some curiosities – in particular, the earlier part (1960–79) of ERA-40 shows a QBO in the upper stratosphere that is distinctly different from the one in the later part (1980–99). Most prominently, a westerly shift of up to 12 m/s is observed in the zonal wind between the two sections. No obvious reason for this was found.

Because few or no observations are available for the upper stratosphere region, especially in the earlier years, it is not clear whether our findings are artifacts of the ERA-40 reanalysis system or whether they represent the real state of the atmosphere. A couple of shifts in upper stratospheric conditions can be related to problems with

or changes of the reanalysis system, such as the warm stratosphere in 1975/76, or the introduction of satellites in 1979.

However, for the long term differences, no satisfying explanation could be given. If we assume the dynamics of the model is working well, reproducing the climate several levels above where observations were available in the pre-satellite period, our work indicates there is substantial variability on time scales longer than the QBO period. On the other hand, there are some caveats with the reanalysis related to data quality, quantity or assimilation, and a more careful review of the data sources used and the assimilation system is required, which is beyond the scope of this work.

Anyway, there is reason to believe that the later portion of the ERA-40 displays the more realistic description of tropical zonal winds and the QBO, as it is based on more and likely higher-quality observations, including detailed satellite data since the late 1970s.

Given these findings, care should be taken when using the ERA-40 reanalysis as a reference, e.g. for model development and validation purposes, where winds in the tropical upper stratosphere play a role. Another outcome of this study is that reliable long term data records from observations are crucial for any statements on interannual atmospheric variability in this region of the atmosphere.

Chapter 3

Net effect of the QBO in a Chemistry Climate Model[1]

3.1 Introduction

The representation of the stratosphere in present-day general circulation models (GCMs) such as those used for the IPCC AR4, is usually simple. Specific processes driving stratospheric variability, in particular the dynamics of waves and the transport and chemistry of trace gases, can not be included in these models for their high computational cost. But the interest in projections for stratospheric ozone concentrations and stratospheric climate impacts has led to the development of the so called chemistry-climate models (CCMs) that cover these processes to different degrees. Recently, Eyring et al. (2006) presented an inter-comparison of such models.

The effects of the quasi-biennial oscillation (QBO) of equatorial zonal winds (see the review of Baldwin et al., 2001) are a prominent example for the complex interaction of dynamics, trace gas transport and trace gas chemistry in the stratosphere. QBO variations were found in satellite observations for many trace gases including ozone, methane and water vapor (Randel and Wu, 1998; O'Sullivan and Dunkerton, 1997; Randel et al., 1998; Dunkerton, 2001; Patra et al., 2003; Randel et al., 2004b). More recently, Schoeberl et al. (2008) presented a comprehensive study of QBO signals in multiple trace gases from HALOE and Aura MLS observations.

The purpose of modeling studies in this context is twofold: Firstly, CCMs provide a unique way to study QBO effects in a consistent manner. Secondly, the representation of the QBO and its effects is an interesting test case for CCMs. Still, like most GCMs, many CCMs fail to represent the QBO entirely, which may lead to significant deficiencies in the results from these models.

Several studies validated or showed QBO signals in CCMs, such as Steinbrecht et al. (2006) who compared ozone concentrations and temperatures in CCMs to satellite observations and reanalyses. Chipperfield et al. (1994), Bruhwiler and Hamilton

[1] Accepted for publication in *Atmospheric Chemistry and Physics Discussions*, 2008, with M.A. Giorgetta as co-author.

(1999) and Tian et al. (2006) discussed the QBO signal in ozone and nitrogen oxides and their chemical connection. Previous analyses have mostly focused on the actual variation of the circulation, trace gas concentrations and chemical processes.

In contrast, the goal of this work is to analyze the average net effect of introducing a realistic QBO into the circulation on the long term. This is done using the chemistry climate model MAECHAM4-CHEM. The nudging technique of Giorgetta and Bengtsson (1999) offers the opportunity to include a realistic QBO, based on observations at Singapore, in the MAECHAM4-CHEM model, which otherwise does not have a QBO, unlike the higher resolved and improved simulations based on ECHAM5 (Giorgetta et al., 2006; Lelieveld et al., 2007). The variations induced by the QBO, e.g. in ozone, can be compared directly to observations, due to the assimilation of observed QBO winds. The comparison of two otherwise largely identical experiments, of which one is nudged to the observed QBO for 20 years and the other one is not, reveals the net effect of the QBO. Here, we are not primarily interested in the difference between selected states of the QBO and the non-QBO state, but in the climatological difference for longer times. The length of the experiments was chosen accordingly to average over a reasonable number of QBO cycles and many different phase combinations of annual and QBO cycles to give a realistic view of the long term effect.

For many considerations on longer time scales, the net effects of the QBO may be far more important than the QBO variations themselves. Specifically, such effects are not limited to the QBO region for a given quantity, and may exceed the actual QBO range in other places, as will be discussed below.

The QBO net effect will be shown for a number of variables that are directly affected by the QBO and its secondary meridional circulation. For the dynamic aspect, we chose zonal wind and temperature. They show pronounced QBO imprints that are well understood (Plumb and Bell, 1982; Huesmann and Hitchman, 2001; Baldwin et al., 2001). Regarding trace gases, we restrict ourselves to the discussion of ozone. Net effects on selected other trace species, i.e., methane, NO_x and water vapor, as well as the net differences in the stream function, are included in an appendix.

The results of this study are particularly interesting in the light of the recent development of global circulation models that produce a QBO. Currently, the Japanese models at CCSR/NIES (Takahashi, 1996) and MRI (Shibata and Deushi, 2005), the SKYHI model of GFDL (Hamilton and Hsieh, 2002), the models UMETRAC and UMSLIMCAT of the UK Met Office (Austin, 2002) and ULeeds (Tian and Chipperfield, 2005) and the models MAECHAM5 (Giorgetta et al., 2006) and HAMMONIA (Schmidt et al., 2006), when used with a high vertical resolution grid, have a representation of the QBO.

Our approach can show the improvement of the general circulation and tracer representation to be expected in such models when compared to conventional, non-QBO models. Some of the aforementioned models may also offer the possibility to remove the QBO by modifications to the model, e.g. by reducing the vertical reso-

lution. In that case, however, these modifications may themselves have an impact on the circulation that is entangled with the QBO's effect. The main advantage of using a nudged model is that the nudging presents a very minor modification to the model simulation and thus the net impact of the QBO can be addressed directly and consistently.

Section 2 describes the CCM runs used for this study and the methods of analysis used. The QBO in the model is evaluated by comparing the anomalies to the ERA-40 reanalysis and results from satellite observations. Section 3 deals specifically with the model's representation of the QBO in ozone. Section 4 shows the net effect of the QBO in wind and temperature in comparison to the amplitude of the QBO while section 5 discusses the net effect on ozone. Implications are discussed in section 6. The appendix presents a synopsis of annual and seasonal net effects of the QBO in the mass stream function, methane, humidity and nitrogen oxides.

3.2 Model and comparison to observations

The MAECHAM4-CHEM CCM consists of the middle-atmosphere version of the ECHAM4 climate model (Manzini and McFarlane, 1998; Roeckner et al., 1996) and the interactively coupled chemistry model CHEM (Steil et al., 1998, 2003; Manzini et al., 2003). The circulation is computed by the spectral transform method at T30 truncation, associated to a Gaussian longitude-latitude grid with a spacing of 3.75 degree, and has 39 vertical layers between the surface and 0.01 hPa. Transport and physical and chemical processes are computed in grid point space. The chemistry scheme includes the most important species and reactions of troposphere and stratosphere. Radiative feedbacks of the computed O_3, H_2O and CH_4 are processed in the climate model.

The two experiments described here run from 1980-2000. Sea surface temperatures are from HadISST1 (Rayner et al., 2003) and greenhouse gases and halogens are as used for the WMO/UNEP assessment 2002 (WMO, 2003). The first experiment (nonQBO) is free-running and does not reproduce the quasi-biennial oscillation. The second experiment (QBO) is in contrast forced to have a QBO equivalent to observations using the nudging technique: tropical stratospheric winds are relaxed linearly to the observed winds from the Singapore radiosondes, which is close to the equatorial maximum of the QBO. The applied forcing is zonally uniform with a Gaussian profile with the full width of half maximum around the Equator ranging from 20 degrees at 70 hPa to 30 degrees at 10 hPa. Observations from seven altitude levels between 70 and 10 hPa are used until 1986, when measurements on 14 levels between 90 and 10 hPa became available. Above 10 hPa, the QBO jets are extended vertically, assuming a steady downward propagation of 2 km/month between 10 and 3 hPa. The nudging applied here neglects hemispheric asymmetry of the QBO in zonal wind. Zonal asymmetries are also assumed to be negligible.

Furthermore, in the nudged experiment, solar activity is parameterized using radiation flux data by Lean et al. (1997) and the aerosol forcing caused by volcanic

eruptions is included by prescribing precalculated net heating rates of Kirchner et al. (1999) and the surface area densities of Jackman et al. (1996) for the chemistry module. These two observational forcings were not included in the simulation without QBO nudging. They introduce additional sources of interannual variability to the QBO run, mainly the 11-year solar cycle and the eruptions of El Chichon in April 1982 and Mt. Pinatubo in June 1991. However, for the quantities of interest here, their impact should be either small or well understood, as e.g. the stratospheric temperature and water vapor response to tropical volcanic eruptions. 2-year time sections following the eruptions of El Chichon and Mt. Pinatubo are excluded from the comparison for this reason. Tourpali et al. (2003) report an ozone variation of 2-3% in the upper stratosphere due to the solar cycle, but on average over the entire period of the experiment these variations will nearly cancel, and the net effect related to the 11-year solar cycle will be far lower than this number. Thus, comparing the two experiments is still very effective for the identification of the QBO's net impact on the stratosphere. The nudged experiment described here has previously been evaluated within the SPARC CCMVal activity (Eyring et al., 2006) on the validation of chemistry-climate models.

Figure 3.1 displays the time series of zonal mean zonal wind at the Equator for the period of the experiments. Figure 1a shows the zonal mean zonal wind for the nudged QBO experiment, Fig. 3.1b for the non-QBO experiment, and Fig. 3.1c for the ERA-40 reanalysis (Uppala et al., 2004). Notice the close agreement of the nudged experiment and the reanalysis in the structure of the QBO jets below 10 hPa where direct wind observations exist. The easterlies are slightly stronger in the reanalysis than in the model. This may be because the additional data sources assimilated in ERA-40 differ from the Singapore winds.

In the non-QBO experiment, the winds are almost constant easterly by 5-10 m/s throughout the lower and middle stratosphere. The semi-annual oscillation (SAO) of the winds in the upper stratosphere is more pronounced than in the QBO experiment. In particular, the SAO westerlies are suppressed in the QBO experiment when there are westerlies at 20 hPa . The SAO easterlies during the solstitial seasons are mostly due to the mesospheric overflow in these seasons and therefore not affected as severely by this effect. Also see the discussion on this issue in Giorgetta et al. (2006), who compared two experiments that have a QBO or no QBO due to different vertical resolutions. They noted similar differences in the SAO due to the presence of the QBO using a model that generates the QBO spontaneously.

In ERA-40, the annual asymmetry between the two cycles of the SAO is more pronounced than in the model experiments, and is generally more variable. The weakening of the SAO phases above equal QBO phases can also be recognized. Compared to the QBO experiment, the SAO also extends further down in the experiment without QBO. This is a consequence of the too low resolved wave driving in the CCM, one reason why it does not produce a QBO spontaneously. Note, however, that there is some uncertainty to the ERA-40 data above 10 hPa, because there are rather few data available at these levels (Uppala et al., 2004; Punge and Giorgetta, 2007).

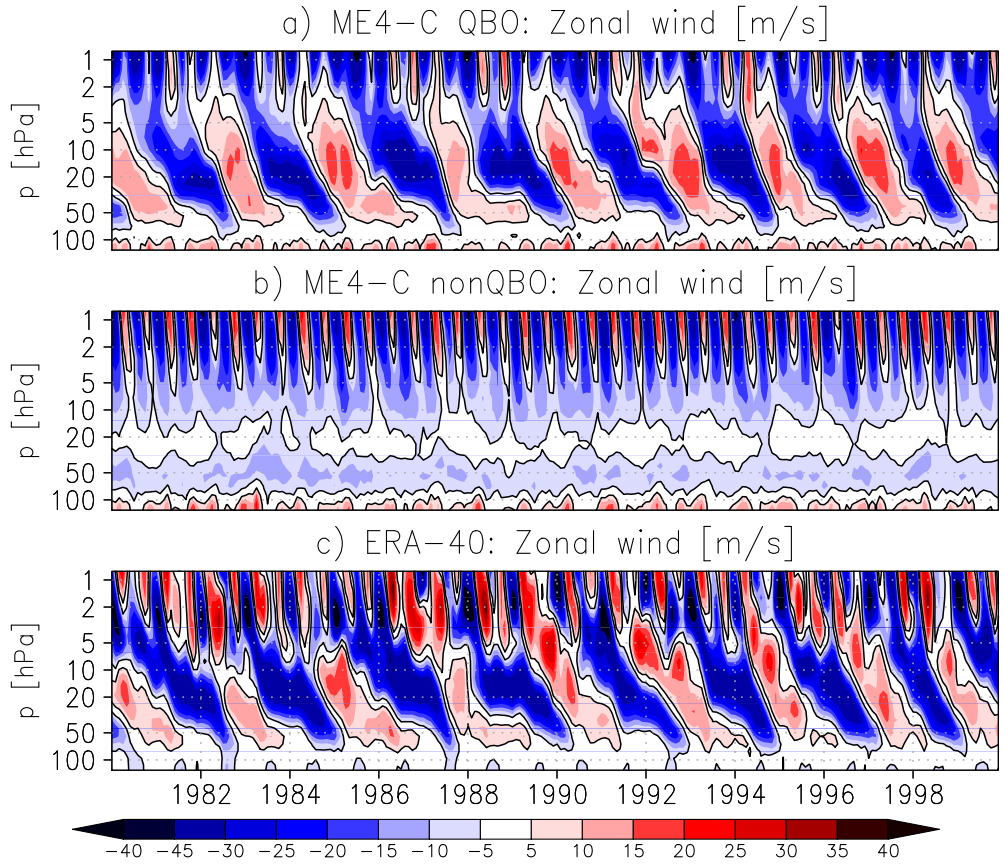

Figure 3.1— Zonal mean zonal wind [m/s] in the equatorial stratosphere in m/s, mean between 5°S and 5°N, **(a)** MAECHAM4-CHEM nudged QBO experiment; **(b)** MAECHAM4-CHEM free running experiment; **(c)** ERA-40 reanalysis.

We conclude from Fig. 3.1 that the representation of the zonal wind in the QBO model experiment is quite realistic and the non-QBO experiment is typical for a climate model without QBO. Thus, the pair of experiments is suitable for our comparison in this respect.

Figure 3.2 shows the temperature anomalies for the two model experiments and the ERA-40 reanalysis. Thermal wind balance explains the temperature QBO signal which is phase-shifted with respect to zonal wind by about 1/4 cycle (e.g., Baldwin et al., 2001). The representation of the temperature QBO is realistic in the nudged model run. In comparison to ERA-40, I notice some differences in the upper stratosphere. One explanation is the different representation of the SAO mentioned above. But some of the differences may again be due to deficiencies in the ERA-40 (Punge and Giorgetta, 2007). For an analysis of the temperature QBO in the nudged version of MAECHAM4-CHEM in comparison to observations we refer to Steinbrecht et al. (2006). They evaluated a model experiment that is almost identical to the QBO

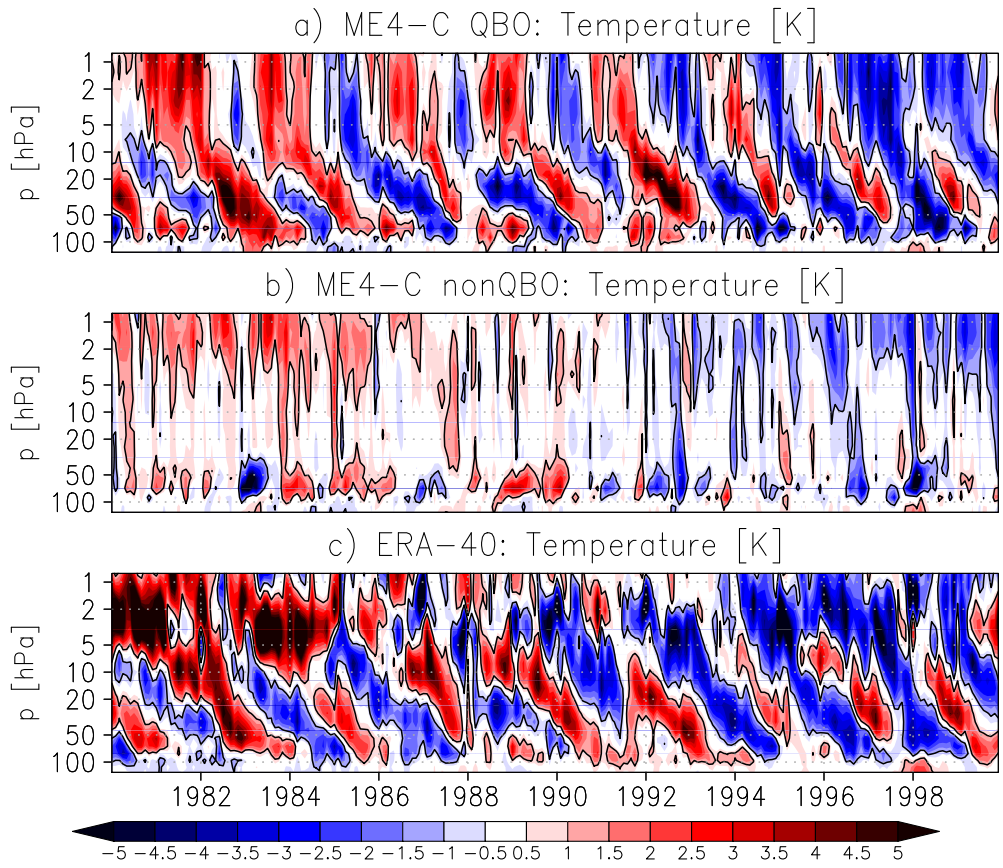

Figure 3.2— As Fig. 3.1, but for the zonal mean temperature anomalies [K] (monthly climatology subtracted).

experiment in this study, except for its duration of 40 years, but did not evaluate a free-running model experiment.

The non-QBO experiment shows little interannual variability. There are cold anomalies in the lower stratosphere in 1983 and 1998 following the El Nino events in these years. These cold anomalies are present in the nonQBO simulations but absent in both the QBO simulation and the ERA-40 data, which suggests that the QBO is important for studies on the impact of El Nino in the tropical stratosphere.

The warm and cold anomalies of the temperature QBO signal correspond to phases of weaker and stronger upwelling in the tropics, respectively. Together with the variation of the latitudinal velocities, this forms the QBO's secondary meridional circulation (SMC) that modulates the Brewer-Dobson circulation, which leads to the QBO imprint on the mass stream function (Plumb and Bell, 1982). It is clear that the secondary meridional circulation impacts any trace gas and substance with vertical or horizontal gradients and sufficiently long life time in the tropical stratosphere

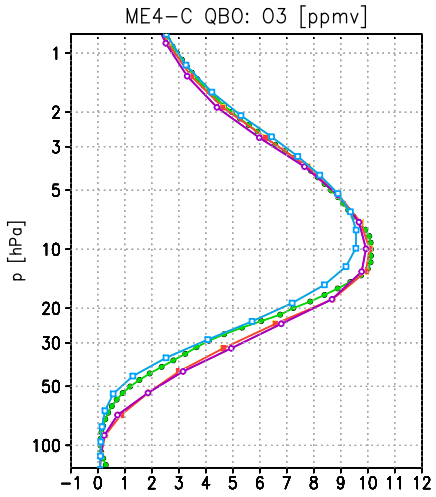

Figure 3.3— Profile of zonal mean ozone mixing ratios [ppmv] in the equatorial stratosphere, averaged over six years of HALOE observations (green) and the respective time interval in the ERA-40 reanalysis (blue) and the MAECHAM4-CHEM model with (red) and without (violet) nudged QBO.

(Trepte and Hitchman, 1992; Chipperfield and Gray, 1992; Randel and Wu, 1998; Randel et al., 1998; Patra et al., 2003; Tian et al., 2006; Schoeberl et al., 2008).

Ozone is the most prominent example for a tracer that varies with the QBO. The modulation of the ozone column in our model was investigated by Steinbrecht et al. (2006). In this article, the vertical distribution of ozone is of particular interest.

Fig. 3.3 shows the 6-year climatological mean vertical profile for the period 1992-1998 of ozone in the two model experiments, in comparison to HALOE satellite observations and the ERA-40 reanalysis. The modelled profile is close to that of HALOE at and above the maximum at 10 hPa in both simulations. In the lower stratosphere, the model overestimates mixing ratios by up to 1 ppmv. The model run with QBO is slightly closer to the HALOE data than the nonQBO run both at most levels, indicating that there is a net effect of the QBO. Reanalyzed ozone mixing ratios are lower than in the HALOE observations both at the maximum and around 50 hPa, but agree well especially in the upper stratosphere. Recent radiosonde observations however suggest that HALOE results underestimate ozone concentrations in the lower stratosphere (Witte et al., 2008).

A number of different effects of the QBO impact the vertical profile of ozone via both transport and chemistry, making modelling a difficult task. In Fig. 3.4, the equatorial (2°S to 2°N) ozone anomalies over the period 1991-1999 are given for available HALOE measurements, the two MAECHAM4-CHEM model runs and the ERA-40 reanalysis. The QBO signal in HALOE O_3 data given here was obtained by interpolation to a monthly time series. A similar evaluation was applied by Cordero et al. (1997).

We find good agreement between the nudged model and the HALOE data. The

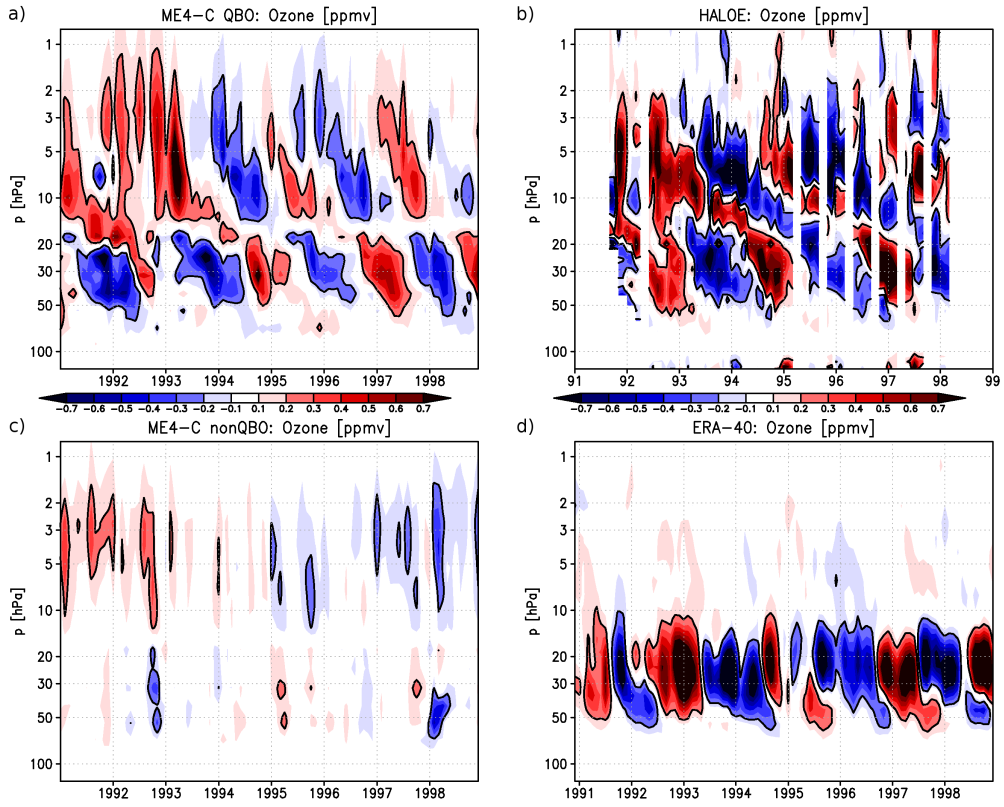

Figure 3.4— Anomalies of the ozone volume mixing ratio [ppmv] in the tropical stratosphere in **(a)** the MAECHAM4-CHEM nudged QBO experiment; **(b)** HALOE observations, **(c)** the MAECHAM4-CHEM free running experiment; **(d)** the ERA-40 reanalysis. Contour spacing is 0.1 ppmv, the zero contour is omitted.

downward propagation of the anomalies, following the QBO jets, is well represented, including the phase shift at 15 hPa. The magnitude of the modelled anomaly is somewhat lower than in the HALOE record, at about 0.5 ppmv both at 8 and 30 hPa compared to about 0.8 ppmv. In the QBO model run, we also find an imprint of the eruption of Mt. Pinatubo during the two years after June 1991 not present in the satellite observations. During this period, volume mixing ratios are decreased below 20 hPa, and increased above, which may relate to the water vapor anomalies due to the eruption.

In the reanalysis, there is hardly any QBO signal above 10 hPa. Instead, the lower branch of the anomalies is much stronger than in satellite observations, and it reaches up to 10 hPa. In the non-nudged model there is interannual variability probably related to the lower stratospheric temperature modulation by ENSO in this run. Anomalies are in phase in the lower and upper stratosphere, with a phase reversal at 15 hPa as in the QBO run. There is a negative trend in the upper stratosphere that is related to increase in chlorine species.

A detailed discussion of the QBO impact on the chemistry and transport of ozone in the model is instructive for the later evaluation of the net effect and follows in the next section.

The Figures 3.1 to 3.4 show the nudging technique is appropriate to introduce a realistic QBO into a model and that the representation of the QBO effects on temperature and ozone is in good agreement with observations.

3.3 Chemistry and transport impact on ozone by the QBO

A vertically resolved record of ozone anomalies due to the QBO in SAGE satellite observations was first shown by Zawodny and McCormick (1991). They argued that the equatorial QBO signal was due to the advection of ozone by the SMC in the lower stratosphere and by modulation of the ozone chemistry above, with anomalies of nitrogen oxides, mainly NO and NO_2, playing a major role in the latter. It is clear that the chemical lifetime of O_3 decreases significantly with altitude (e.g., Brasseur et al., 1999), thereby limiting the direct impact of advection at higher levels. In the upper stratosphere, the modulation of temperatures due to the modulation of upwelling by the SMC is assumed to alter the equilibrium state of ozone chemistry and cause variations in phase with the upwelling.

The respective roles of ozone transport and chemistry in the formation of the QBO signal have however been debated. Hasebe (1994) presented anomalies of the ozone QBO in the tropical mean volume mixing ratio in SAGE data with an amplitude of about 0.5 and 1 ppmv, or about 10%, in the lower and upper branch of the signal, respectively. Randel et al. (1998) updated and extended the analysis of the SAGE record, and another update was given in Logan et al. (2003). Logan et al. (2003) also presented the ozone QBO signal derived from sonde measurements at Nairobi and San Christobal. They report a signal of 15-20% in the lower branch near the Equator. This is somewhat stronger than in the SAGE data, which suggest an amplitude of 10-15% if only measurements close to the Equator (2°S to 2°N) are taken into account. The QBO signal in HALOE ozone data given in Fig. 3.4 was also analyzed by Cordero et al. (1997), who report an amplitude of 0.8 ppmv in both branches for the latitude range 4°S to 4°N, similar to the equatorial SAGE evaluations. Dunkerton (2001) and Schoeberl et al. (2008) also evaluate HALOE data and found an amplitude of about 0.4 ppmv in the tropics. Recently, Witte et al. (2008) found good agreement between HALOE records and sonde observations from the SHADOZ network in the lower branch of the QBO anomaly within 10° of the Equator, with an amplitude of about 1 ppmv.

In all records that have coverage in this altitude range, the signal is split at about 15 hPa in the tropics, where time series show a phase shift of nearly 180°. This phase reversal occurs below the maximum volume mixing ratio at 10 hPa, were it would be expected if advection alone were responsible for the signal. A contribution of NO_x to the QBO signal at these altitudes, as suggested by the

studies of Chipperfield and Gray (1992) could in principle explain the shift of the phase reversal. Recently, Butchart et al. (2003) reproduced a near realistic QBO signal in ozone using a chemistry-climate model that generated a QBO internally but did not include variations in NO_x. However, the phase reversal occurs near 10 hPa, close to the maximum of O_3 in their model.

Bruhwiler and Hamilton (1999) showed in their model, which had a nudged QBO of fixed period and did not include chlorine chemistry, that the QBO anomaly of net chemical production, mainly by NO_x anomalies, largely compensates the anomaly by transport above 30 hPa, and can be dominant above 15 hPa. Their model produces an ozone phase shift near 13 hPa, and the magnitude 0.3 ppmv in both upper and lower branch, which appears to be a low estimate.

Tian et al. (2006) used their CCM with internally generated QBO to produce a realistic QBO signal in ozone. The magnitude of the upper branch QBO signal of about 6% agrees well with their analysis of the SAGE data, while the lower branch of the signal appears slightly underestimated.

The advantage of the MAECHAM4-CHEM model in the version with QBO nudging presented here over previous model studies is that the modelled QBO exactly follows the observed QBO, and hence the modelled QBO in ozone can be compared directly to the observed profile. The good match of the modelled and observed patterns of the signal suggests that, despite the too low amplitude, the relevant processes are represented well in the model.

To distinguish the relative importance of transport and chemical processes for the modelled ozone QBO, it is instructive to separate the ozone gain and loss terms associated with these. The long term averages of these over the course of the QBO experiment are given in Fig. 3.5a in units of molecules per cm^3 and second. While chemical production and loss terms were taken directly from the model, the total transport contribution was obtained by summing up advection and eddy transport terms from a transformed Eulerian mean (TEM) analysis of the 6-hourly model output.

Production is mainly due to photolysis of oxygen (orange line), with a minor contribution from the reactions of HO_2 and CH_3O_2 with NO (magenta). The above mentioned catalytic loss of ozone by nitrogen oxides (violet), for which $NO_2 + O^3P \rightarrow NO_3 + O_2$ is the rate limiting reaction, dominates on the loss side between 20 and 3 hPa. Other significant contributions come from the reactions with chlorine (ClO_x, aqua) and hydrogen oxides (HO_x, light blue) and the recombination $O_3 + O^3P \rightarrow 2\ O_2$(light green).

It is clear from Fig. 3.5a that chemical production and loss terms cancel to a large degree, especially at higher altitudes. Deviations from the climatological monthly mean are given for two opposite phases of the QBO in Fig. 3.5b and c. The vertical zonal wind shear is easterly at 20 hPa in September 1995 and westerly one year later, which corresponds to increased and reduced upwelling in these years due to the SMC. In the region between 7 and 25 hPa we find an anomaly in the NO_x loss rates, which amounts to about 10% at 13 hPa. It can be explained by the model's

NO_2 anomalies, which are in phase with the upwelling of the QBO and amount to about 1 ppbv or 10% at 10 hPa, in agreement with Randel and Wu (1998).

In the region of maximum easterly (westerly) shear, at 17 hPa, there is also a decrease (increase) in the loss rates via the HO_x and O + O_3 reactions, which can be related to the lower (higher) local ozone concentrations in September 1995 (1996). Interestingly, the higher losses in the westerly shear are cancelled to some extent by increased photolytic production between 5 and 15 hPa, but this adjustment is smaller in the easterly shear.

Fig. 3.6a shows the respective contributions of chemistry and transport to the ozone budget at the Equator, now in ppmv/d, which is the more instructive unit to study transport. In the long term mean, transport, due to the tropical upwelling, causes loss in the lower stratosphere that is mostly balanced by chemical production. Above the ozone maximum, this relation is reversed, as the ozone vertical gradient is. There is also a significant contribution from eddy transport at higher levels, as suggested by Bruhwiler and Hamilton (1999). The chemical and transport terms do however not cancel entirely. Apparently, diffusion plays a role as well, and acts to transport ozone away from the level of maximum mixing ratio.

The sum of the chemical QBO anomalies (Fig. 3.6b and c) is lower than the advective one below the 13 hPa level. As noted above, there is considerable positive chemical net production (loss) at 10 hPa in the easterly (westerly) phase in September 1995 (1996), while the advective anomaly is zero, for there is no ozone gradient at this level. Still, diffusion will act to lower this anomaly and distribute it to the neighboring levels. For this reason, the total anomaly zeroes below the 12 hPa level, at about 15 hPa.

Consequently, the ozone trend anomaly, that is, the difference between the following October and the September, minus the climatological mean of that difference, which produces the QBO anomalies in the mixing ratios, is reversed at 15 hPa. At the levels above 10 hPa, transport and chemistry contributions should be in phase. But in the chosen example, the wind shear is reduced at these levels and the QBO is in the easterly (westerly) state at 5 hPa. As can be seen in Fig. 3.4, the ozone anomaly is zero there.

This section shows that both chemistry and transport anomalies are important for the formation of the QBO anomalies in ozone at the Equator. Both are primarily due to the anomalies of upwelling that are part of the QBO's secondary circulation. The direct effect by advection of ozone is combined with an indirect one caused by the advection of nitrogen oxides to form the characteristic pattern of anomalies. Both are approximately in phase above 15 hPa. However, both observations and model results suggest that the phase shift at 15 hPa is by slightly more than 180°. One should keep in mind that ozone chemistry takes about 1 month at this altitude range to reach its steady state. That will cause the chemical contribution to the signal to be lagged, as it is observed in both model and satellite record.

We also like to stress that while the ozone production anomaly is small compared to the single production and loss terms, it is still much larger than the observed

rate of change in ozone in the middle stratosphere, as is the advective contribution. Hence the ozone anomaly is the residual of large contributions and quite sensitive to the circulation.

In the model, diffusion is making a considerable contribution to create the anomaly. As noted before, it is likely overestimated in the model. It will act to dampen the anomalies and explain the too low amplitude of the ozone QBO in the model. Also, an increased vertical resolution should benefit the simulation of the signal, as the advective and the chemical contributions change greatly with altitude.

3.4 Net effect of the QBO on the circulation

In this section net effects of the QBO are analyzed in zonal wind, temperature and mass stream function. Climatologies are computed for the three quantities based on the long term simulations , which average over the effects of several QBO east and west phases. As explained above, two year periods after the eruptions of El Chichon and Mt. Pinatubo are spared from the analysis to avoid false detection due to the volcano impacts. Furthermore, the year 1999 is spared from the analysis to obtain an integer number of QBO cycles, six in this case. For comparison, the magnitude of the respective QBO variations in the model will be shown, computed using the method of Baldwin and Gray (2005).

First, we analyze the QBO's net effect in zonal wind. It is shown in Fig. 3.7a. On average, winds are more westerly in the QBO experiment than in the non-QBO experiment both in the lower stratosphere around 50 hPa and in the upper stratosphere around 5 hPa. This is mostly because the non-QBO simulation produces easterly winds in the tropics. But in the QBO simulation the asymmetry in the strength and the duration of easterly and westerly phases as in the Singapore radiosonde record is reproduced, and thus the 20-year climatological annual mean zonal wind in the tropical stratosphere of this experiment is different from zero. The easterly QBO jet is strong in the middle stratosphere between 10 and 40 hPa so that in the long term mean, winds are more easterly than in the non-QBO experiment at the Equator. Winds are also more easterly in the uppermost stratosphere at around 1 hPa. This is due to the interaction of the QBO and the SAO, which is also reflected in a secondary maximum of the QBO amplitude in Fig. 3.7b and the different strengths of the SAO in Fig. 3.1a and b. Different absorption of tropical waves in the different wind conditions of the two model experiments is the main explanation for this effect. In summary, we have a four layer structure for the QBO's net effect on zonal wind which extends from 20°S to 20°N in the tropical stratosphere. There is no significant net effect on the annual mean zonal wind in the extratropics.

Figure 3.8 shows the net effect of the QBO on zonal mean zonal wind during boreal winter, spring, summer and fall. It is found that in the QBO experiment, especially during the solstitial seasons, but also during the following equinoctials, the winds are more westerly in the low latitudes of the summer hemisphere, in a wide range between 70 and 2 hPa. This illustrates that mainly the weakening

of the summer hemisphere easterlies causes the net westerly effect in the annual mean. The net easterly effect at 1 hPa occurs only in the equinoctial seasons, in the westerly phase of the SAO, which is more pronounced in the nonQBO experiment. Slight changes of the winter time westerly jets is noted, but the differences are not significant at the 95% level in Students t-test because of the high year-to-year variability. In northern fall, winds are a bit more westerly on both hemispheres.

Circulation differences resulting from the QBO can be illustrated effectively by discussing differences in the stream function. However, a detailed discussion of the effects is not essential for understanding of the processes involved. Hence we present the net effects of the QBO on the annual and seasonal means of stream function in Appendix 1, and just summarize briefly the derived differences from the inclusion of the QBO on transport:

- Reduced upward transport in the tropical stratosphere below 60 hPa and between 10 and 3 hPa
- Increased upward transport in the tropical middle stratosphere between 60 and 10 hPa and in the upper stratosphere above 3 hPa
- Increased poleward transport from the tropics around 10 hPa, especially in winter and, with reduced reach, fall on each hemisphere
- Reduced poleward transport around 60 hPa, especially in winter
- Reduced poleward transport at around 4 hPa

The effects of these differences in circulation on temperature and ozone shall be discussed in the following.

The temperature QBO signal (Fig. 3.9b) is a direct consequence of the modulation of the Brewer-Dobson circulation. Due to the positive gradient of potential temperature with height, increased upwelling leads to cooling and decreased upwelling or subsidence produces warm anomalies. This direct connection between vertical motion and temperature also holds in the long term annual mean difference between the two experiments, as Fig. 3.9a illustrates. The pattern of four warm and cold regions in the equatorial stratosphere corresponds well to the four-layer structure in the stream function. In the subtropics, the signal is reversed, as the vertical motion anomaly of the SMC is, but it is much weaker than in the tropics. The strongest changes occur in the tropical lower stratosphere, which is warmer by about 2 K in the QBO experiment, and the tropical upper stratosphere, which is colder by 1.5 K. We also note a weak cooling of the southern polar lower stratosphere, although the QBO variation of temperature is very small in this region. On the other hand, the QBO signal in the northern polar stratosphere does not produce a net effect in the annual mean.

A more detailed picture of the QBO's net effect on temperatures is obtained from the seasonal analysis in Fig. 3.10a-d. The equatorial signal is similar for all seasons, except for the upper stratospheric cooling, which mostly occurs during

the equinoctial seasons, a consequence of the more easterly wind shear due to the modified SAO. Theses cold anomalies are accompanied by warm anomalies in the autumn hemisphere, which appear to propagate downward until winter, when they contribute to the relatively strong subtropical warming between 15 and 70 hPa on the winter hemisphere. Generally, the subtropical signals are stronger on the winter hemisphere, as the QBO variation itself is (see, e.g., Gray, 2000).

Interestingly, temperatures are colder by about 2 K during fall at northern polar latitudes in the QBO model. At southern polar latitudes, the relative cooling is limited to spring (100-10 hPa) and summer (below 60 hPa), the pattern is apparently emerging from the polar vortex and propagating downwards. These polar anomalies can not be understood directly from our analysis of the mass stream function. The cold fall temperatures in northern fall are consistent with the slightly stronger westerlies there. This supports an earlier formation of the northern vortex, which may be aided by the weaker summer easterlies. Quite likely, the difference also relates to changes in the propagation of Rossby waves (Holton and Tan, 1980; O'Sullivan and Salby, 1990; Baldwin and Gray, 2005; Calvo et al., 2007). E.g., Holton and Tan (1980) found that QBO westerly conditions in the lower stratosphere is associated with weaker wave one activity in early winter and a stronger vortex. On the other hand, the net effects in temperature can also be caused by net effects in radiatively active trace gases, which themselves originate from the change in circulation. These are the the subject of the next section.

3.5 Net effects of the QBO on ozone

In this section we apply the same analysis of QBO net effects on the ozone volume mixing ratios. Analogous effects on methane, NO_x and water vapor are given in the appendix. In short, the QBO model run has increased methane and N_2O concentrations above about 10 hPa resulting from the differences in the circulation. NO_x concentrations are increased by 10-15% in the upper stratosphere, and water vapor is increased in the lower stratosphere due to increased tropopause temperature and higher up due to the increased methane.

One might expect that the strong increase in NO_x in the upper stratosphere especially at the Equator seriously impacts the modelled ozone concentrations, as the loss via the NO_x cycle makes a major contribution to the ozone budget given in Fig. 3.5a. But there is no evidence for this in the QBO's net effect on ozone in our model in Fig. 3.12a.

Fig. 3.11a compares the relative contributions to the ozone budget in the model runs with and without QBO. There is indeed a considerable net effect in the NO_x contribution to ozone loss, it amounts to about 10% and is thus of a magnitude comparable to that of the QBO variation. It occurs at a higher altitude though, and is partly balanced by reduced losses by ClO_x and O_3 + O, and the net total loss is almost completely balanced by increased production.

Consequently, the advective contribution to the ozone budget outweighs the total

chemical loss above 3 hPa, as can be seen in Fig. 3.11b, despite the relatively short lifetime of ozone at these levels. Only between 3 and 15 hPa we find the net effect on the total chemical budget to be larger than that on total transport. Below 15 hPa, the higher upwelling in the QBO model leads to a transport loss that is partially balanced by increased total chemical production, in agreement with the findings on the total budget in Fig. 3.6a.

As for the mean profile, diffusion will act to balance the remaining anomalies. Nonetheless, positive (negative) net anomalies in the total change rates of ozone coincide with net increased (reduced) mixing ratio in Fig. 3.12a at 12 and 50 hPa (5 and 30 hPa).

Fig. 3.12b shows the QBO amplitude in ozone, which has a minimum at the Equator at the location of the phase reversal seen in Fig. 3.4. The QBO signal at mid-latitudes caused by the SMC (e.g., Randel et al., 1998) is also reproduced, as well as an impact on Arctic ozone mixing ratios (e.g., O'Sullivan and Salby, 1990).

However, in the annual mean, there is no net effect of the QBO on lower- and mid- stratospheric ozone at mid-latitudes. Instead, there is a net decrease of about 3% in the experiment with the QBO at around 5 hPa at mid-latitudes and a slight net decrease in the southern vortex area.

Figure 3.13 shows the seasonal variation in the QBO's net effect on ozone. In the tropical upper stratosphere, above 3 hPa, an increase is only noted during the equinoctial seasons, when the temperature is significantly colder in the QBO model. At mid-latitudes, higher ozone volume mixing ratios are found during winter and spring in the lower stratosphere and the lower mixing ratios in the upper stratosphere are particularly pronounced during summer and fall. These patterns resemble those found for the temperature net effect, and hence suggest that the net effects on ozone are linked to the net effects on the vertical transport.

To confirm the net effect on mid-latitude ozone, a second pair of experiments that run from 2000-2019 and only differ in the representation of the QBO was evaluated. Both experiments follow the specifications of the REF2 experiments of the CCMVal activity (Eyring et al., 2006), except for the QBO, which is included in one of the simulations only. Trace gas concentrations for these experiments are based on the IPCC A1B scenario, SSTs prescribed from a simulation of the UK Met Office HadGEM1 atmosphere-ocean GCM also assuming the A1B scenario. Halogen concentrations are based on the B2 scenario in the UNEP/WMO assessment of ozone depletion (WMO, 2003). The QBO is repeated from the past, chosen such that the phase agrees with observations at the beginning in January 2000. A detailed description of this procedure is given on the CCMVal website (`http://www.pa.op.dlr.de/CCMVal/Forcings/qbo_data_ccmval/u_profile_195301-200412.html`).

The net effects on zonal wind, temperature and trace gases for these experiments (not shown) agree qualitatively with the findings for the experiments 1980-1999, but those for ozone do not. Fig. 3.14 does not show the difference in mid-latitude upper stratospheric ozone volume mixing ratios found for the experiments for 1980-1999. This result is at first surprising. It suggests that the net effect of the QBO on ozone

depends on the different forcings in the future and past experiments. Specifically, the increase in CFCs during 1980-1999, which causes an increase of ClO_x levels in the stratosphere and thereby affects the modelled ozone concentrations in both QBO- and nonQBO experiments, levels off during 2000-2019. In contrast, the greenhouse gas emission trend is similar in both time periods, and any climatic differences due to the increased greenhouse gas levels or the different SST boundary conditions in the past and future experiments could cause differences in the net QBO effect on ozone primarily via a difference in the net effect on the circulation, which is not found in the simulations.

Hence it seems that while the net effect on mid-latitude upper stratospheric ozone is absent at constant chlorine concentrations, there is a net effect due to the positive chlorine trend in 1980-1999. The model with a QBO appears to adjust faster to the increasing CFCs, which causes the lower ozone concentrations in the 20 year mean of 1980-1999. Besides differences in the transport and chemistry of the CFCs, the effects of the volcanic eruptions of El Chichon and Mt. Pinatubo may play a role in causing this different adjustment in the two simulations, so the effect can not be attributed to the QBO alone based on our results.

3.6 Conclusions

In summary, we have found a realistic representation of the QBO and its immediate effects in a CCM. The QBO in ozone results from the QBO's secondary circulation in the meridional plane, with contributions from variations in (a) ozone transport with the mean flow and (b) transport of nitrogen oxides that cause ozone depletion. The combination of these two effects causes the characteristic phase shift of the ozone QBO at 13 hPa. Compared to HALOE satellite observations, the signal is slightly underestimated in the model, which is certainly related to the relatively low vertical resolution of the model in the given configuration.

Furthermore, in the long term, we found significant annual and seasonal net effects of introducing the QBO into the model on the circulation and trace gases by comparing a pair of otherwise identical CCMs. Most of the differences at mid- and low-latitudes are related to the QBO's secondary meridional circulation. E.g., reduced upwelling in the lower tropical stratosphere leads to increased temperatures at and above the tropical tropopause.

The net effects on tropical temperatures and ozone mixing ratios generally correspond to the net effects in upwelling. In the case of ozone, the net chemical production also differs for the two cases and partially cancels the transport effect in the lower stratosphere. In the upper tropical stratosphere, the QBO modulates the strength of the SAO, which, in combination with the higher upwelling, leads to net colder temperatures and higher NO_x, especially in the equinoctial seasons. The higher losses via the NO_2 cycle are however largely balanced by increased photolysis rates. The transport contribution prevails over the chemical change rate below 15 and between 1 and 3 hPa.

At mid-latitudes, we find lower ozone volume mixing ratios for the period 1980-99 between 10 and 3 hPa when the QBO is included in the model. A time series analysis (not shown) reveals a faster decrease of volume mixing ratios in the QBO simulation compared to the free running one. This indicates that the adjustment to the changes in the forcing, specifically the increasing CFC concentrations during 1980-99, differs among the models with and without QBO representation. However, it has to be kept in mind that some of the perturbations caused by the eruptions of El Chichon and Mt. Pinatubo only present in the model run with QBO, like the increased water vapor (see Appendix), may have consequences relevant to ozone beyond the two year period following the eruptions that is omitted in this work. Similarly, the 11-year solar variability present in the QBO experiment affects ozone concentrations in this region and complicates the identification of the QBO net effect. For a future study, it would be desirable to evaluate a pair of experiments with equal, constant boundary conditions except for the QBO and another pair with a linear trend in CFCs to clear this point.

There are also significant net effects at polar latitudes in our experiments. The slight increase noted in the strength of the southern vortex when the QBO is incorporated may be due to dynamic effects related to the propagation of waves (Holton and Tan, 1982; Kinnersley and Tung, 1999). Planetary waves are barred from the tropical stratosphere during the easterly phase (e.g., Shuckburgh et al., 2001), leading to a slightly weaker BDC (Haynes et al., 1991) and a stronger, more isolated vortex. The differences in ozone and other trace gas concentrations among the two model runs can however also influence vortex dynamics. The northern vortex is slightly stronger in fall, likely for similar reasons, but not in winter and spring. Again, one could think of a further pair of experiments with no coupling of chemistry to assess the respective roles of direct and indirect effects of the changed dynamics at polar latitudes.

In this work however, we focused on the period 1980-99, for which extensive observations were available to determine to what extent the nudged QBO model produces realistic results and to elaborate the net effect of the QBO for this period.

We wish to state clearly that details of the presented net effects may be specific to the model system used here, because of its specific limitations as discussed in Eyring et al. (2006).

Nonetheless, the overall net effects determined in this study demonstrate that the QBO affects the stratospheric circulation in multiple ways and in regions beyond those where QBO variations can be detected. There are considerable impacts on the trace gas concentrations which will feed back on the circulation via radiative heating. Accurate modelling of the stratosphere therefore requires an accurate representation of the QBO.

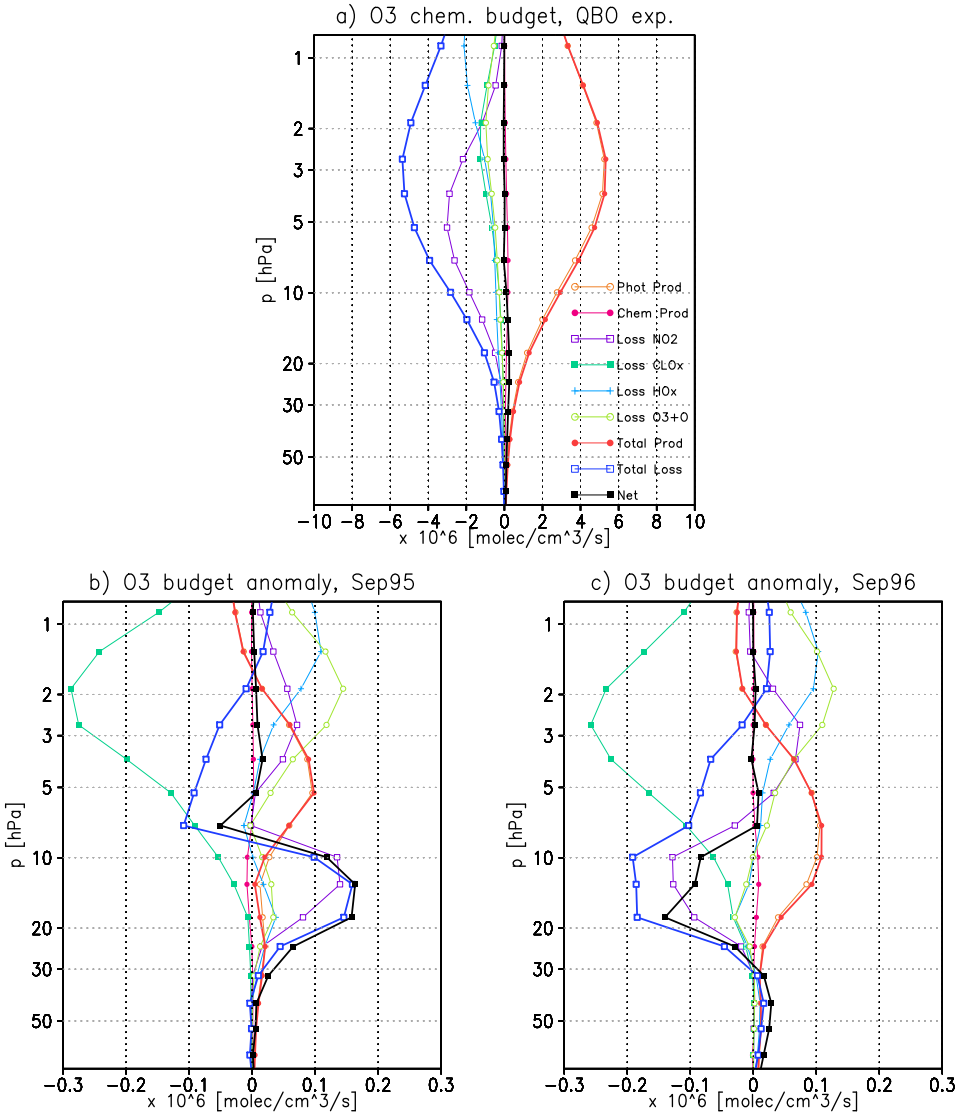

Figure 3.5— Contributions to ozone chemical production and loss in the MAECHAM4-CHEM model run with nudged QBO [10^6 molec/cm^3/s]. **(a)** 20-year mean contributions to chemical production and loss. Net chemical production and net advective gain are also shown. **(b)** Deviation from the 20-year climatological monthly mean in September 1995, when winds are easterly at 10 hPa (easterly shear at 20 hPa). **(c)** Deviation from the 20-year climatological monthly mean in September 1996, when winds are westerly at 10 hPa (westerly shear at 20 hPa).

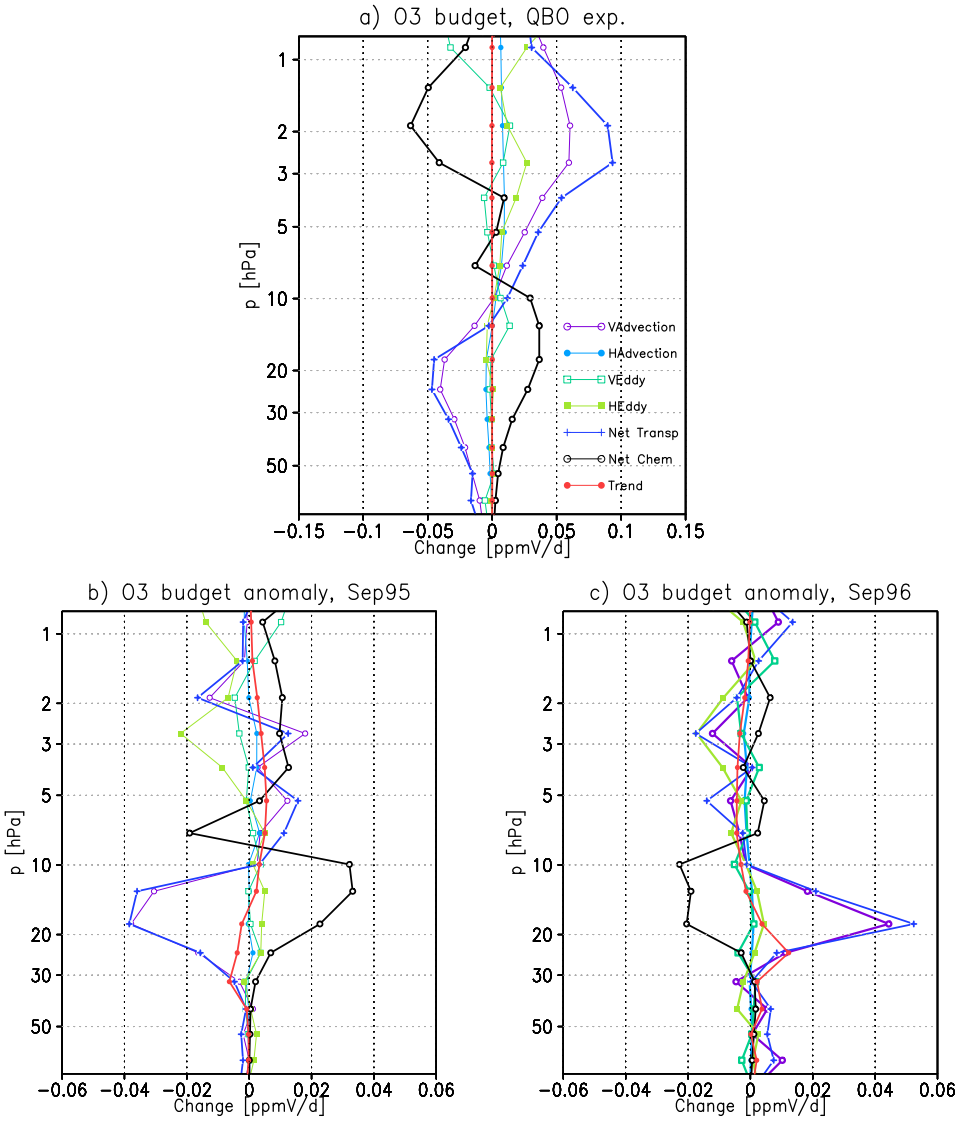

Figure 3.6— Contributions transport and chemistry to the total ozone budget and trend in the nudged MAECHAM4-CHEM model run [ppmv/d]. **(a)** 20-year mean. **(b)** Deviation from the 20-year climatological monthly mean in September 1995, when winds are easterly at 5 hPa (easterly shear at 20 hPa). **(c)** Deviation from the 20-year climatological monthly mean in September 1996, when winds are westerly at 5 hPa (westerly shear at 20 hPa).

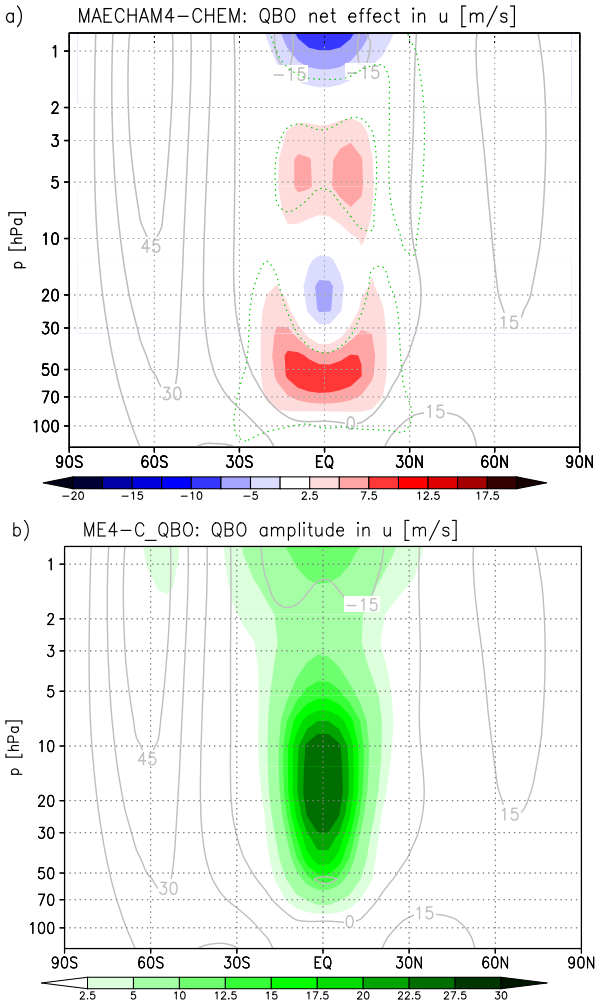

Figure 3.7— (a) Shades give the net effect of the QBO on zonal mean zonal wind [m/s], obtained by subtracting the climatological annual and zonal mean in the nonQBO experiment from the one in the QBO experiment. The solid grey contours show the annual climatological mean zonal wind in the nonQBO experiment. Dotted green contours surround the areas where the net effect is significant on the 95% confidence level. (b) QBO amplitude in the zonal wind [m/s] in the QBO experiment, zonal mean. Solid grey contours show the climatological annual mean zonal wind in the QBO experiment.

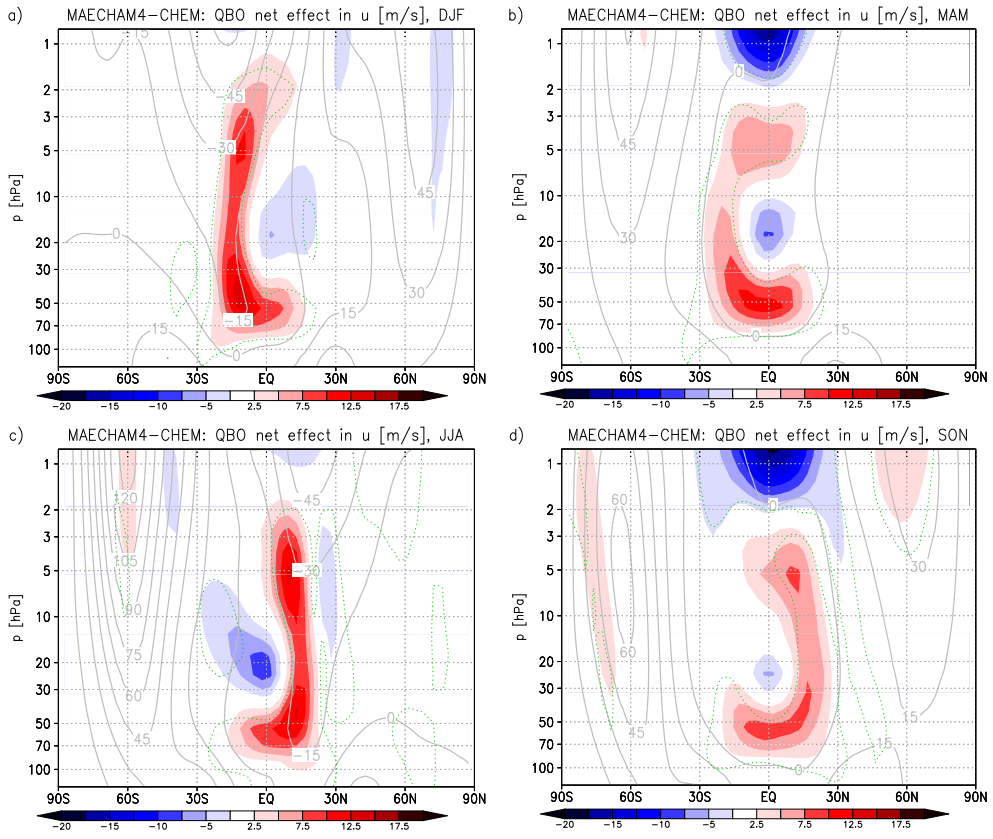

Figure 3.8— As Fig. 3.7a, but for seasons: (a) DJF; (b) MAM; (c) JJA; (d) SON.

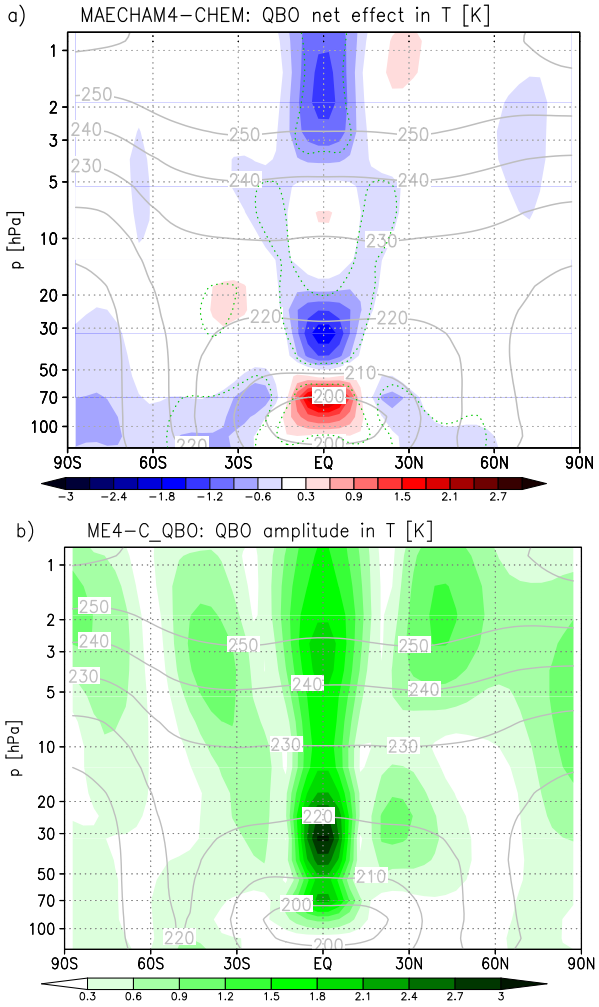

Figure 3.9— (a) Shades give the net effect of the QBO on temperature [K], obtained by subtracting the climatological annual and zonal mean in the nonQBO experiment from the one in the QBO experiment. The solid grey contours show the climatological annual mean temperature in the nonQBO experiment. Dotted green contours delimit the areas where the net effect is significant on the 95% confidence level. (b) QBO amplitude in temperature [K] in the QBO experiment, zonal mean. Solid grey contours show the climatological annual and zonal mean temperature in this experiment.

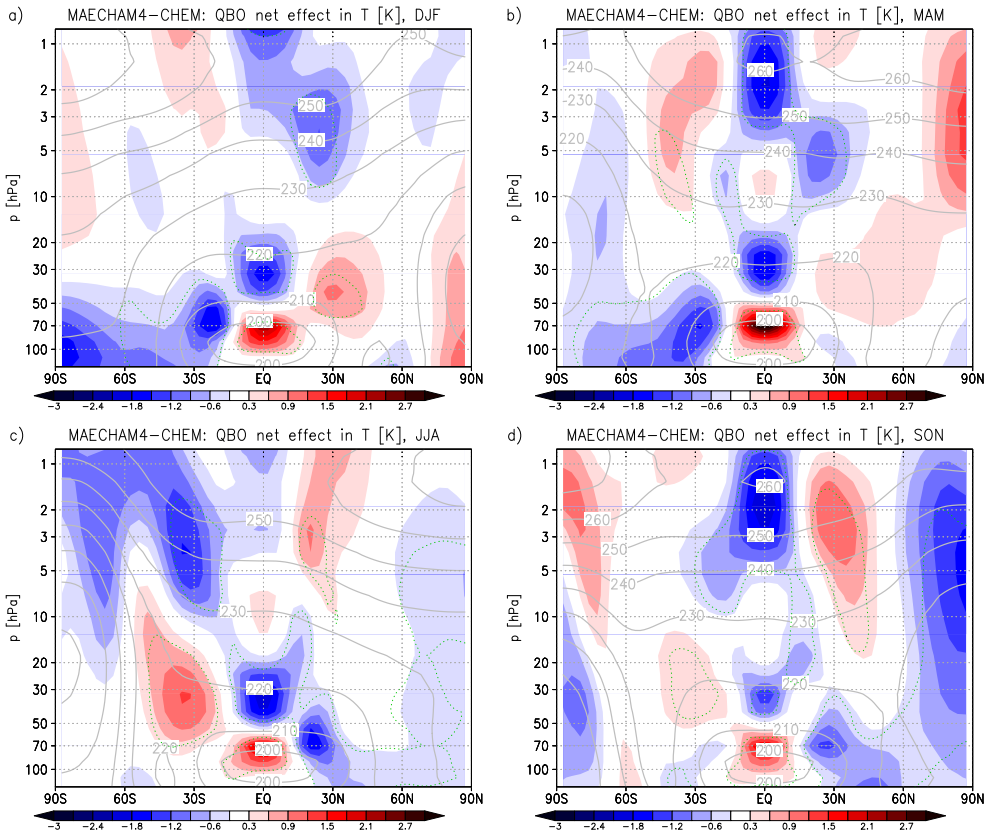

Figure 3.10— As Fig. 3.9a, but for seasons: **(a)** DJF; **(b)** MAM; **(c)** JJA; **(d)** SON.

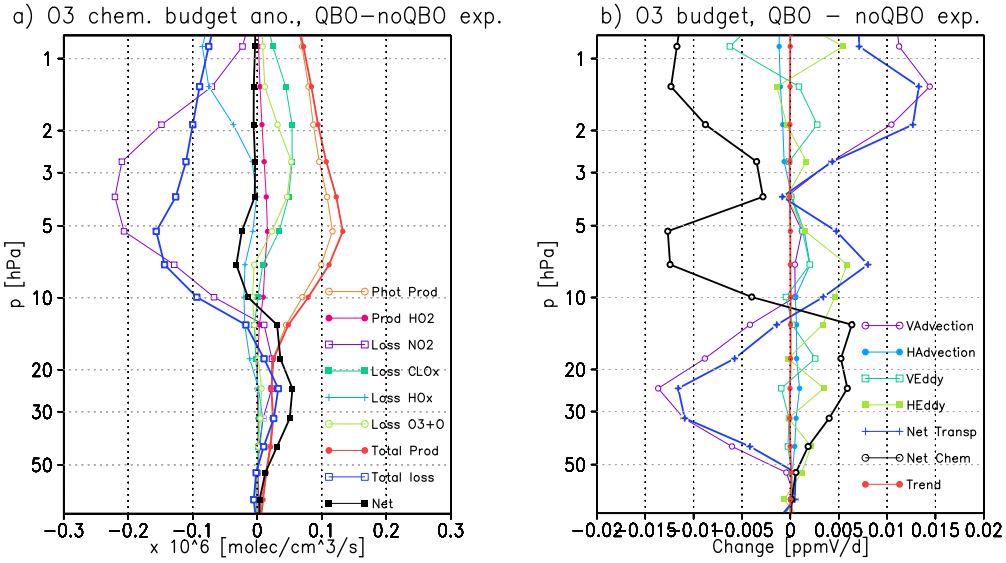

Figure 3.11— **(a)** Net difference in the 20-year mean contributions to ozone chemical production and loss between the MAECHAM4-CHEM model runs with and without nudged QBO at the Equator, zonal mean [10^6 molec/cm^3/s]. **(b)** Net difference in the contributions of transport and chemistry to the total ozone budget and in the ozone trend for the QBO and nonQBO experiments, equatorial zonal mean.

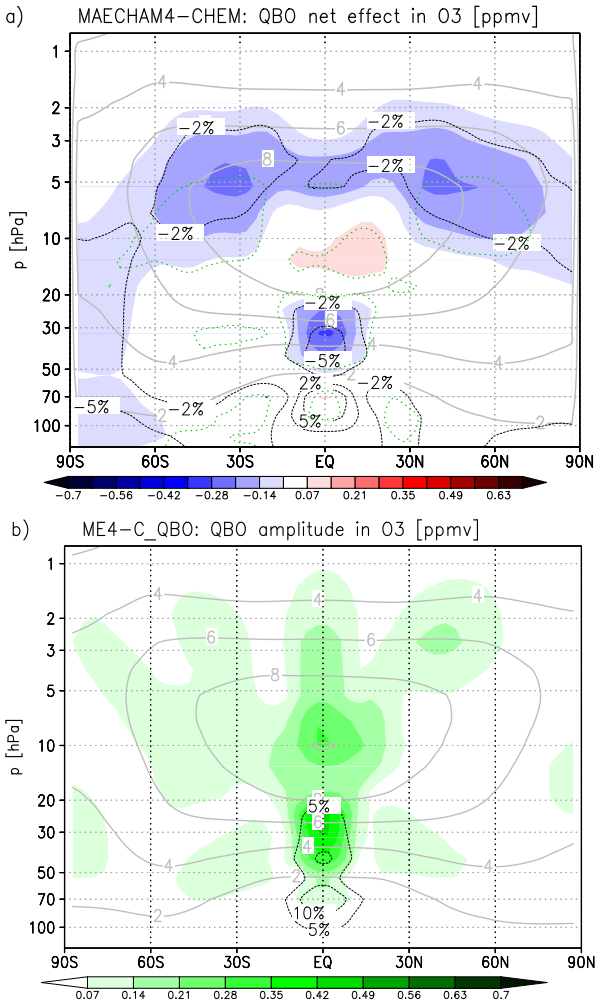

Figure 3.12— (a) Shades give the net effect of the QBO on ozone, obtained by subtracting the climatological annual and zonal mean volume mixing ratio [ppmv] in the nonQBO experiment from the one in the QBO experiment. Solid grey contours show the climatological annual mean mixing ratio in the nonQBO experiment, and solid black contours the relative difference between the two experiments in percent. Dotted green contours delimit the areas where the net effect is significant on the 95% confidence level. (b) QBO amplitude in the mole fraction of ozone [ppmv] for the QBO experiment, zonal mean. Solid grey contours show the climatological annual mean of the mole fraction in this experiment.

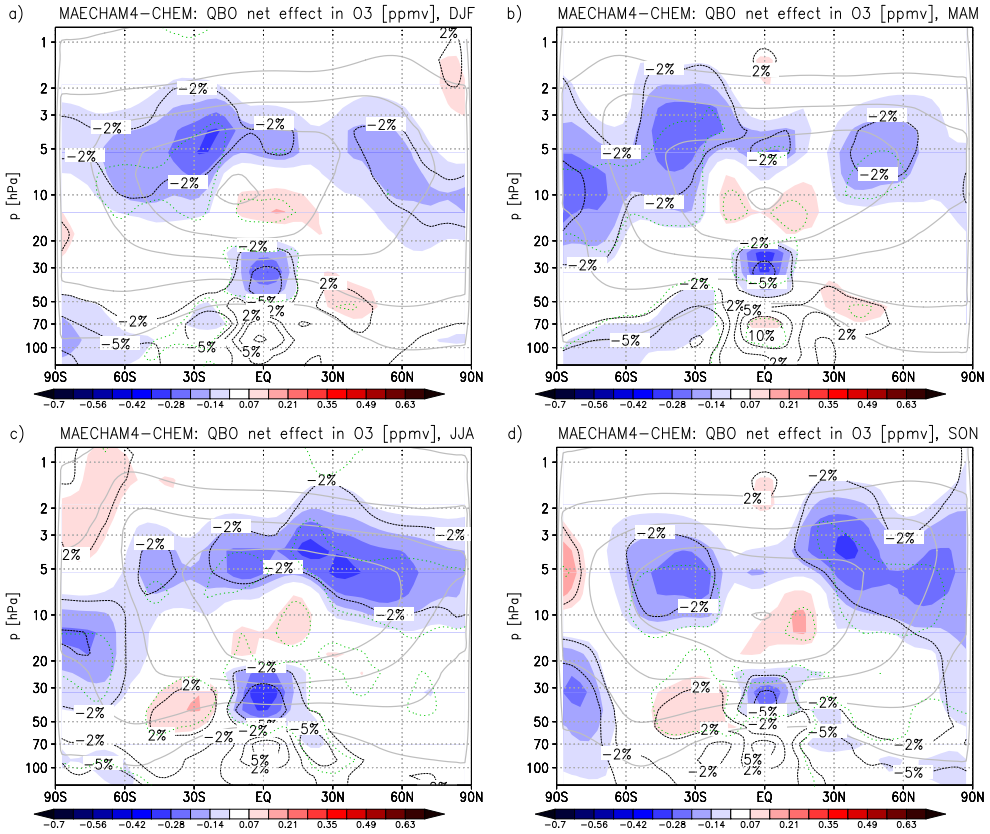

Figure 3.13— As Fig. 3.12a, but for seasons: (a) DJF; (b) MAM; (c) JJA; (d) SON.

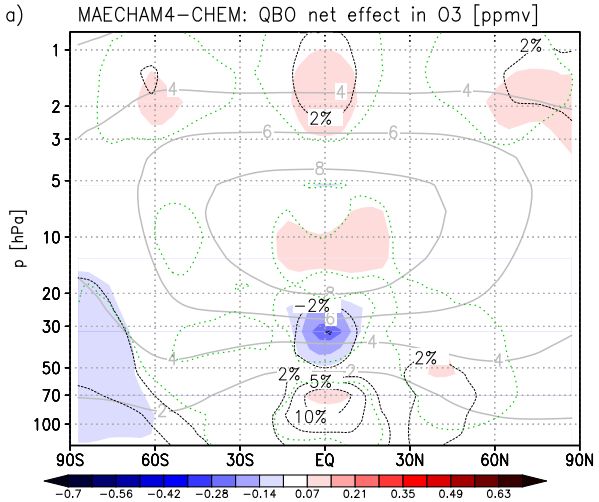

Figure 3.14— As Fig.3.12a, but for a second pair of experiments running from 2000-2019.

Chapter 4

Effects of the quasi-biennial oscillation on low-latitude transport in the stratosphere as derived from model driven trajectory calculations

4.1 Introduction

The properties of stratospheric air, such as its temperature and composition, are largely determined by the large scale circulation of the stratosphere commonly referred to as Brewer-Dobson circulation (BDC). Young air that has recently crossed the tropopause undergoes upwelling in the tropical pipe (Plumb and Bell, 1982) moves poleward, and descends to eventually re-enter the troposphere. While this simple conception explains many aspects of the real atmosphere, such as the tape recorder signal in water vapor (Mote et al., 1996) or the approximate distribution of long-lived tracers, the real situation is more complicated in a number of ways.

Firstly, the strength and direction of the circulation varies with time. It is stronger in the winter hemisphere than in the summer hemisphere due to the larger Equator-Pole temperature gradient in the troposphere that leads to higher wave activity which drives the BDC (Haynes et al., 1991). The higher level of the wave forcing in the northern hemisphere causes seasonal variations of the tropical upwelling. Furthermore, especially in the tropics and subtropics, the BDC is modulated by the secondary meridional circulation (SMC) of the quasi-biennial oscillation (QBO) (Plumb and Bell, 1982; Baldwin et al., 2001; Ribera et al., 2004), which is illustrated in Fig. 1.2. The easterly (westerly) shear phase of the QBO coincides with enhanced (reduced) upwelling and hence cold (warm) temperature anomalies at the Equator (Reed, 1964; Angell and Korshover, 1964). This configuration goes along with horizontal divergence and convergence in the QBO easterly and westerly

phases and vertical flow anomalies in the subtropics compensating for the equatorial ones. Niwano et al. (2003) showed the effect of the QBO on vertical transport as derived from HALOE satellite observations of water vapor and methane.

Secondly, especially in mid-latitudes, air is also dispersed by large scale planetary waves that cause horizontal transport and thereby act to weaken latitudinal gradients and promote the homogenization of air. This effect is most prominent in the mid-latitudes of the winter hemisphere, the so called surf zone (e.g., McIntyre and Palmer, 1984; Plumb, 2002). There have been multiple approaches to study the variability of horizontal transport. For example, strong potential vorticity (PV) gradients indicate transport barriers, as in the absence of friction and vertical gradients of the heating rate, PV is a conserved quantity. Based on a trajectory model study, Gray (2000) argued that the characteristics of the subtropical edge of the surf zone depended on the QBO phase. Neu et al. (2003) derived the variation of the actual position of the edge from HALOE methane mixing ratios and found that it is mostly due to the annual cycle and the QBO variation is small, in agreement with Waugh (1996) and Chen (1996). Chen (1996) and O'Sullivan and Chen (1996) also found a strong effect of the QBO on planetary wave breaking in winter. While these waves are blocked and dissipate at the Equator during the easterly phase of the QBO, they propagate across the Equator to dissipate at the summer hemisphere easterlies during the westerly phase of the QBO.

Thirdly, mixing by small scale processes also changes the composition of air masses, especially when there is strong wind shear, as, e.g., vertically, between the easterly and westerly jets of the QBO. The effects of this mixing are particularly pronounced in the presence of large gradients in the properties of neighboring air masses, as, e.g., horizontally, at the tropical-subtropical edge. Using the concept of "effective diffusivity", Haynes and Shuckburgh (2000) and Shuckburgh et al. (2001) found propagation of planetary waves to the low latitudes of the summer hemisphere during the westerly phase of the QBO but not during the easterly phase. A more recent study by Garny et al. (2007) found a QBO signal in Lyaponuv exponents calculated from NCEP/NCAR reanalysis winds and indicates that mixing at low latitudes is enhanced in summer during the westerly phase compared to the easterly phase.

Furthermore, concentrations of radiatively active trace gases such as ozone or water vapor, varying either directly due to transport or due to chemical reactions taking place at varying rates, also affect the circulation via their radiative impact. Similarly, aerosol distributions vary with time and have a radiative feedback.

In this work, we use a modelling framework to illustrate the impacts of the first two listed effects, i.e. the variation of the BDC and the horizontal exchange at the topical-subtropical edge, on transport, with a focus on the role of the QBO. To this purpose, a novel modelling approach is chosen. Model experiments carried out with the Eulerian chemistry-climate model MAECHAM4-CHEM (ME4C) (Manzini et al., 2003; Steil et al., 2003) describe the dynamics of the stratosphere including the QBO, taking into account feedbacks due to chemistry.

This model alone offers limited capabilities to assess transport effects. Therefore, the output of the ME4C model is used to drive the Chemical Lagrangian Model of the Stratosphere (CLaMS) (McKenna et al., 2002) to study pathways of air masses for different phase combinations of the quasi-biennial and annual cycles. In this work, only the trajectory module of this model is used.

With this setup, it is possible to assess exactly how the instantaneous equatorial circulation anomalies associated with the QBO transform to transport anomalies in the tropical region. It is also suited to test the understanding of properties of barriers to horizontal transport suggested by the dynamics and observed trace gas gradients, analyzed e.g. by Shuckburgh et al. (2001) in a purely Eulerian framework. The Lagrangian view taken with the calculation of trajectories allows for a more process-based understanding of the transport effects and provides a link from diagnosed circulation anomalies to the resulting anomalies in trace gas distributions. Our general approach is similar to that of Gray (2000), but with a strong focus on the two questions mentioned above, and is based on calculations carried out over a longer time period in order to better separate the effects of QBO and annual cycle and underline their significance.

In the following section, the model framework used will be explained in detail. The third section focuses on the impact of the QBO on vertical transport, while the fourth assesses the impact on horizontal transport. Conclusions are discussed in section 4.5.

4.2 Model Setup

4.2.1 Chemistry-climate Model Simulations

For the Eulerian calculations, the chemistry climate model MAECHAM4-CHEM (Manzini et al., 2003; Steil et al., 2003) is used. It consists of the middle atmosphere general circulation model MAECHAM4 (Manzini et al., 1997), which is based on ECHAM4 climate model (Manzini and McFarlane, 1998; Roeckner et al., 1996) and the interactively coupled chemistry model CHEM (Steil et al., 1998). Simulations are carried out in the version with spectral truncation T30, associated with a Gaussian grid with a spacing of 3.75° and 39 vertical layers, of which the uppermost is centered at 0.01 hPa.

The two model experiments used in this work, running from 1980-1999, also described in Punge and Giorgetta (2008), differ chiefly in the representation of the QBO. In both experiments, sea surface temperatures from the HadISST1 data set (Rayner et al., 2003) and greenhouse gas and halogen emissions as in the WMO/UNEP assessment 2002 (WMO, 2003) are used as lower boundary conditions.

The first experiment ("nonQBO") is free-running and does not produce an intrinsic QBO at the given vertical resolution. The second experiment ("QBO") is in contrast forced to have a QBO equivalent to observations using the nudging tech-

nique: Winds in the tropical stratosphere are relaxed linearly towards the observed wind record from the Singapore radiosondes, which are launched close to the equatorial maximum of the QBO. The applied forcing is zonally uniform with a Gaussian profile around the Equator with a full width of half maximum ranging from 20° at 70 hPa to 30° at 10 hPa. Observations from seven altitude levels between 70 and 10 hPa are used until 1986, when measurements on 14 levels between 90 and 10 hPa became available. Above 10 hPa, the vertical propagation of the QBO jets is continued at a constant rate, but with decreasing strength. The nudging applied here neglects hemispheric asymmetry of the QBO in zonal wind. Zonal asymmetries are also assumed to be negligible.

Furthermore, in the nudged experiment, solar activity is parameterized using radiation flux data of Lean et al. (1997) and the aerosol forcing caused by volcanic eruptions is included by prescribing precalculated net heating rates Kirchner et al. (1999) and the surface area densities of Jackman et al. (1996) for the chemistry module. These two observational forcings were not included in the simulation without QBO nudging. The forcings are additional sources of interannual variability in the QBO run, mainly by introducing effects of the 11-year solar cycle and the eruptions of El Chichon in April 1982 and Mt. Pinatubo in June 1991.

In this study, the impact of the 11-year solar cycle (e.g., Tourpali et al., 2003) can be neglected, as most considerations here are on shorter time scales and the effect is small in the considered altitude range anyway. The volcanic eruptions do however impact transport due to the heating effects caused by aerosols (e.g., Trepte and Hitchman, 1992; McCormick et al., 1995). Consequently, a significant slowdown of the BDC is observed in the "QBO" model run after the eruption, and for this reason, the post-eruption periods are not suitable for the elaboration of QBO effects.

The nudged experiment has previously been evaluated within the CCMVal activity (Eyring et al., 2006) on the validation of chemistry-climate model and a slightly different experiment was used by Steinbrecht et al. (2006) to compare with observed total ozone values.

For using the CCM output within the CLaMS setup, some processing is required. Zonal and meridional wind components, temperatures and net heating rates are extracted and interpolated from the hybrid pressure-height coordinate σ of the ME4C model to the vertical coordinate ζ of the CLaMS model, which is a hybrid of pressure p in the troposphere and potential temperature θ in the stratosphere (Konopka et al., 2007). At the levels considered here, $\zeta = \theta$ and $\sigma = p$.

We use potential vorticity (PV), computed on isentropic levels, to illustrate the difference between the two model runs. PV is zero at the Equator, and increases (decreases) towards the North (South) pole. Its meridional gradient is not uniform though, and, as noted before, strong gradients indicate transport barriers, while weak gradients indicate a well-mixed region. Following Nash et al. (1996), the singular points of the second derivative of PV along equivalent latitudes can be used to define a latitudinal barrier.

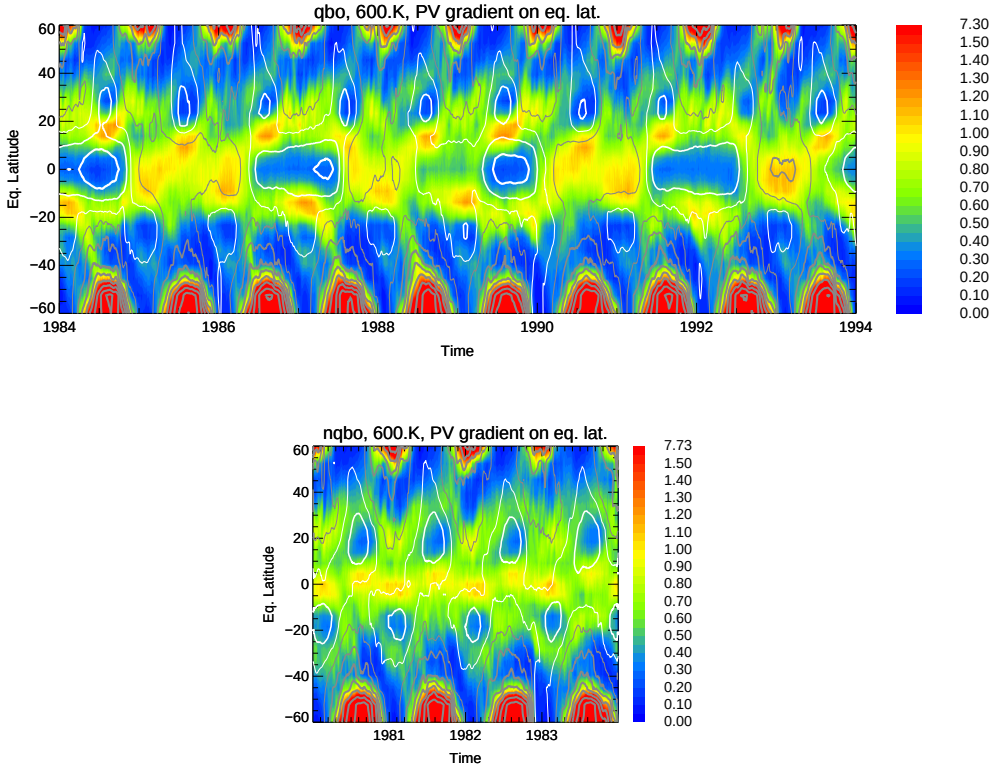

Figure 4.1— Shades show the horizontal gradient of potential vorticity, as analyzed at the 600K (≈ 32 hPa) potential temperature level: **(a)** QBO experiment **(b)** nonQBO experiment. Gray contours denote westerly zonal wind at [5, 15, 25, 35, 45, 55, 65] m/s, while white contours show easterlies with the same spacing.

Fig. 4.1a shows the daily zonally averaged PV gradient at the 600 K (≈ 32hPa) over several years in the run including the QBO, Fig. 4.1b in the run neglecting the QBO. In both cases, the increased PV gradient at the winter vortex edge on both hemispheres can clearly be discerned. At lower latitudes, in the nonQBO run, PV gradients are strongest around the Equator, with a tendency towards the summer hemisphere, suggesting a transport barrier there. There is a region of notable PV gradient at around 20°N (15°S) during northern (southern) winter that migrates towards 35°N (30°S) during spring and summer to form the edge between the relatively well-mixed regions of subtropical summer easterlies and summer high latitudes.

At mid-latitudes, there is considerable variability in PV, especially during fall, and the winter time surf zone appears to develop thoroughly only by mid-winter. The variability of the winter PV field is a consequence of the exchange of air masses from the near tropics and the mid-latitudes. The large scale eddies generated by the

planetary waves, which are strong on the winter hemisphere (especially the northern), cause transport on a time scale of several days and leave an imprint on PV gradients, even though equivalent latitude is used in Figure 4.1. Corresponding variability is also seen in the (10-day averaged) zonal wind field. The planetary waves from the winter hemisphere appear to reach up to the edge of the subtropical easterlies in the summer hemisphere, where they are damped and a barrier is established (Haynes and Shuckburgh, 2000).

Interestingly, the situation in the QBO run is similar to the nonQBO case during the westerly phases, just the subtropical PV gradients are smaller. The westerly winds allow the planetary waves to propagate through the equatorial region, but are damped where winds become more easterly slightly north of the Equator, causing a barrier as above Shuckburgh et al. (2001).

When there are easterlies though, there is no PV gradient in the tropics between 10°S and 10°N. This can be understood by considering the latitudinal part of the meridional circulation (Fig. 1.2). During the easterlies, equatorial, low PV air is moving polewards. There is a strong PV gradient at the summer edge of the easterly QBO jet, and again a weak PV gradient in the region of summer easterlies. The apparent barrier in the summer subtropics can however hardly be generated by planetary waves from the winter hemisphere, as they are blocked in the strong easterly jet. An explanation for this barrier is not found easily.

The example shows that it is difficult to reach conclusions for transport from the analysis of PV fields alone. The trajectory calculations allow to analyze latitudinal transport in detail and to deduce the integrated effect over a longer time period. This will be done in section 4, with a focus on the barrier diagnosed at the summer edge of the easterly QBO jet.

4.2.2 Trajectory calculations

Because of the modular structure of CLaMS, the trajectory module of CLaMS can be used for stand-alone calculations. It uses a fourth-order Runge-Kutta algorithm to infer the motion of air parcels from winds and heating rates (McKenna et al., 2002). Trajectories are started on a regular 1° x 1° grid between 80°S and 80°N, omitting the polar regions. The total number of trajectories on each level is 360 × 160 = 57,600. The time step for the trajectories is 30 minutes.

Four isentropic levels (500, 600, 675, and 870 K, corresponding to about 50, 32, 20, and 9 hPa) were selected to compute backward trajectories over 90 days. At low latitudes the impact of mixing over such a time span is assumed to be small enough for the trajectory distribution to give a reasonable representation of the origin of the air that is found at these levels. Starting dates were chosen at four dates at the end of January, April, July and October over several years in order to represent the seasonal differences and the interannual variations in both the QBO and nonQBO experiments.

The combined modelling approach chosen here has several advantages compared

to using operational analysis or reanalysis to drive the CLaMS model. The isentropic ascent rates can be taken from the model calculation directly rather than being inferred from often noisy analyzed vertical wind.

While MAECHAM4-CHEM has no QBO in the free-running setup, an accurate and consistent representation of the QBO and its effects can be obtained by the nudging of equatorial stratospheric winds (Giorgetta and Bengtsson, 1999) as applied in this work. This allows for a comparison of transport in largely similar model simulations with and without QBO representation.

The full CLaMS model can be used for extensive Lagrangian studies of the stratosphere (e.g., Konopka et al., 2007; Khosrawi et al., 2005), and the modelling approach presented here offers the possibility of further, more detailed analyses based on Eulerian calculations.

4.3 QBO effect on vertical transport

To analyze how transport within the tropics is affected by the QBO, the backward trajectories of parcels starting at the 870 K level, corresponding to 9 hPa, in the tropics between 12° S and 12° N are considered, hence of $24 \times 360 = 8640$ parcels. In the QBO model run, for a given start date, years with pronounced easterly wind, westerly shear, westerly wind or easterly shear phase of the QBO at that level were selected. A case from the CCM simulation with no QBO is given for comparison.

We start out presenting the results for trajectories run during an equinoctial season, when the circulation is expected to be approximately symmetric about the Equator. Fig. 4.2 shows the distribution of trajectories starting on the 28th of April. The location of the air parcels in the meridional plane is depicted in 15 day intervals after binning them to a $1\,\mathrm{K} \times 1^\circ$ grid. The resulting density distribution is smoothed by a simple filter and cut off at 0.1 for a smoother display.

Over the course of 90 days, the air is ascending by 150 to 250 K, depending on the QBO phase. The overall ascent is weakest for the trajectories started in the westerly shear phase (WS, Fig. 4.2d) but strongest in the easterly phase (E, Fig. 4.2c). From the secondary meridional circulation (SMC, see Fig. 1.2), one would have expected the strongest ascent during easterly shear. But the circulation pattern of the SMC depicts only the motion at one instant, while for transport of air parcels, their history needs to be considered. Air parcels, while following the general upwelling in the tropical pipe, subsequently enter the downward propagating QBO shear zones and jets, in which the circulation may differ considerably, as will be discussed in more detail below.

The shape of the distribution also differs distinctly among the cases. It is evident from the shear cases in Fig. 4.2b and Fig. 4.2d that the modulation of upwelling by the SMC is strongest at the Equator and has an approximately Gaussian profile, as the QBO itself. Over the course of 90 days, these meridional differences apparently level off by horizontal dispersion, and the mean potential temperature is approximately the same in the entire equatorial region. We also note that the initial

dispersion of the parcels upon their release is stronger in the shear phases than in the easterly and westerly wind phases. This suggests that the conditions are more favorable for mixing of air masses in these phases.

Furthermore, while the parcels mostly originate from within 15°S to 15°N in the easterly case, they stem from the 25°S to 25°N range in the westerly case and the westerly shear case. This is the effect of the equator-ward motion associated with the westerly phase (Fig. 1.2).

The Brewer-Dobson circulation (BDC) is hemispherically asymmetric during the solstitial seasons, which affects also transport at tropical latitudes. Fig. 4.3 shows the same distributions of air parcels as Fig. 4.2 but for release of parcels on July 28 and for different years but with similar QBO phases as above. It is evident from the Figure that air masses ascending in the equatorial region during this time of the year are influenced by the seasonal circulation anomaly. Most of the parcels originate from the northern subtropics, which is due to the extension of the southern cell of the BDC to the northern hemisphere during boreal summer. Only for the parcels that come from the tropics, the upwelling is different between easterly and westerly shear cases, as for the equinox case. Also note that the parcel distribution is spread out on the extratropical winter hemisphere especially in the westerly case and the easterly shear case, which is likely due to perturbations caused by planetary waves propagating from higher latitudes. When the tropical wind is easterly, these waves can not propagate and are blocked from the tropics. Also, slightly more parcels stem from the 10°N-30°N range in the westerly phase, which is again interpreted as the effect of the SMC. However, planetary waves from the winter hemisphere may also cause dispersion of the trajectory groups in this region (Chen, 1996; Shuckburgh et al., 2001).

While the selected cases presented in Figs. 4.2 and 4.3 give a clear impression of the QBO under solstice and equinox conditions, it is also useful to investigate the variability of the ascent due to the combination of seasonal and QBO cycle over a longer time period. To that end, the course of backward trajectories that arrive at three selected levels within +/− 2° off the Equator was analyzed in three month intervals over a period of ten years covering various phase states of the QBO, and for the experiment with no QBO. At each date, $360 \times 4 = 1440$ parcels start in this region. Fig. 4.4a shows the ascent of parcel ensembles driven by the QBO simulation and Fig. 4.4b the corresponding ascent in the simulation with no QBO. Trajectories are started at 500, 675, and 870 K on the 28th of April, July, October and January from 1984 till 1994 in the QBO simulation and in the period 1980-1984 in the nonQBO simulation. The median level of the groups of trajectories is given by the solid black line and the area between the 10th and 90th percentiles is colored by season. The curvature and ascent of the lines clearly depend on the QBO phase which can be inferred from the zonal wind shown in the background; gray shading marks westerly wind, while white shades stand for easterlies.

In the case with no QBO, shown in Fig. 4.4b, the annual cycle in the vertical trajectory distributions is clearly seen. It is due to the annual variations in both

upwelling and horizontal transport of air parcels.

Ascent differs by about a factor of two between trajectories started in July and those started in April. However, the ascent variation by the QBO affects only a region close to the Equator. Especially at higher levels, a considerable fraction of parcels is advected to the Equator from outside that corridor over 90 days in the solstitial seasons, as seen in Fig. 4.3, which causes the higher width of the parcel distributions in these seasons.

In Figure 4.4a, the additional variability due to the QBO is seen. The figure shows clearly how parcels ascending in the tropics move through the different descending QBO phases. While the QBO phase difference between 400 and 870 K (70 and 9 hPa) at any instant is about π, the parcel will usually undergo a full QBO cycle within about one year when travelling between these two levels, due to the change in the QBO phase during the travel.

Assuming a parcel stays within the tropics, its cross-isentropic vertical motion will be determined by the local heating rates, which vary with the QBO, and the ascent of a parcel is the integral of the heating rates experienced. When parcels start in the easterly phase at 870 K, as in April 1991 (also see Fig. 4.2c), they have ascended from an easterly shear phase (ES) before and experienced strong ascent there. At the same time, the parcels started in the ES phase, as in April 1993 (also see Fig. 4.2b), although their ascent was the strongest for the first 15 days of the calculation, have come from a westerly jet, where ascent was slower, which explains why the total ascent over 90 days was higher in the easterly case than in the ES case in Fig. 4.2. For the westerly (W, Fig. 4.2e) and westerly shear (WS, Fig. 4.2d) phases, the ascent rate was lower, and so was the QBO phase difference between the start and the end of the trajectories. Thus the effect of the integration over 90 days is lower, explaining that the WS phase case has the lowest total ascent over the 90 day period.

Due to the change of the circulation with time, cases with no ascent over 90 days are rarely found, despite the occurrence of weakly negative heating rates during the westerly shear phase. One exception is found in the parcels released at 675 K in July 1992, which may however be affected by the anomalous heating rates caused by the anomalous aerosol load after the eruption of Mt. Pinatubo (McCormick et al., 1995). Often the westerly shear and associated weak ascent lasts for a short period only. E.g., for the trajectories started at 675 K in a westerly shear in July 1987, a few parcels actually descend during the first month; still the median is ascending.

In general, we expect that not only the phase states of QBO and annual cycle influence the distributions, but also the variable phase propagation, of the QBO—a constant phase sustained oven imprint on transport than a phase that passes quickly.

Nonetheless, a relation between QBO phase and upward transport was found. In Fig. 4.5, the total ascent over 90 days to the 675 K level is displayed as a function of the QBO phase. The radii of black and colored circles give the annual and seasonal means of the ascent, respectively. The QBO phase was derived from the zonal wind u and the vertical shear of zonal wind, $u_z = \frac{du}{dz}$ (also see Huesmann and Hitchman,

2004). The relation of these two quantities, when normalized to their respective variances σ_u and σ_{u_z}, define the phase state ϕ of the QBO:

$$\phi = \arctan \frac{u\sigma_{u_z}}{u_z\sigma_u} \tag{4.1}$$

In other words, in a plane spanned by u (on the ordinate) and u_z (on the abscissa), ϕ is the angle spanned by the positive abscissa and the point (u_z,u) at any given time. E.g., at the beginning of a westerly phase, u_z is positive but decreasing, and by the time u becomes maximum positive, approaches 0, hence $\phi \longrightarrow \pi/2$ and (u_z,u) is located on the positive ordinate. At the time when wind shear becomes easterly, u_z is negative and ϕ enters the second quadrant, and so on.

The phase was computed at the start of the trajectories at the approximated level of release, in this case 675 K. In the Figure, symbols mark the median and bars show the 10th and 90th percentiles, and colors again distinguish seasons. Clearly, the trajectories of parcels that are released in a westerly shear phase have lower total ascent than the seasonal average, and those released in an easterly shear show above-average ascent. The phase of maximum ascent is shifted towards the easterly phase, as discussed above. While this is true for all four seasons, no significant seasonal dependence of this phase shift is found, more cases would be required to analyze this.

4.4 QBO effect on horizontal transport

The analysis of PV gradients at the 600 K level in section 4.2 suggested a transport barrier at the summer tropical-subtropical edge during the easterly phase of the QBO only. In this section, we elaborate on this finding by studying a methane profile in the CCM simulation with a representation of the QBO and the motion of trajectories based on this run.

In the stratosphere, methane is a well-suited trace gas for transport studies. It has sources only below the tropopause, a long stratospheric lifetime, but also has a sink in the stratosphere. Upon its ascent in the tropical pipe from the tropical tropopause region it is oxidized gradually, increasingly in the upper stratosphere. Therefore, methane concentrations in the extra-tropics are determined by the descent from above and by isentropic transport from the tropics. Hence there are gradients of the volume mixing ratio in both the horizontal and vertical directions, and variations in vertical and horizontal transport are reflected in methane concentrations. The effects of the QBO on methane are discussed by Randel et al. (1998); Dunkerton (2001) and Patra et al. (2003).

Fig. 4.6a shows the zonally averaged latitudinal profile of the methane volume mixing ratio at 600 K ($\approx$ 32 hPa) in July for easterly and westerly QBO phases. The blue and orange line are the profiles in the westerly phase of 1990 and the easterly phase of 1989, respectively. The thick can line is the July average of the years 1985, 1990, 1995, 1997, and 1999, in which the QBO is in a pronounced westerly phase and

the thick red line is the July average of the years 1984, 1989, 1994, 1996, and 1998 with a pronounced easterly QBO phase. The July concentrations averaged from five years are higher than the 1989 and 1990 examples due to the positive methane trend in the stratosphere.

It is evident that in the years with easterly wind the equatorial volume mixing ratio is higher than in the years with westerly wind, due to the integral upwelling modulation caused by the SMC, which was described in the previous section, in combination with the vertical gradient of methane. This result is in agreement with the findings of Randel et al. (2004b).

On the winter hemisphere, the methane profiles look similar in all years. There is a sharp decrease in the subtropics, a rather weak gradient in the mid-latitudes between 25°S and 45°S, and a stronger decrease at the antarctic polar vortex edge. This is in agreement with the conception of a well-mixed surf zone at mid-latitudes (McIntyre and Palmer, 1984) and transport barriers at the vortex edge (Nash et al., 1996) and in the subtropics (Gray, 2000), see also Plumb (2002).

As expected, there is a considerable difference between easterly and westerly years in the summer hemisphere subtropics, compare the can and red lines in Fig. 4.6 between 15 and 40°N. Volume mixing ratios are higher here in the westerly cases. This seems to be in contrast to the concept of the SMC, which would predict increased poleward transport during the easterly phase but relative equator-ward flow during the westerly phase, thus higher methane in the easterly phase. However, variation of the strength of the transport barrier with QBO phase offers an explanation for this finding.

Fig. 4.6b shows the absolute latitudinal gradients of the concentrations given in Fig. 4.6a. It confirms that there is a large difference between easterly and westerly years in the summer subtropics at about 15-20°N. The large gradient in easterly years is consistent with the proposed subtropical transport barrier in summer, whereas in westerly years, transport from the tropics into this region appears to be enhanced, causing the higher subtropical methane concentrations, and a significantly weaker gradient reaches its maximum beyond 30°N.

Figure 4.6b also shows that the CH_4 gradient at the winter tropical-subtropical edge is higher in the easterly cases. This is in part due to the vertical transport effect of the SMC induced by the QBO discussed above that causes higher tropical concentrations and lower subtropical concentrations in easterly years. This also affects the gradients on the summer hemisphere, but does not explain the strong difference in the northern hemisphere profile found in Fig. 4.6b. O'Sullivan and Chen (1996) found a similar effect of the QBO on the summer hemisphere for their artificial tracer using an Eulerian transport scheme in a middle atmosphere GCM. Also note that at the Equator, between 10°S and 10°N, the gradients are indeed lower in the easterly than in the westerly phase, which is consistent with the SMC.

Parcel trajectories can be used in various ways to study transport barriers (e.g., Bowman, 1996). The approach chosen here is to analyze whether the backward trajectories started at a given latitude remain at this latitude during the considered

period, that is, whether the air originates from a latitude close to its final latitude or not. If parcels do not move much latitudinally between the start and the end of their trajectories, this indicates a transport barrier, but if they do, it indicates that there is transport in the latitudinal direction.

Fig. 4.7 shows the time air parcels released in northern hemisphere summer at a given horizontal position have remained within a 10° channel around their original latitude during three months of backward trajectory calculations. In both the easterly (1989, Fig. 4.7a) and westerly (1990, Fig. 4.7b) years, air is rapidly removed from its starting latitude in the surf zone on the southern hemisphere and in the antarctic vortex. If the vortex was circular, our trajectory diagnostic could identify the transport barrier at its edge. But as it is not, each parcel is shifted latitudinally within a few days of its rapid circumpolar motion.

An alternative diagnostic was tested, in which the total time spent in the range of the starting latitude was analyzed. In this case, the vortex is clearly identified, as parcels that reenter the starting latitude channel after being deflected by the vortex asymmetry are taken into account. This diagnostic is however less suitable at lower latitudes, where large scale mixing, being a counter-indicator of transport barriers, can have the same effect. Moreover, in the tropics the circulation does not show pronounced zonal variations in the altitude range considered, and hence no zonally variable location of the barrier is expected, in contrast to the vortex.

On the northern hemisphere, the eddy motion of the summer circulation is evidently much slower than in the southern hemisphere and there are occasionally air masses that remained for some time at their original latitude.

The situation in the tropics and—especially northern—subtropics, the effect of the QBO is seen clearly. In the westerly year (Fig. 4.7b), although the situation is rather inhomogeneous, some air stays at its original latitude for a month or more during the three months under consideration between 20°S and 30°N, but only within some filaments on a smaller scale than in the northern extra-tropics.

In the easterly year, however, most of the air parcels retain their location between 10°N and 30°N for the entire period. It is clear that hardly any latitudinal transport takes place under such conditions. Between 20°S and 10°N though, much fewer air parcels reside around their start location.

Analysis of the vertical motion of the air parcels (not shown) tells that, in the easterly situation, air has ascended strongly in both the tropics and northern subtropics in July 1996, but ascent has been weaker in a narrow strip at around 20°N. At the same time, an analysis of stream function (given in Punge and Giorgetta (2008), their Fig. A1g) shows that the subtropical air is influenced by the southern winter circulation cell, which, as seen in Fig. 4.3, drags air towards the southern hemisphere. A qualitative explanation of the observed stalling of the parcel trajectories would thus be that the opposed influences of seasonal cycle and QBO cancel, creating a region of little latitudinal motion. The northward flow of the SMC dominates in the tropics but is weaker than the southbound flow by the BDC, which leads to convergence and hence subsidence in the barrier region. However, the ab-

sence of net advection does not per se explain the observed barrier, and the different planetary wave forcing in the tropical and extratropical regions during the easterly QBO phase certainly plays a role here.

Apart from the cases presented in Fig. 4.7, it is interesting to investigate the residence times in the different QBO phases over a longer period and also during austral summer. In Fig. 4.8, the zonal mean of residence times computed as in Fig. 4.7 is displayed in form of a bar that extends over the runtime of the trajectories.

In boreal summer (Fig. 4.8a), situations with reduced horizontal motion at about 15-20° N are found in easterly QBO years as in 1984, 1989, 1994, and 1996, but not in the westerly years 1985, 1990, 1993, and 1995. In situations with no pronounced easterly or westerly QBO phase, such as the westerly and easterly shear phases in 1987 and 1988, residence times are longer in the northern subtropics than elsewhere, but clearly shorter than in the easterly years.

The same picture is found in austral summer (Fig. 4.8b). Regions of high residence time are found at 15-20°S for trajectories started in January of 1984, 1987, 1989, 1990, and 1994, when winds are easterly, but are absent in the cases with westerlies as for the trajectories started in January 1986, 1988, 1991, 1993, and 1995. Generally, subtropical residence times are shorter on the southern hemisphere compared to the northern hemisphere, and the QBO-related differences are less pronounced in the southern hemisphere. It appears that the weaker planetary wave forcing on the southern hemisphere compared to the northern one leads to a less pronounced barrier due to the less pronounced wave induced mixing in the surf zone (Plumb, 2002).

4.5 Conclusions

The effect of the QBO on stratospheric transport at low latitudes has been illustrated by means of trajectory calculations based on a general circulation model with representation of the stratospheric circulation and chemistry.

Ensembles of trajectories running backward over three months following the GCM winds and heating rates show a clear modulation of tropical ascent associated with the QBO independent of the season. Upwelling is enhanced when the vertical wind shear caused by the QBO jets at a selected level is easterly but reduced or even turned to subsidence in westerly shear conditions at the Equator, as expected due to the secondary meridional circulation of the QBO (Plumb and Bell, 1982). The effect of this circulation anomaly on transport is pronounced in both easterly and westerly shear phases, but as the QBO jets are descending while the air is ascending, the exposition time of individual air parcels to the different shear phases is limited and the differences in integrated ascent over longer periods are smaller than the differences in instantaneous ascent rates. Nonetheless, the effect of the SMC is clearly seen after three months of integration.

Additionally, the phase of maximum integral ascent over the last three months lags the phase of maximum easterly shear and thus the associated maximum instan-

taneous ascent by several months; the exact amount of this lag however varies with the rate of downward propagation of the QBO. In fact, the impact of the changing QBO phase is stronger in the cases with easterly wind shear or easterly wind, which have a higher total ascent than the westerly wind shear or westerly wind cases. Hence the phase relationship between the QBO phase as diagnosed from wind and wind shear to the ascent variation over 90 days will generally not be a linear one but will vary with the QBO cycle. This should be taken into account in studies that diagnose the effect of the QBO on the distributions of long-lived trace gases as methane (Randel et al., 1998) or N_2O (Schoeberl et al., 2008), or, potentially, SF_6 (Stiller et al., 2008).

The trajectory calculations also show that the effect of the SMC on upwelling is strongest in a narrow region around the Equator, but isentropic exchange leads to a homogenization of the ascent in the equatorial region on a time scale of a few months. During solstitial seasons, the asymmetry of the BDC leads to general flow towards the winter hemisphere and a larger fraction of the air stems from the summer hemisphere. The QBO modulation of equatorial ascent appears to be largely unaffected by season.

Effects of the horizontal part of the SMC are less clearly identified from the trajectory distributions, probably because isentropic transport is less uniform than the vertical transport. As suggested by Ribera et al. (2004), the horizontal circulation anomaly due to the SMC may not always coincide with the phases of the strongest easterly and westerly jets (see Fig. 1.2) that were selected here. Nonetheless, especially in the equinoctial seasons, the width of the latitude range from which most parcels originate varies clearly with the phase of the QBO and is narrowest in the selected Easterly phase, as expected.

In the solstitial seasons, the circulation anomaly towards the winter pole due to the hemispheric asymmetry of the BDC is superimposed to the symmetric horizontal branch of the SMC. This leads to zones with no large scale latitudinal transport in the near subtropics at around 15-20° latitude on the summer hemisphere during the easterly phase. As evident from Fig. 4.7, the trajectories of parcels in this region show almost no latitudinal transport in this situation at all. Following the same reasoning as above, one would expect a similar zone of no large scale latitudinal transport in the winter subtropics during the westerly phase, which is however not evident in Fig. 4.7. It seems likely that the poleward flow of the BDC dominates over the equator-ward flow due to the SMC in this situation. Furthermore, in the absence of an easterly tropical jet, planetary wave-induced isentropic mixing leads to dispersion of air parcels at these latitudes even if net advection is zero. This is supported by the high mixing anomaly in the westerly phase found by Garny et al. (2007).

In the easterly phase on the summer hemisphere, however, a transport barrier develops and this kind of dispersion is absent. As suggested by earlier studies in an Eulerian framework (Haynes and Shuckburgh, 2000; Shuckburgh et al., 2001), the fact that planetary waves can not enter the easterly QBO jets appears to be

the reason for the evolution of that barrier. The barrier separates the tropical domain with easterly winds and little influence of extratropical waves from the extratropics, where these extratropical waves drive isentropic transport in the surf zone (McIntyre and Palmer, 1984). While one would expect the barrier to be stronger in winter and the equinoctial seasons, when the wave forcing and surf zone mixing is stronger, our results suggest that the poleward general circulation hinders the evolution of a stationary subtropical barrier in these cases. In the westerly QBO phase, the separation of the tropical and extratropical domains is weaker and the mean latitudinal flow does not allow for the evolution of a barrier. To support this reasoning on the tropical-subtropical transport barrier, further, more detailed studies would be desirable. In particular, the respective roles of isentropic mixing and horizontal advection deserve further investigation. More advanced statistical evaluation techniques of parcel motion may be valuable tools here. A quantification of the barrier strength from its effects on trace gas distributions observed in the atmosphere is needed to validate the model results presented in this work. Also, its vertical extent needs to be analyzed, which was not done in this study, where trajectories are released only at a few levels.

As a conclusion, we find that trajectory calculations within a setup of a general circulation model proved to be a valuable tool for transport diagnostics. The consistent dynamical fields of the CCM, as opposed to reanalyses or operational analyses in which many different observations are assimilated, are suitable for accurate quantification of the QBOs effect on transport in the stratosphere by means of Lagrangian analysis. When the present setup is extended by including the mixing and chemistry modules of the CLaMS model, this allows to study effects of the QBO on small scale mixing, age of air and trace gas distributions from a Lagrangian point of view.

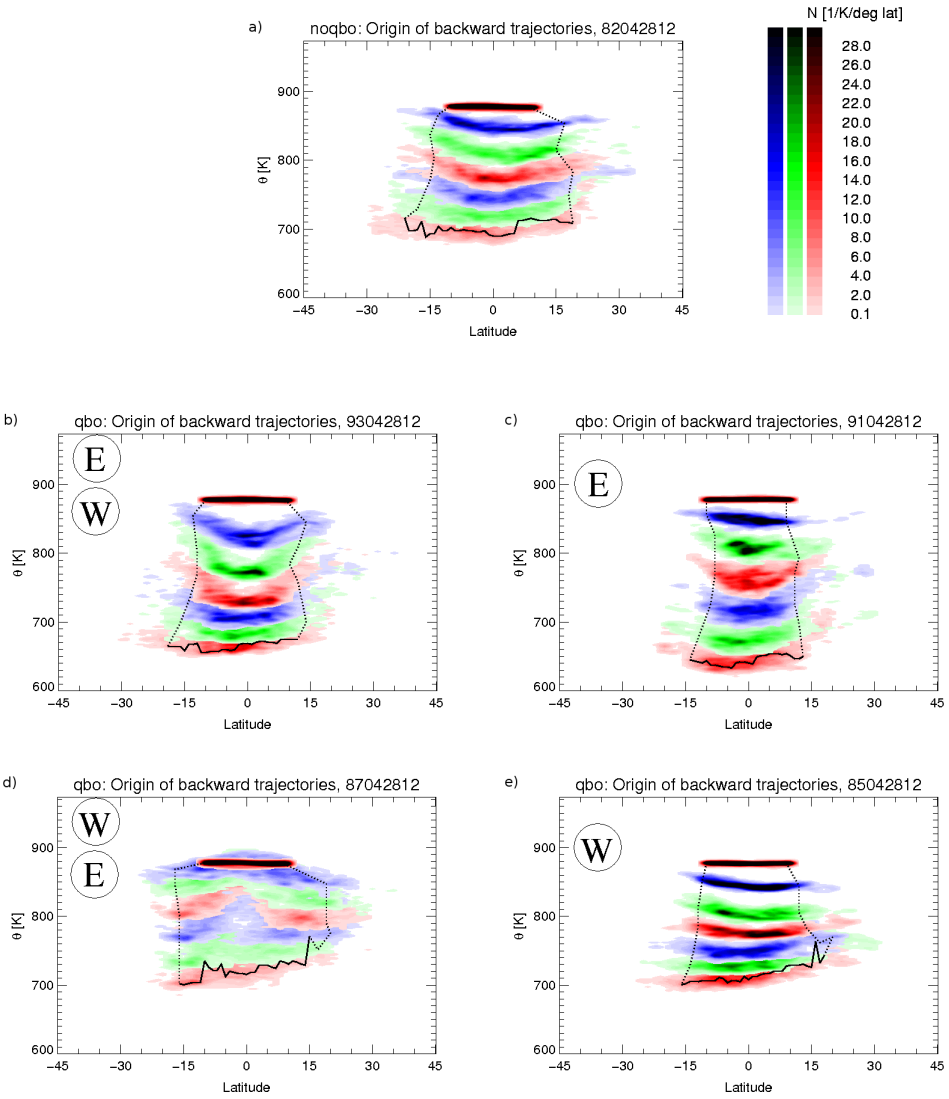

Figure 4.2— Density distribution of backward trajectories starting at 870 K on 28 April, depicted in 15 day intervals in different colors to illustrate the propagation. (**a**) shows trajectories in spring of 1982 in the model that does not have a QBO representation. For the QBO model four years were selected that have a well defined QBO phase at 870 K: (**b**) 1993: easterly wind shear; (**c**) 1991: easterly wind; (**d**) 1987: westerly wind shear; (**e**) 1985: westerly wind. The two dashed lines are chosen such that 3% of the parcels are located north and south of them respectively at each time step; the solid line gives the mean altitude for parcels at day 90 of the calculations.

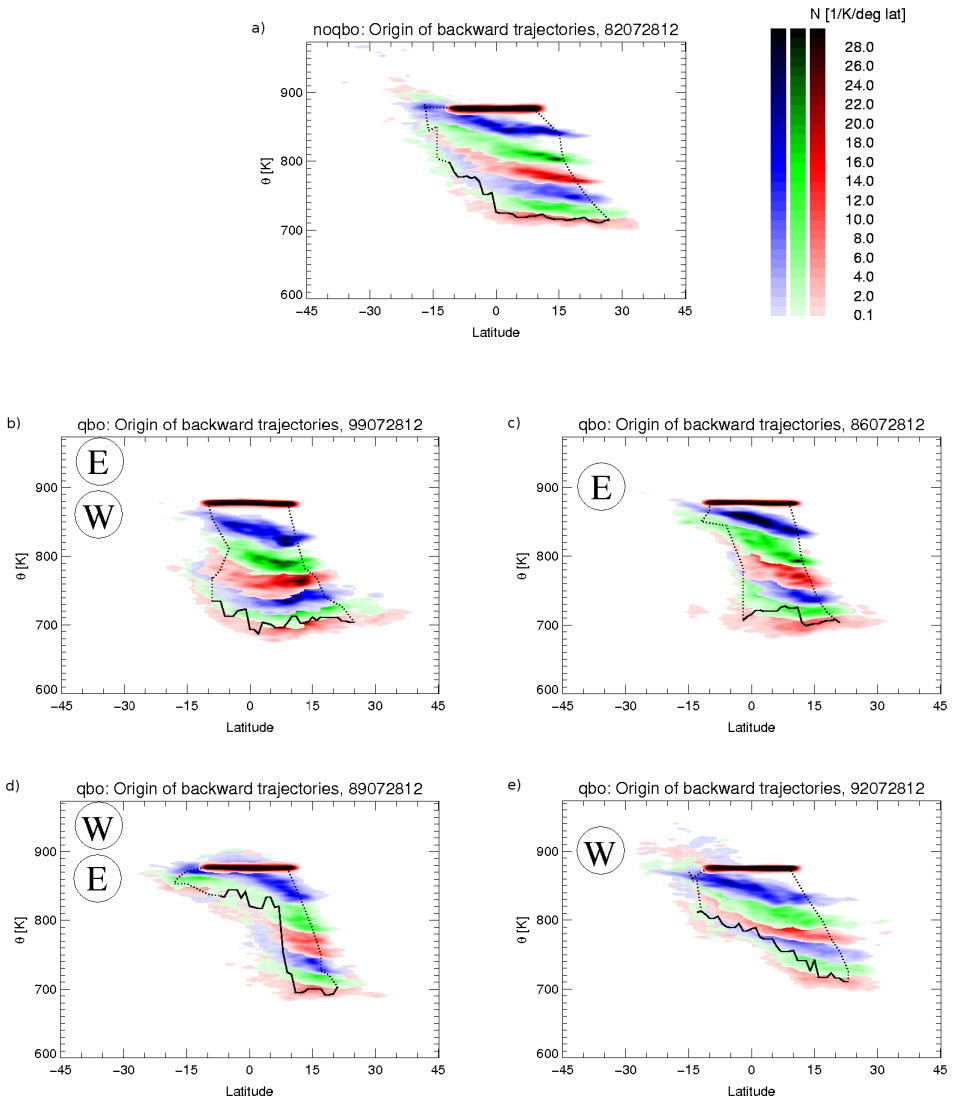

Figure 4.3— As Fig. 4.2, but for trajectory runs started the 28th of July: (**a**) no QBO (1982); (**b**) easterly shear (1999); (**c**) easterly wind (1986); (**d**) westerly shear (1989); (**e**) westerly wind (1992).

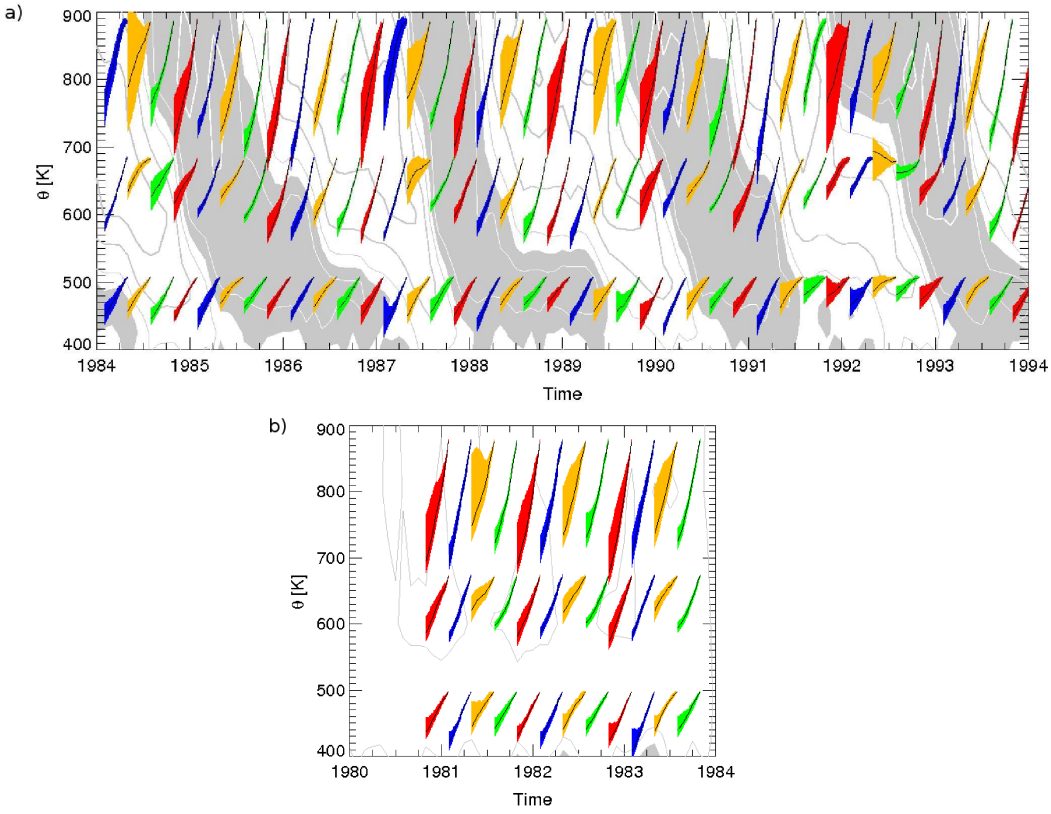

Figure 4.4— (a) Vertical transport of air parcels within [2°S, 2°N] in the QBO model. Stripes represent the course of the backward trajectories started at various dates from the (500, 675 and 890 K) levels. The solid line marks the median vertical positions of the air parcel groups during 90 days before their arrival at the start level, while the 10th and 90th percentiles of the group bound the colored stripes. The colors stand for the starting date: red for 28 January, blue for 28 April, yellow for 28 July and green for 28 October. The zonal wind fields in the background show the descending westerly (gray shading with white contours at [5, 15, 25] m/s) and easterly (white shading with gray contours at [5, 15, 25, 35] m/s) QBO jets. (b) Same as a, but for the experiment with no QBO representation.

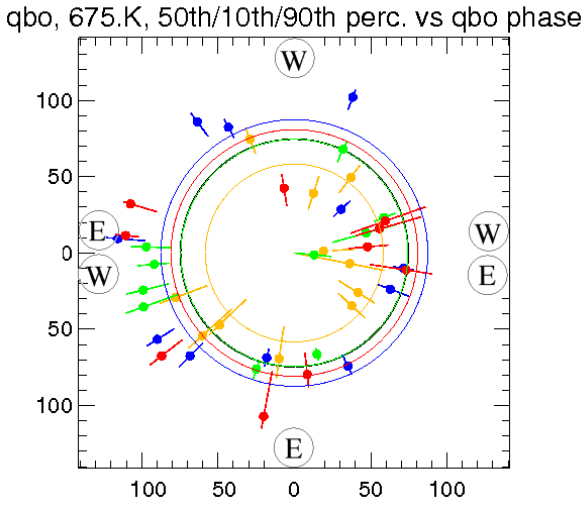

Figure 4.5— Polar plot of ascent vs. QBO phase. The radii of the circles give the mean ascent of the 675 K air parcels as in Fig. 4.4a over the course of 90 days in K. The black one stands for the climatological average of all starts over the 7 years, and colors distinguish between seasons as in Fig. 4.4. Marks with bars stand for the individual trajectory runs and are plotted at the QBO phase at the start of the trajectory calculations. They give the median and 10th/90th percentiles of the vertical distribution at day 90. The QBO phase is rotating counterclockwise and is westerly on the positive ordinate.

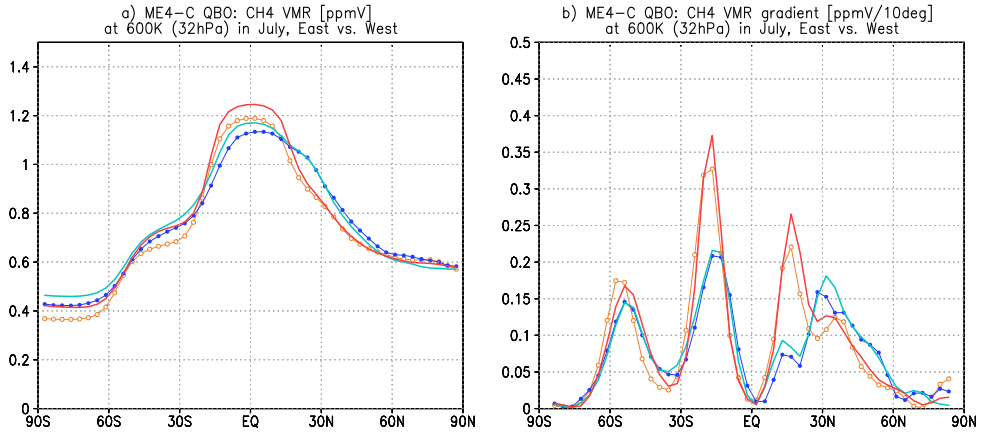

Figure 4.6— (a) Modelled methane concentration at 600 K (32 hPa) during the westerly phase of the QBO in July 1990 (thin blue line) and during the easterly phase of the QBO in July 1989 (thin orange line). The thick red line gives the average of five years when the QBO was easterly in July, the can line of five years with westerly QBO phase in July. (b) Gives the absolute value of the horizontal gradient of the respective curves [ppmv/10°].

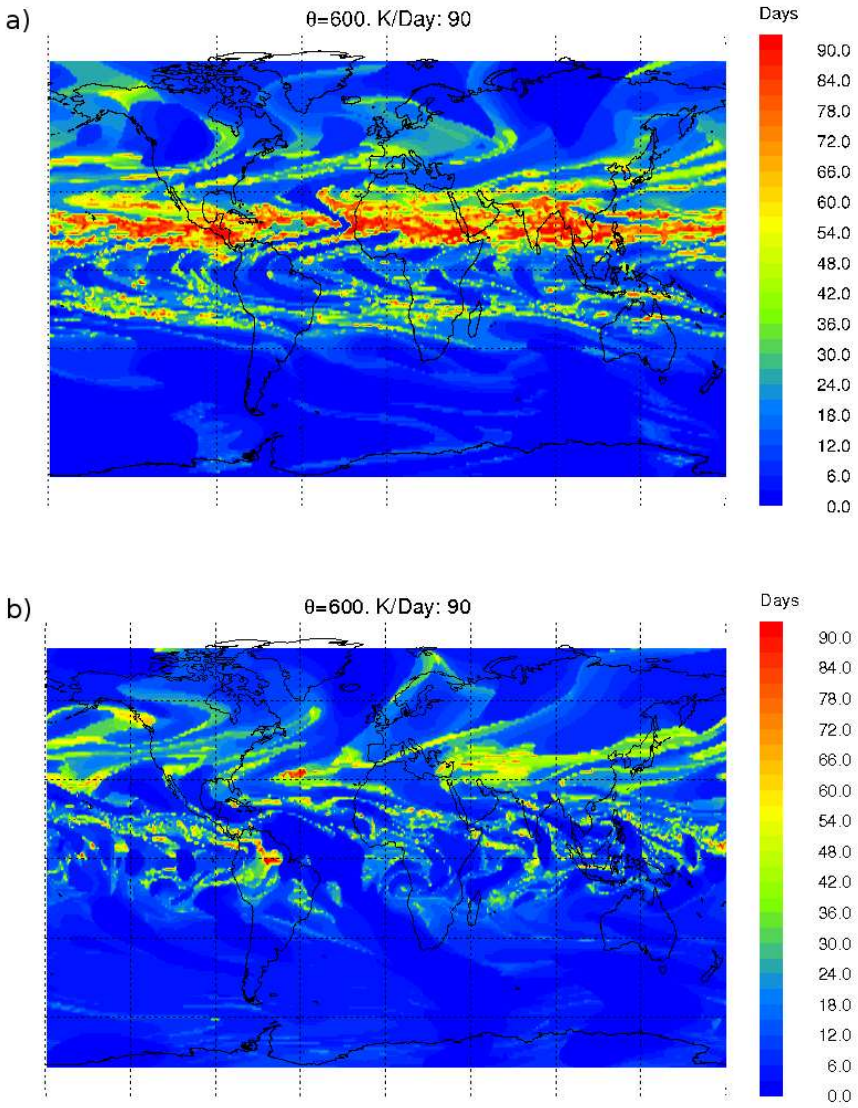

Figure 4.7— Time out of the last 90 days for which parcels have been in their present latitude range (+/– 5 deg) before their arrival at 600 K (**a**) during the easterly phase of the QBO in July 1989, (**b**) during the westerly phase of the QBO in July 1990.

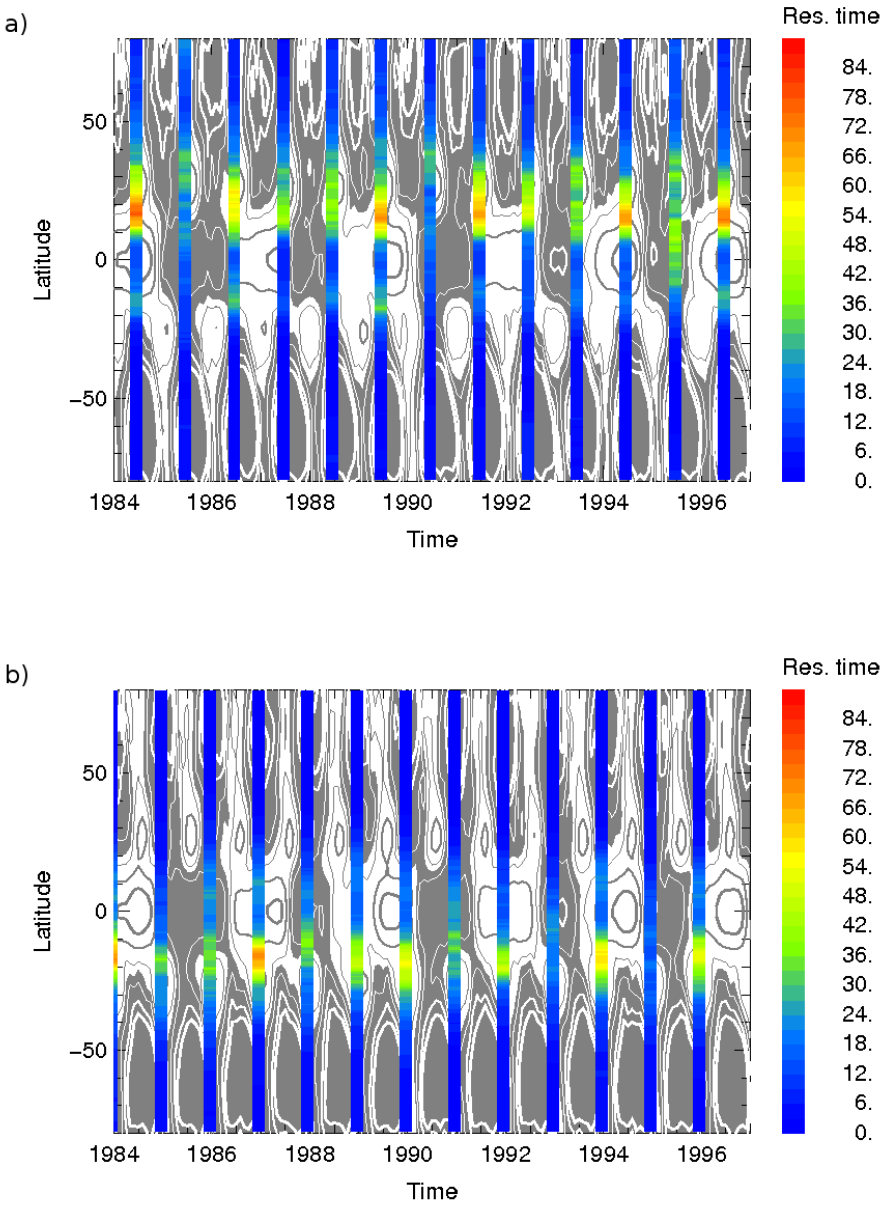

Figure 4.8— Bars show the zonal mean residence time in a channel of +/–5° around the release latitude in days for backward trajectories started on (a) 28 July and (b) 28 January of each year from 1984-1996 at the 600 K level. The background shows the zonal mean zonal wind. Easterlies are colored in white with contour levels at -5, -15, -25 m/s, westerlies in grey with contours at 5, 15, 25 m/s.

Chapter 5

Summary and Outlook

5.1 General summary

To summarize the results obtained from this study, I return to the questions posed in section 1.3.

- *What is the quality of the representation of the tropical stratospheric circulation including the QBO in a current reanalysis? What are the potential weaknesses, and is there evidence for trends?*

  Recent efforts to include the quasi-biennial oscillation in numerical model simulations have proven successful in several ways. Reanalyses using weather forecast models, in particular ERA-40, do include the QBO rather accurately (Baldwin and Gray, 2005; Pascoe et al., 2005), especially below 10 hPa. this is confirmed in our analysis in chapter 2. But above that level, the evolution of wind and temperature fields on interannual to decadal time scales in ERA-40 are still questionable due to the sparse, generally lower quality data available for the earlier parts of the reanalyses. The amount of observations has increased significantly with the availability of satellite observations from the 1980s on (Uppala et al., 2004). However, no direct relation of the observed differences between the earlier and later parts of the reanalysis and changes to the assimilation scheme could be identified. Hence, the observed differences may either be an artefact due to other changes in the model circulation or depict the changes in the real atmosphere. The cooling trend in the upper stratosphere would be in agreement with the expected response to anthropogenic chlorofluorocarbon (CFC) and greenhouse gas (GHG) forcings (Baldwin et al., 2007), but I think the finding is not reliable enough to be regarded as proof for this concept, considering the large variability due to the QBO and the uncertainties discussed above.

- *How does the reanalysis compare to a GCM with internally generated QBO in this respect?*

  Simulating the QBO in a climate model, especially one with focus on the

middle atmosphere has the advantage that a much larger fraction of relevant processes are modelled and the model is less dependent on external forcings. This more self-consistent method allows for more detailed studies of the stratospheric circulation.

The results from the diploma thesis (Punge, 2007) show that there is some variability in the long-term mean fields and QBO amplitudes of wind and temperature similar to that found in ERA-40 even in models with reduced external sources of variability, e.g. with climatological monthly sea surface temperatures only. This appears to be caused by the variable phase relationship between QBO and annual cycle. Increasing long-term variability is found in a model with representation of chemistry. This supports that some variability on the time scale of a decade as found in ERA-40 may be present in the real atmosphere.

- *Does nudging towards observed winds in the QBO region lead to a realistic QBO representation in general circulation models with extension into the stratosphere and inclusion of chemistry? Can such models help understanding observed QBO variations in trace gases?*

  In models that do not generate a QBO internally, a realistic QBO representation can be achieved by the nudging technique, as shown by (Giorgetta and Bengtsson, 1999). The present study shows how the QBO effects on ozone at the Equator can be analyzed in detail, the advantage compared to previous efforts like those of Tian et al. (2006) and Bruhwiler and Hamilton (1999) being in the correct phase relationship to the observed QBO variations. Application of the nudging technique in a model that does generate a QBO internally may yield the same effect. From the results of chapter 2 I expect that a higher horizontal and vertical resolution in model simulations will still improve the analysis of such complex QBO signals as that in ozone.

- *What are the systematic weaknesses in the circulation of models that have no QBO representation? How are trace gas concentrations affected by the net differences in the dynamics?*

  As shown in Chapter 3 significant differences are found in the wind, temperature, mass stream function and several trace gas fields between models with and without QBO representation. The differences in the mean wind field are due to the asymmetry of the QBO with its pronounced westerly phases in the lower stratosphere and pronounced easterlies in the middle stratosphere in combination with the weak easterly wind field in a model with no QBO. Many of the differences seen at low latitudes in temperature and trace gas fields, as e.g. in lower stratospheric ozone, can be understood as effects of the net secondary meridional circulation of the QBO. The much higher water vapor mixing ratios in the simulation with QBO due to the increased temperature at the tropopause is another good example how the circulation changes by the QBO affect the constitution of the stratosphere. An interesting side result is

that the water vapor in the lower subtropical stratosphere are not affected by the tropical tropopause warming (see Fig. A.2k). Hence it appears to enter the stratosphere locally, which indicates that a relation to the Asian monsoon (Dethof et al., 1999; Randel and Park, 2006) is present in the model.

Further net differences in the circulation, like the reduced annual asymmetry of the circulation in the case with QBO, appear to play a role for other trace gases, including methane and the nitrogen oxides. These differences are not easily understood quantitatively though.

- *How do the instantaneous QBO-induced variations of the mean meridional circulation translate to anomalies in the long-term transport of air and trace gas distributions? What is the role of seasonal variations of the Brewer-Dobson-circulation in the tropics and how do they relate to the QBO?*

  Chapter 4 illustrates in detail how the instantaneous, dynamical variations by the QBO affect transport and thus translate to trace gas variations on inter-annual time scales. In particular the ascent variation at the Equator due to the secondary meridional circulation (Plumb and Bell, 1982) is seen clearly. It leaves an imprint in the total ascent of air over three months that is shifted in phase by several months relative to the instantaneous ascent anomaly, indicating that air carries a "memory" of the ascent rates in the past. However, this phase shift will always also depend on the rate of change of the QBO phase, therefore no exact estimate is given.

  It is also shown how the variability of the ascent differs significantly between the two version of MAECHAM4-CHEM with and without QBO. This can affect trace gas concentrations. For example, the higher variability of the ascent leads to the more frequent occurrence of high gradients in long lived trace gases of tropospheric origin and thereby enhances the homogenizing effects of mixing. This could contribute to the higher methane and N_2O levels diagnosed in chapter 3.

- *How does the QBO affect transport at the tropical-subtropical edge? What is the role of the QBO effect on planetary wave propagation (Shuckburgh et al., 2001) relative to the horizontal branch of the secondary circulation?*

  Previous studies of the effect of the QBO on the horizontal transport mostly focused on the effect of the QBO jets on wave dynamics (Gray, 2000; Shuckburgh et al., 2001) rather than the meridional circulation anomaly. However, our results suggest that the combined effect of the SMC, the seasonal asymmetry of the BDC and the effect of the QBO jets on the propagation of planetary waves leads to strong variations of transport at the tropical-extratropical edge that are also reflected in trace gas distributions. It seems that a barrier can only develop when a low horizontal flow, reached by a compensation of summer circulation and easterly QBO anomaly, coincides with a distinct separation of the tropical and extratropical circulation regimes due to the inability of westward propagating extratropical planetary waves to enter the easterly QBO jet.

This finding is a nice example for the complexity of processes occurring in the stratosphere on interannual time scales. The trajectory calculations proved very helpful for getting to the level of qualitative understanding discussed in chapter 4.

5.2 Outlook

Despite constant improvements to numerical models of the atmospheric circulation and their usefulness for understanding processes at work, many challenges remain. This is in particular true for the stratosphere. Its relevance for surface UV conditions has been recognized following the emergence of the ozone hole, but its relation to tropospheric climate is hardly understood (Baldwin et al., 2007).

The studies presented in this work highlight some areas were further improvements are necessary, by showing weaknesses of models and by revealing lack of complete understanding of processes.

Reanalyses are valuable especially for understanding of long-term changes and variability. Although the weaknesses in and sparsity of historic observations can generally not be helped, the way this information is used can be improved. For example, the four-dimensional variational analysis (4dVar) assimilation scheme makes more sophisticated use of the available observations than the 3dVar used for the ERA-40 reanalysis. Together with further improvements, this resulted in a much better representation of the stratospheric circulation in a test run over several years of the reanalysis ERA-interim (B. Legras, S. Fueglistaler, pers. comm.). From a longer term run, it could be assessed what long-term changes of those discussed in chapter 2 remain or are eliminated due to the improvements.

Especially in the light of expected climate change, long term changes to the stratospheric circulation deserve further attention (Baldwin et al., 2007; Shaw and Shepherd, 2008). As shown in chapter 2, temperatures in the tropical stratosphere are closely linked to the zonal wind field, which is only one example for the complex relationships in the stratosphere that may be affected by increased greenhouse gas concentrations.

To cover such processes will be worthwhile for climate models as used for the IPCC studies (on Climate Change , IPCC; Shaw and Shepherd, 2008). A representation of the QBO is an essential ingredient here. While for such studies the ultimate goal is to produce a QBO as realistic as possible, nudging may be used for studies of past trends or short term projections with a QBO continued from the past, as proposed in the CCMVal activity. Furthermore, nudging will continue to be a valuable method to obtain a reality-synchronous QBO for further studies on the effects of the QBO.

The spread in the acceleration of the Brewer-Dobson circulation in response to anthropogenic climate change diagnosed by Butchart et al. (2006) shows that many processes influencing the large scale transport of air in the stratosphere are still sparsely understood. From chapter 4, it is clear that the QBO's meridional circu-

lation plays an important role. One particularly useful diagnostic for studies on transport is that of age of air (Hall and Plumb, 1994; Waugh and Hall, 2002). Taking a Lagrangian view, it is diagnosed for how long a parcel of air has spent in the stratosphere upon entering through the tropopause. Typically, a spectrum of ages is found for ensembles of parcel trajectories, and the mean characterizes the strength of the BDC. It can be derived from observations of linearly increasing trace gases such as SF_6 (Stiller et al., 2008), and from Lagrangian models such as the CLaMS (McKenna et al., 2002), which are usually driven by observed or reanalyzed meteorological fields. The advantage of CLaMS is a realistic representation of small scale mixing (e.g., Konopka et al., 2005), which is particularly important for the age spectrum.

The approach taken in this study to combine a Eulerian GCM and and a Lagrangian transport model is promising in this respect as it allows a reliable derivation of age from a climate model and study its future evolution. A further application of this approach would be a comparison of the trace gas distributions generated in the two different models to derive the respective strength and weaknesses in the chemistry and transport representations.

Clearly, further high-resolved measurements of trace gases are needed for the validation of models. For example, improved observations of methane are needed to identify the effect of the transport barrier seen in the model (Fig. 4.6). On the other hand, as seen in chapter 2, a long continuation of existing observations is necessary to derive reliable estimates of variability and trends of the stratospheric circulation.

Appendix A

Net effect in stream function and further trace gases

The method to calculate the net effect of the QBO as described in the text was applied to further quantities besides zonal wind, temperature and ozone. As for the latter, the QBO amplitude and the seasonal net differences were also computed. The results are given in Figs. A.1 and A.2.

The mass stream function was chosen because it best illustrates the net effect of the QBO on the meridional circulation. In Fig. A.1a, the contours give the stream function for the QBO experiments. In the stratosphere there are two large circulation cells of opposite sign on the two hemispheres that describe the Brewer-Dobson circulation. Contour lines give the direction of the flow, which is clockwise for positive stream function and anti-clockwise for negative streamfunction, and the density of isolines gives the strength of the flow.

The net effect of the QBO as shown in the shades of Fig. A.1a is largely antisymmetric with respect to the Equator. In the lower stratosphere, upwelling is weaker in the simulation with a QBO which affects the time scale of the tape recorder signal in water vapor (Giorgetta et al., 2006). Higher up, at around 30 hPa, the effect is reversed and the circulation is stronger by up to 5% in the QBO experiment. There are two further alternating pairs of cells in the upper stratosphere, located at 7 and 2 hPa. The panels a-d of Figure A.2 show the large seasonal variations of the stream function.

In addition to ozone, we give the QBO effects and amplitudes for three further prominent trace gases in the stratosphere. Methane, water vapor and nitrogen oxides ($NO_x = NO + NO_2 + NO_3 + 0.5\ N_2O_5$) were selected for their roles in the radiation budget and the chemistry of ozone.

The net effect of the QBO on methane, shown in Fig. A.1c, is a substantial increase in the mole fraction over a wide range of the stratosphere above 40 hPa. The absolute net effect is largest in the tropics between 10 and 5 hPa, which can be attributed to the increased upwelling in the middle stratosphere. At mid-latitudes, the net difference between the methane concentrations in the QBO and nonQBO ex-

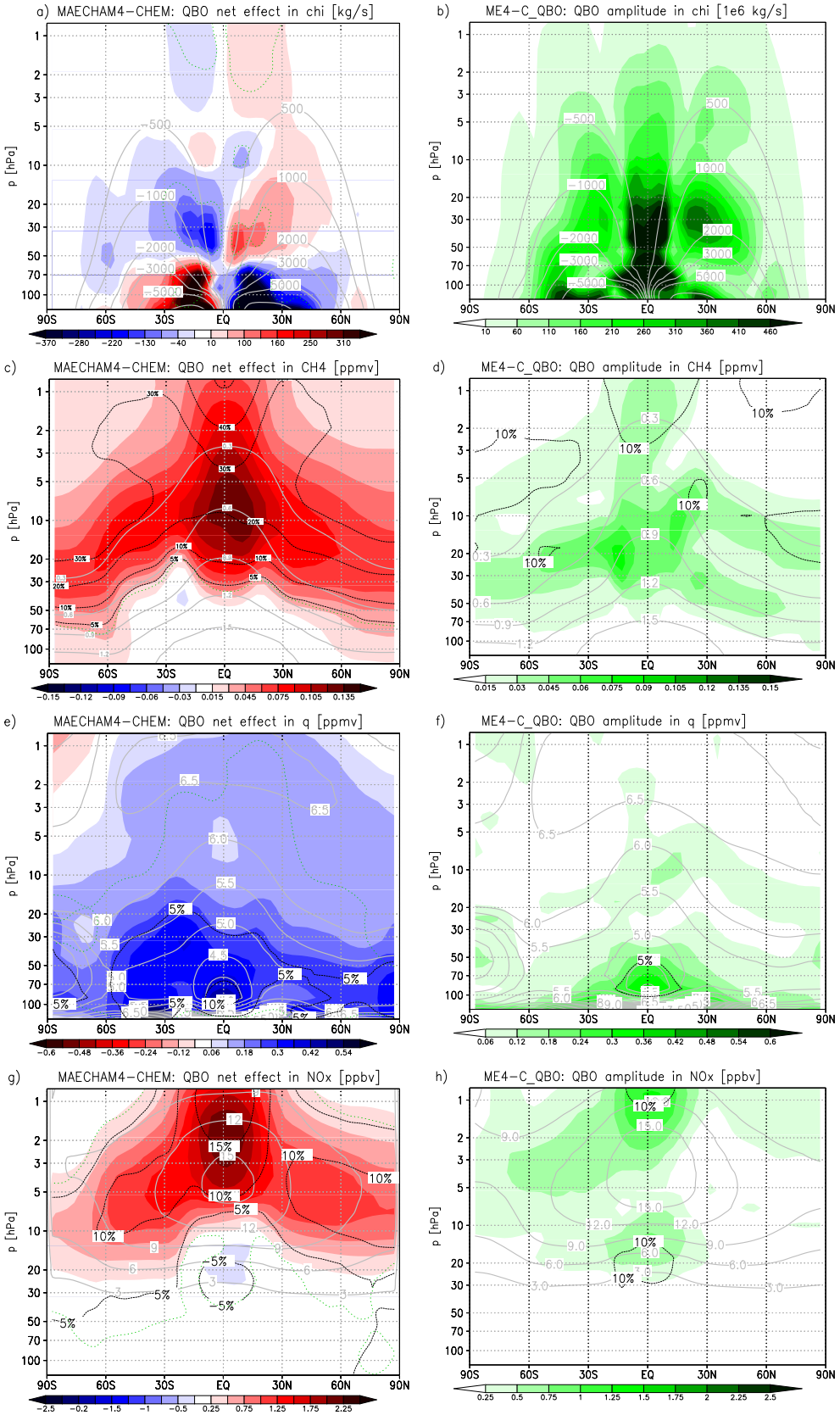

Figure A.1— As Fig. 3.7, but for mass stream function [10^6 kg/s] (**a-b**), and the volume mixing ratios of methane [ppmv] (**c-d**), water vapor [ppmv] (**e-f**) and nitrogen oxides [ppbv] (**g-h**).

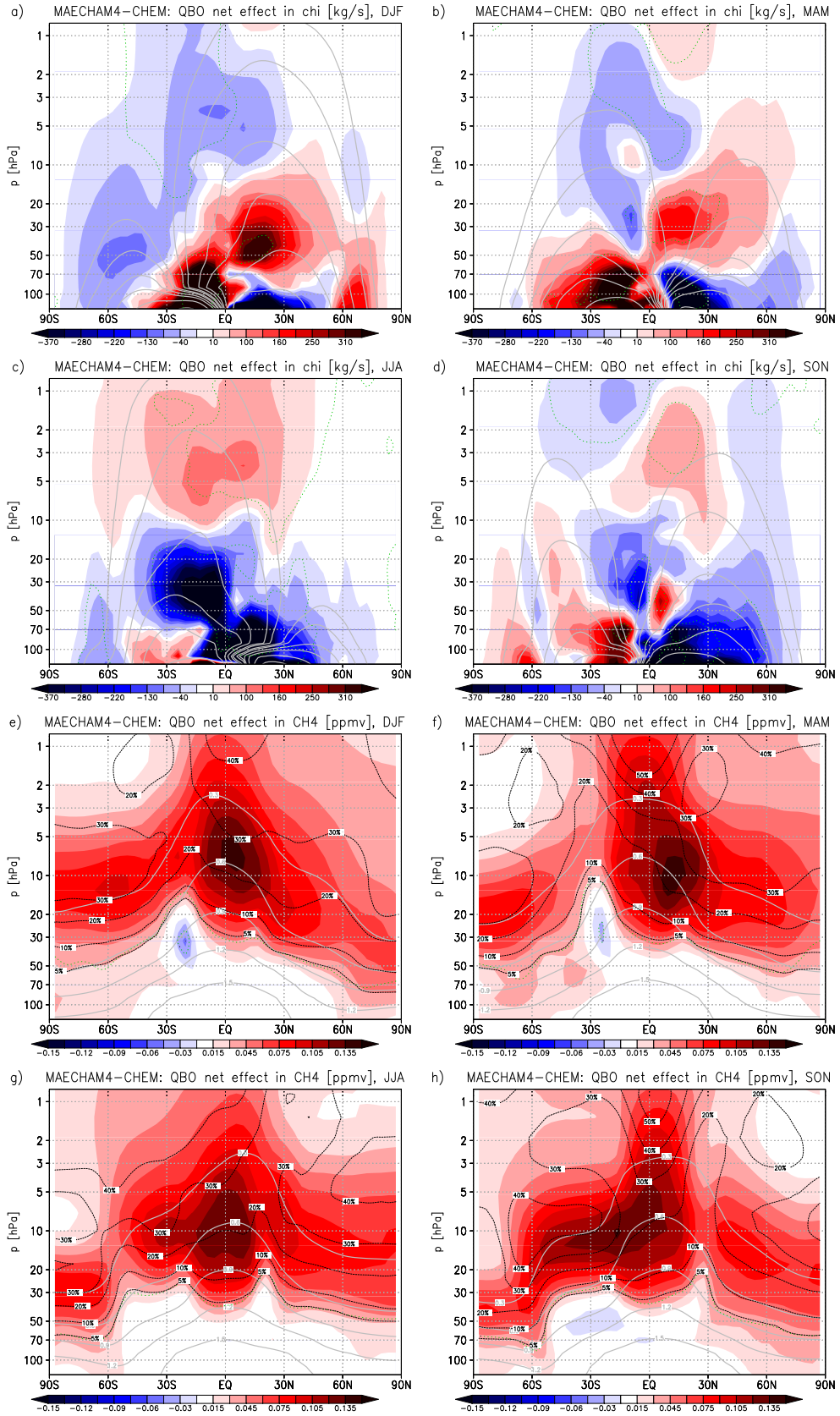

Figure A.2— As Figure 3.8, but for mass stream function [10^6 kg/s] (**a-d**), and the volume mixing ratios of methane [ppmv] (**e-h**), water vapor [ppmv] (**i-l**) and nitrogen oxides [ppbv] (**m-p**).

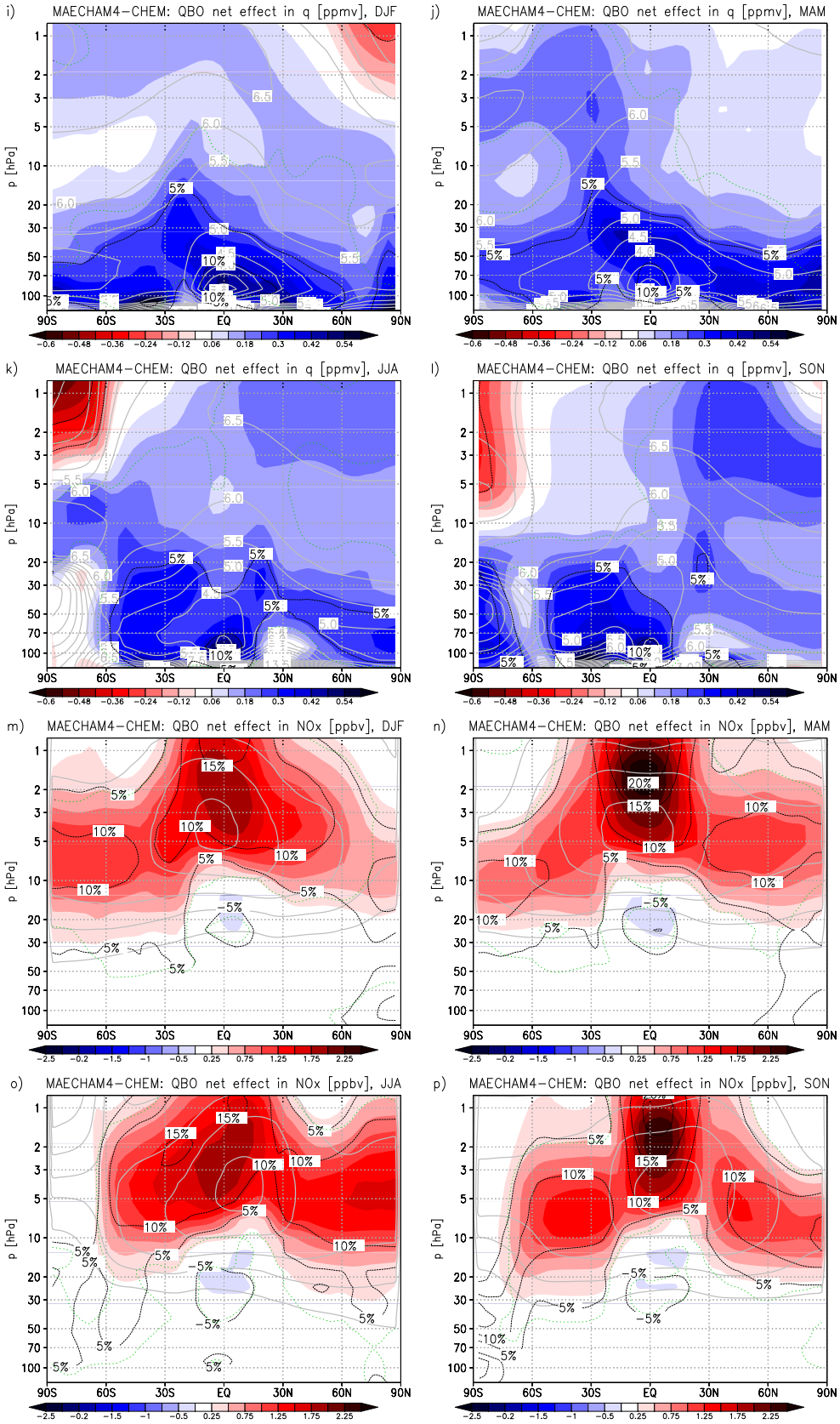

Figure A.2— (continued).

periments is strongest at around 10 hPa. It can be explained by the higher poleward transport at these levels indicated by the differences between the stream functions in the two experiments. Figure A.1d shows the amplitude of the QBO variations in methane in the nudged model experiment. The dark contours show that the amplitude is of the order of 5-10% of the mean volume mixing ratio in a large part of the extratropical stratosphere.

Figures A.2e-h confirm that the increased methane volume mixing ratios occur mainly in winter and spring on both hemispheres, as can be expected from the analysis of the mass stream function. There is a slight reduction of the methane mole fraction between 20°N and 30°N at around 30 hPa during summer and spring, especially on the southern hemisphere.

The stratospheric concentrations of water vapor are elevated up to 6 years after the big volcanic eruptions in the model run with QBO, while they are not in the nonQBO run. To eliminate the resulting net difference in the 20-year means between the two experiments, six years after the eruptions of El Chichon and Mt. Pinatubo were excluded for the analysis of the water vapor field, in contrast to the other quantities. Unfortunately, this leaves only 8 years or about three QBO cycles and hence reduces the reliability of the results. Fig. A.1e shows that nonetheless a QBO signal in tropical water vapor is retained. It occurs at 10 hPa, thus at a lower altitude than in satellite observations (Randel et al., 1998, 2004b; Schoeberl et al., 2008), as mentioned in section 3.2. In the model, the signal is about half as strong as analyzed in the HALOE record by Schoeberl et al. (2008).

The net effect of the QBO, given in Fig. A.1e, is clearly dominated by the tropopause temperature effect. There is a surplus of up to 10% above the tropical tropopause and around 5% in most of the lower stratosphere in the model simulation with nudged QBO compared to the free running model.

The seasonal analysis in the Panels i-l of Figure A.2 confirms that most of the net effect in the lower stratosphere seen in Fig. A.1e is due to the QBOs net effect on tropopause temperatures. A comparison to Fig. A.2e-h reveals that in the middle and upper stratosphere, regions with higher water vapor in the QBO run coincide with the regions where methane mole fraction is not elevated with respect to the nonQBO run.

At the Equator, volume mixing ratios of NO_x are maximum at around 5 hPa. Fig. A.1h shows that there is a QBO signal in NO_x in two regions above and below the maximum. It thus seems that the QBO in NO_x is caused by the QBO in upwelling and the tracer gradient. As discussed in the text, this signal makes an important contribution to the QBO in ozone.

The net effect in NO_x is shown in Fig. A.1g. In the QBO simulation, there is slightly less NO_x in the tropics between 15 and 30 hPa than in the QBO less reference simulation. The net downwelling between 5 and 10 hPa and net upwelling above are consistent with elevated NO_x below and above the maximum. However, we assume that most of the net effect comes from increased production of NO_x from N_2O, for which the pattern of the net effect (not shown) is very similar to that in methane.

The panels m-p of Fig. A.2 show the net effect in NO_x for the four seasons. The net gain in NO_x in the upper stratosphere is strongest during the equinoctial seasons. This supports the connection to temperatures - the colder temperatures due to the weaker SAO westerlies in the QBO west phase lead to the higher NO_x concentrations. On the other hand, a larger part of the excess NO_x will be advected towards the winter hemisphere during the solstitial seasons. An increase of NO_x volume mixing ratios at mid-latitudes by 10-15 % above 20 hPa is however found during all seasons in the QBO versus the nonQBO experiment.

Bibliography

Ambaum, M. H. P. and Hoskins, B. J.: The NAO Troposphere-Stratosphere Connection, Journal of Climate, 15, 1969–1978, 2002.

Andrae, U., Sokka, N., and Onogi, K.: The radiosonde temperature bias corrections used in ERA-40, ERA-40 Project Report Series, 15, 1–37, 2004.

Angell, J. K. and Korshover, J.: Quasi-biennial variations in temperature, total ozone, and Tropopause Height, J. Atmos. Sci., 21, 479–492, 1964.

Austin, J.: A Three-Dimensional Coupled Chemistry-Climate Model Simulation of Past Stratospheric Trends, J. Atmos. Sci., 59, 218–232, doi:10.1175/1520-0469(2002)059⟨0218:ATDCCC⟩2.0.CO;2, 2002.

Baldwin, M. P. and Gray, L. J.: Tropical stratosphere zonal winds in ECMWF ERA-40 reanalysis, rocketsonde data, and rawinsonde data, Geophys. Res. Lett., 32, L09806, doi:10.1029/2004GL022328, 2005.

Baldwin, M. P., Gray, L. J., Dunkerton, T. J., Hamilton, K., Haynes, P. H., Randel, W. J., Holton, J. R., Alexander, M. J., Hirota, I., Horinouchi, T., Jones, D. B. A., Kinnersley, J. S., Marquardt, C., Sato, K., and Takahashi, M.: The Quasi-Biennial Oscillation, Rev. of Geophysics, 39, 179–229, 2001.

Baldwin, M. P., Dameris, M., and Shepherd, T. G.: How Will the Stratosphere Affect Climate Change?, Science, 316, 1576–1577, doi:10.1126/science.1144303, 2007.

Bengtsson, L., Hodges, K. I., and Hagemann, S.: Sensitivity of the ERA40 reanalysis to the observing system: determination of the global atmospheric circulation from reduced observations, Tellus, 56A, 456–471, 2004.

Bowman, K. P.: Rossby Wave Phase Speeds and Mixing Barriers in the Stratosphere. Part I: Observations., J. Atmos. Sci., 53, 905–916, 1996.

Brasseur, G. P., Orlando, J. J., and Tyndall, G. S.: Atmospheric Chemistry and Global Change, Oxford University Press, New York, NY, 1999.

Bruhwiler, L. P. and Hamilton, K.: A numerical simulation of the stratospheric ozone quasi-biennial oscillation using a comprehensive general circulation model, J. Geophys. Res., 104, 30 525–30 557, 1999.

Butchart, N., Scaife, A. A., Austin, J., Hare, S. H. E., and Knight, J. R.: Quasi-biennial oscillation in ozone in a coupled chemistry-climate model, J. Geophys. Res., 108, 4486, 2003.

Butchart, N., Scaife, A. A., Bourqui, M., de Grandpré, J., Hare, S. H. E., Kettleborough, J., Langematz, U., Manzini, E., Sassi, F., Shibata, K., Shindell, D., and Sigmond, M.: Simulations of anthropogenic change in the strength of the Brewer Dobson circulation, Climate Dynamics, 27, 727–741, doi:10.1007/s00382-006-0162-4, 2006.

Calvo, N., Giorgetta, M. A., and Peña-Ortiz, C.: Sensitivity of the boreal winter circulation in the middle atmosphere to the quasi-biennial oscillation in MAECHAM5 simulations, J. Geophys. Res., 112, D10 124, 2007.

Chattopadhyay, J. and Bhatla, R.: Possible influence of QBO on teleconnections relating Indian summer monsoon rainfall and sea-surface temperature anomalies across the equatorial pacific, International Journal of Climatology, 22, 121–127, 2002.

Chen, P.: The Influences of Zonal Flow on Wave Breaking and Tropical-Extratropical Interaction in the Lower Stratosphere, J. Atmos. Sci., 53, 2379–2392, 1996.

Chipperfield, M. P. and Gray, L. J.: Two-Dimensional Model Studies of the Interannual Variability of Trace Gases in the Middle Atmosphere, J. Geophys. Res., 97, 5963–5980, 1992.

Chipperfield, M. P., Gray, L. J., Kinnersley, J. S., and Zawodny, J.: A two-dimensional model study of the QBO signal in SAGE II NO2 and O3 [NO_2 O_3], Geophys. Res. Lett., 21, 589–+, 1994.

Cordero, E. C., Kawa, S. R., and Schoeberl, M. R.: An analysis of tropical transport: Influence of the quasi-biennial oscillation, J. Geophys. Res., 102, 16 453–16 462, doi:10.1029/97JD01053, 1997.

Crooks, S. A. and Gray, L. J.: Characterization of the 11-year solar signal using a multiple regression analysis of the ERA-40 dataset, J. of Climate, 18, 996–1015, 2005.

Dethof, A., Oneill, A., Slingo, J. M., and Smit, H. G. J.: A mechanism for moistening the lower stratosphere involving the Asian summer monsoon, Q. J. R. Meteorol. Soc., 125, 1079–1106, doi:10.1256/smsqj.55601, 1999.

Dunkerton, T. J.: Quasi-Biennal and subbiennal Variations of Stratospheric Trace Constituents Derived from HALOE Observations, J. Atmos. Sci., 58, 7–25, 2001.

Eyring, V., Butchart, N., Waugh, D. W., Akiyoshi, H., Austin, J., Bekki, S., Bodeker, G. E., Boville, B. A., Brühl, C., Chipperfield, M. P., Cordero, E.,

Dameris, M., Deushi, M., Fioletov, V. E., Frith, S. M., Garcia, R. R., Gettelman, A., Giorgetta, M. A., Grewe, V., Jourdain, L., Kinnison, D. E., Mancini, E., Manzini, E., Marchand, M., Marsh, D. R., Nagashima, T., Newman, P. A., Nielsen, J. E., Pawson, S., Pitari, G., Plummer, D. A., Rozanov, E., Schraner, M., Shepherd, T. G., Shibata, K., Stolarski, R. S., Struthers, H., Tian, W., and Yoshiki, M.: Assessment of temperature, trace species and ozone in chemistry-climate model simulations of the recent past, J. Geophys. Res., 111, doi:10.1029/2006JD007327, 2006.

Garny, H., Bodecker, G. E., and Dameris, M.: Trends and variability in stratospheric mixing: 1979-2005, Atmos. Chem. Phys., 7, 5611–5624, 2007.

Giorgetta, M. A. and Bengtsson, L.: Potential role of the quasi-biennial oscillation in stratosphere-troposphere exchange as found in water vapor in general circulation model experiments, J. Geophys. Res., 104, 6003–6020, 1999.

Giorgetta, M. A., Bengtsson, L., and Arpe, K.: An Investigation of QBO signals in the east Asian and Indian monsoon in GCM experiments, Climate Dyn., 15, 435–450, 1999.

Giorgetta, M. A., Manzini, E., Roeckner, E., Esch, M., and Bengtsson, L.: Climatology and Forcing of the Quasi-Biennial Oscillation in the MAECHAM5 Model, J. of Climate, 19, 3882–3901, 2006.

Gleisner, H., Thejll, P., Stendel, M., Kaas, E., and Machenhauer, B.: Solar signals in tropospheric re-analysis data: Comparing NCEP/NCAR and ERA40, J. of Atmos. and Sol.-Terr. Phys., 67, 785–791, 2005.

Gray, L. J.: A model study of the influence of the quasi-biennial oscillation on trace gas distributions in the middle and upper stratosphere, J. Geophys. Res., 105, 4539–4552, doi:10.1029/1999JD900320, 2000.

Hall, T. M. and Plumb, R. A.: Age as a diagnostic of stratospheric transport, J. Geophys. Res., 99, 1059–1070, doi:10.1029/93JD03192, 1994.

Hamilton, K. and Hsieh, W. W.: Representation of the quasi-biennial oscillation in the tropical stratospheric wind by nonlinear principal component analysis, J. Geophys. Res., 107, 4232–+, doi:10.1029/2001JD001250, 2002.

Hasebe, F.: Quasi-Biennial Oscillations of Ozone and Diabatic Circulation in the Equatorial Stratosphere, J. Atmos. Sci., 51, 729–745, 1994.

Hastenrath, S.: Equatorial zonal circulations: Historical perspectives, Dyn. Atmos. and Oceans, 43, 16–24, 2007.

Haynes, P. and Shuckburgh, E.: Effective diffusivity as a diagnostic of atmospheric transport 1. Stratosphere, J. Geophys. Res., 105, 22 777–22 794, 2000.

Haynes, P. H., McIntyre, M. E., Shepherd, T. G., Marks, C. J., and Shine, K. P.: On the 'Downward Control' of Extratropical Diabatic Circulations by Eddy-Induced Mean Zonal Forces., J. Atmos. Sci., 48, 651–680, 1991.

Holton, J. R. and Lindzen, R. S.: An updated theory for the quasi-biennial cycle of the tropical stratosphere, J. Atmos. Sci., 29, 1076–1080, 1972.

Holton, J. R. and Tan, H.-C.: The influence of the equatorial quasi-biennial oscillation on the global circulation at 50 mb, J. Atmos. Sci., 37, 2200–2208, 1980.

Holton, J. R. and Tan, H.-C.: The quasi-biennial oscillation in the Northern Hemisphere lower stratosphere, J. of the Meteorol. Soc. of Japan, 60, 140–148, 1982.

Huesmann, A. S. and Hitchman, M. H.: The stratospheric quasi-biennial oscillation in the NCEP reanalyses: Climatological structures, J. Geophys. Res., 106, 11 859–11 874, 2001.

Huesmann, A. S. and Hitchman, M. H.: The 1978 shift in the NCEP reanalysis stratospheric quasi-biennial oscillation, Geophys. Res. Lett., 30, 1048, doi: 10.1029/2002GL016323, 2004.

Jackman, C. H., Fleming, E. L., Chandra, S., Considine, D. B., and Rosenfield, J. E.: Past, present, and future modeled ozone trends with comparisons to observed trends, J. Geophys. Res., 101, 28 753–28 768, doi:10.1029/96JD03088, 1996.

Khosrawi, F., Grooß, J.-U., Müller, R., Konopka, P., Kouker, W., Ruhnke, R., Reddmann, T., and Riese, M.: Intercomparison between Lagrangian and Eulerian simulations of the development of mid-latitude streamers as observed by CRISTA, Atmos. Chem. Phys., 5, 85–95, 2005.

Kinnersley, J. S. and Tung, K.: Mechanisms for the Extratropical QBO in Circulation and Ozone, Journal of Atmospheric Sciences, 56, 1942–1962, 1999.

Kirchner, I., Stenchikov, G. L., Graf, H.-F., Robock, A., and Antuña, J. C.: Climate model simulation of winter warming and summer cooling following the 1991 Mount Pinatubo volcanic eruption, J. Geophys. Res., 104, 19 039–19 056, doi:10.1029/1999JD900213, 1999.

Konopka, P., Grooß, J.-U., Hoppel, K. W., Steinhorst, H.-M., and Müller, R.: Mixing and Chemical Ozone Loss during and after the Antarctic Polar Vortex Major Warming in September 2002., J. Atmos. Sci., 62, 848–859, 2005.

Konopka, P., Günther, G., Müller, R., Dos Santos, F. H. S., Schiller, C., Ravegnani, F., Ulanovsky, A., Schlager, H., Volk, C. M., Viciani, S., Pan, L. L., McKenna, D.-S., and Riese, M.: Contribution of mixing to upward transport across the tropical tropopause layer (TTL), Atmos. Chem. Phys., 7, 3285–3308, 2007.

Lean, J. L., Rottman, G. J., Kyle, H. L., Woods, T. N., Hickey, J. R., and Puga, L. C.: Detection and parameterization of variations in solar mid- and near-ultraviolet radiation (200-400 nm)., J. Geophys. Res., 102, 29 939–29 956, 1997.

Lelieveld, J., Brühl, C., Jöckel, P., Steil, B., Crutzen, P. J., Fischer, H., Giorgetta, M. A., Hoor, P., Lawrence, M. G., Sausen, R., and Tost, H.: Stratospheric dryness: model simulations and satellite observations, Atmos. Chem. Phys., 7, 1313–1332, 2007.

Lindzen, R. D.: Planetary waves on beta-planes, Mon. Weather Rev., 95, 441–451, 1967.

Lindzen, R. S. and Holton, J. R.: A theory of quasi-biennial oscillation, JAS, 25, 1095–1107, 1968.

Logan, J. A., Jones, D. B. A., Megretskaia, I. A., Oltmans, S. J., Johnson, B. J., Vömel, H., Randel, W. J., Kimani, W., and Schmidlin, F. J.: Quasibiennial oscillation in tropical ozone as revealed by ozonesonde and satellite data, J. Geophys. Res., 108, 4244–+, doi:10.1029/2002JD002170, 2003.

Manzini, E. and McFarlane, N. A.: The effect of varying the source spectrum of a gravity wave parameterization in a middle atmosphere general circulation model., J. Geophys. Res., 103, 31 523–31 539, 1998.

Manzini, E., McFarlane, N. A., and McLandress, C.: Impact of the Doppler spread parameterization on the simulation of the middle atmosphere circulation using the MA/ECHAM4 general circulation model, J. Geophys. Res., 102, 25 751–25 762, doi:10.1029/97JD01096, 1997.

Manzini, E., Steil, B., Brühl, C., Giorgetta, M. A., and Krueger, K.: A new interactive chemistry-climate model: Sensitivity of the middle atmosphere to ozone depletion and increase in greenhouse gases and implications for recent stratospheric cooling, J. Geophys. Res., 108, 4429, doi:10.1029/2002JD002977, 2003.

McCormick, M. P., Thomason, L. W., and Trepte, C. R.: Atmospheric effects of the Mt Pinatubo eruption, Nature, 373, 399–404, doi:10.1038/373399a0, 1995.

McIntyre, M. E. and Palmer, T. N.: The 'surf zone' in the stratosphere, J. Atmos. Terr. Phys., 46, 825–849, 1984.

McKenna, D. S., Konopka, P., Grooß, J.-U., Günther, G., Müller, R., Spang, R., Offermann, D., and Orsolini, Y.: A new Chemical Lagrangian Model of the Stratosphere (CLaMS) 1. Formulation of advection and mixing, J. Geophys. Res., 107, 4309–+, doi:10.1029/2000JD000114, 2002.

Mote, P. W., Rosenlof, K. H., McIntyre, M. E., Carr, E. S., Gille, J. C., Holton, J. R., Kinnersley, J. S., Pumphrey, H. C., Russell, III, J. M., and Waters, J. W.: An atmospheric tape recorder: The imprint of tropical tropopause temperatures

on stratospheric water vapor, J. Geophys. Res., 101, 3989–4006, doi:10.1029/95JD03422, 1996.

Nash, E. R., Newman, P. A., Rosenfield, J. E., and Schoeberl, M. R.: An objective determination of the polar vortex using Ertel's potential vorticity, J. Geophys. Res., 101, 9471–9478, doi:10.1029/96JD00066, 1996.

Neu, J. L., Sparling, L. C., and Plumb, R. A.: Variability of the subtropical edges in the stratosphere, J. Geophys. Res., 108, 4482, doi:10.1029/2002JD002706, 2003.

Niwano, M., Yamazaki, K., and Shiotani, M.: Seasonal and QBO variations of ascent rate in the tropical lower stratosphere as inferred from UARS HALOE trace gas data, J. Geophys. Res., 108, 4794, doi:10.1029/2003JD003871, 2003.

on Climate Change (IPCC), I. P.: Climate Change 2007: The Physical Science Basis. Contribution of Working Group I to the Fourth Assessment Report of the Intergovernmental Panel on Climate Change [Solomon, S., D. Qin, M. Manning, Z. Chen, M. Marquis, K.B. Averyt, M. Tignor and H.L. Miller (eds.)], Cambridge University Press, 2007.

O'Sullivan, D. and Chen, P.: Modelling the quasi-biennial oscillation's influence on isentropic transport in the subtropics, J. Geophys. Res., 101, 6811–6822, doi:10.1029/96JD00001, 1996.

O'Sullivan, D. and Dunkerton, T. J.: The influence of the quasi-biennial oscillation on global constituent distributions, J. Geophys. Res., 102, 21 731–21 744, 1997.

O'Sullivan, D. and Salby, M. L.: Coupling of the Quasi-biennial Oscillation and the Extratropical Circulation in the Stratosphere through Planetary Wave Transport, J. Atmos. Sci., 47, 650–673, 1990.

Pascoe, C. L., Gray, L. J., Crooks, S. A., Juckes, M. N., and Baldwin, M. P.: The quasi-biennial oscillation: Analysis using ERA-40 data, J. Geophys. Res., 110, D08105, doi:10.1029/2004JD004941, 2005.

Patra, P. K., Lal, S., Venkataramani, S., and Chand, D.: Halogen Occultation Experiment (HALOE) and balloon-borne in situ measurements of methane in stratosphere and their relation to the quasi-biennial oscillation (QBO), Atmos. Chem. Phys., 3, 1051–1062, 2003.

Plumb, R. A.: Stratospheric transport, J. of the Meteorol. Soc. of Japan, 80, 793–809, 2002.

Plumb, R. A. and Bell, R. C.: A model of the quasi-biennial oscillation on an equatorial beta-plane, Q. J. R. Meteorol. Soc., 108, 335–352, 1982.

Punge, H. J.: Interdecadal Variability of the QBO in the ERA-40 reanalysis and in the MAECHAM5 and HAMMONIA climate models, Thesis equivalent to a german Diplomarbeit, Universität Hamburg, Hamburg, Germany, 2007.

Punge, H. J. and Giorgetta, M. A.: Differences between the QBO in the first and in the second half of the ERA-40 reanalysis and in the MAECHAM5 and HAMMONIA climate models, Atmos. Chem. Phys., 7, 599–608, 2007.

Punge, H. J. and Giorgetta, M. A.: Net effect of the QBO in a chemistry-climate model, Atmos. Chem. Phys. Diss., 2008.

Randel, W., Udelhofen, P., Fleming, E., Geller, M., Gelman, M., Hamilton, K., Karoly, D., Ortland, D., Pawson, S., Swinbank, R., Wu, F., Baldwin, M., Chanin, M. L., Keckhut, P., Labitzke, K., Simmons, E. R. A., and Wu, D.: The SPARC Intercomparison of middle-atmospheric climatologies, Journal of Climate, 17, 986–1003, 2004a.

Randel, W. J. and Park, M.: Deep convective influence on the Asian summer monsoon anticyclone and associated tracer variability observed with Atmospheric Infrared Sounder (AIRS), J. Geophys. Res., 111, 12 314–+, doi:10.1029/2005JD006490, 2006.

Randel, W. J. and Wu, F.: Isolation of the Ozone QBO in SAGE II Data by Singular-Value Decomposition, J. Atmos. Sci., 53, 2546–2559, doi:10.1175/1520-0469(1996)053⟨2546:IOTOQI⟩2.0.CO;2, 1998.

Randel, W. J., Wu, F., Russel, J. W., Roche, A., and Waters, J.: Seasonal cycles and QBO variations in stratospheric CH4 and H2O observed in UARS HALOE data, J. Atmos. Sci., 55, 163–185, 1998.

Randel, W. J., Wu, F., Oltmans, S. J., K.Rosenlof, and Nedoluha, G. E.: Interannual changes of stratospheric water vapor and correlations with tropical tropopause temperatures, J. Atmos. Sci., 61, 2133–2147, 2004b.

Rayner, N. A., Parker, D. E., Horton, E. B., Folland, C. K., Alexander, L. V., Rowell, D. P., Kent, E. C., and Kaplan, A.: Global analyses of sea surface temperature, sea ice, and night marine air temperature since the late nineteenth century, J. Geophys. Res., 108, 4407, doi:10.1029/2002JD002670, 2003.

Reed, R. J.: A tentative model of the 26-month oscillation in tropical latitudes, Q. J. R. Meteorol. Soc., 90, 441–466, doi:10.1002/qj.49709038607, 1964.

Reed, R. J., Campbell, W. J., Rasmussen, L. A., and Rogers, D. G.: Evidence of downward propagating annual wind reversal in the equatorial stratosphere, J. Geophys. Res., 66, 813–818, 1961.

Ribera, P., Peña-Ortiz, C., Garcia-Herrera, R., Gallego, D., Gimeno, L., and Hernández, E.: Detection of the secondary meridional circulation associated with the quasi-biennial oscillation, J. Geophys. Res., 109, 18 112, doi:10.1029/2003JD004363, 2004.

Roeckner et al., E.: The atmospheric general circulation model ECHAM4: Model description and simulation of present-day climate, Max-Planck-Institut für Meteorologie - Report No. 218, Hamburg, p. 90 pp., 1996.

Santer, B. D., Wigley, T. M. L., Simmons, A. J., Kallberg, P. W., Kelly, G. A., Uppala, S. M., Ammann, C., Boyle, J. S., Brüggemann, W., Doutriaux, C., Fiorino, M., Mears, C., Meehl, G. A., Sausen, R., Taylor, K. E., Washington, W. M., Wehner, M. F., and Wentz, F. J.: Identification of anthropogenic climate change using a second-generation reanalysis, J. Geophys. Res., 109, D21 104, doi: 10.1029/2004JD005075, 2004.

Scaife, A. A., Butchart, N., Warner, C. D., Stainforth, D., Norton, W., and Austin, J.: Realistic quasi-biennial oscillations in a simulation of the global climate, Geophys. Res. Lett., 27, 3481–3484, doi:10.1029/2000GL011625, 2000.

Schmidt, H., Brasseur, G. P., Charron, M., Manzini, E., Giorgetta, M. A., Diehl, T., Fomichev, V. I., Kinnison, D., Marsh, D., and Walters, S.: The HAMMONIA chemistry climate model: Sensitivity of the mesopause region to the 11-year solar cycle and CO2 doubling, J. of Climate, 19, 3903–3931, 2006.

Schoeberl, M. R., Douglass, A. R., Newman, P. A., Lait, L. R., Lary, D., Waters, J., Livesey, N., Froidevaux, L., Lambert, A., Read, W., Filipiak, M. J., and Pumphrey, H. C.: QBO and Annual Cycle Variations in Tropical Lower Stratosphere Trace Gases from HALOE and Aura MLS Observations, J. Geophys. Res., 113, doi:10.1029/2007JD008678, 2008.

Shaw, T. A. and Shepherd, T. G.: Raising the roof, Nature Geo., 1, 12–13, doi: 10.1038/ngeo.2007.53, 2008.

Shibata, K. and Deushi, M.: Partitioning between resolved wave forcing and unresolved gravity wave forcing to the quasi-biennial oscillation as revealed with a coupled chemistry-climate model, Geophys. Res. Lett., 32, L12 820, 2005.

Shuckburgh, E., Norton, W., Iwi, A., and Haynes, P.: Influence of the quasi-biennial oscillation on isentropic transport and mixing in the tropics and subtropics, J. Geophys. Res., 106, 14 327–14 338, 2001.

Steil, B., Dameris, M., Brüh1, C., Crutzen, P. J., Grewe, V., Ponater, M., and Sausen, R.: Development of a chemistry module for GCMs: first results of a multiannual integration, Annales Geophysicae, 16, 205–228, 1998.

Steil, B., Brühl, C., Manzini, E., Crutzen, P. J., Lelieveld, J., Rasch, P. J., Roeckner, E., and Krueger, K.: A new interactive chemistry-climate model: 1. Present-day climatology and interannual variability of the middle atmosphere using the model and 9 years of HALOE/UARS data, J. Geophys. Res., 108, 4290, doi: 10.1029/2002JD002971, 2003.

Steinbrecht, W., Haßler, B., Brühl, C., Dameris, M., Giorgetta, M. A., Grewe, V., Manzini, E., Matthes, S., Schnadt, C., Steil, B., and Winkler, P.: Interannual variation patterns of total ozone and lower stratospheric temperature in observations and model simulations, Atmos. Chem. Phys., 6, 349–374, 2006.

Sterl, A.: On the (In)Homogeneity of Reanalysis Products, J. of Climate, 17, 3866–3873, 2004.

Stiller, G. P., von Clarmann, T., Höpfner, M., Glatthor, N., Grabowski, U., Kellmann, S., Kleinert, A., Linden, A., Milz, M., Reddmann, T., Steck, T., Fischer, H., Funke, B., Lpez-Puertas, M., and Engel, A.: Global distribution of mean age of stratospheric air from MIPAS SF_6 measurements, Atmos. Chem. Phys., 8, 677–695, `http://www.atmos-chem-phys.net/8/677/2008/`, 2008.

Takahashi, M.: Simulation of the stratospheric quasi-biennial oscillation using a general circulation model, Geophys. Res. Lett., 23, 661–664, 1996.

Tian, W., Chipperfield, M. P., Gray, L. J., and Zawodny, J. M.: Quasi-biennial oscillation and tracer distributions in a coupled chemistry-climate model, J. Geophys. Res., 111, doi:10.1029/2006JD006871, 2006.

Tian, W. S. and Chipperfield, M. P.: A new coupled chemistry-climate model for the stratosphere: The importance of coupling for future O3-climate predictions, Q. J. R. Meteorol. Soc., 131, 281–303, 2005.

Tourpali, K., Schuurmans, C. J. E., van Dorland, R., Steil, B., and Brühl, C.: Stratospheric and tropospheric response to enhanced solar UV radiation: A model study, Geophys. Res. Lett., 30, 35–1, 2003.

Trepte, C. R. and Hitchman, M. H.: Tropical stratospheric circulation deduced from satellite aerosol data, Nature, 355, 626–628, doi:10.1038/355626a0, 1992.

Uppala, S., Kallberg, P., Hernandez, A., Saarinen, S., Fiorino, M., Li, X., Onogi, K., Sokka, N., Andrae, U., and Bechtold, V. D. C.: ERA-40: ECMWF 45-year reanalysis of the global atmosphere and surface conditions 1957-2002, *ECMWF* Newsletter, 101, 2–21, 2004.

Uppala, S., Kallberg, P., , Simmons, A. J., Andrae, U., Bechtold, V. D. C., Fiorino, M., Gibson, J. K., Haseler, J., Hernandez, A., Kelly, G. A., Li, X., Onogi, K., Saarinen, S., Sokka, N., Allan, R. P., Andersson, E., Arpe, K., Balmaseda, M. A., Beljaars, A. C. M., van de Berg, L., Bidlot, J., Bormann, N., Caires, S., Chevallier, F., Dethof, A., Dragosavac, M., Fisher, M., Fuentes, M., Hagemann, S., Holm, E., Hoskins, B. J., Isaksen, L., Janssen, P. A. E. M., Jenne, R., McNally, A. P., Mahfouf, J. F., Morcrette, J. J., Rayner, N. A., Saunders, R. W., Simon, P., Sterl, A., Trenberth, K. E., Untch, A., Vasiljevic, D., Viterbo, P., and Woollen, J.: The ERA-40 re-analysis, Q. J. R. Meteorol. Soc., 131, 2961–3012, 2005.

van Noije, T. P. C., Segers, A. J., and van Velthoven, P. F. J.: Time series of the stratosphere-troposphere exchange of ozone simulated with reanalyzed and operational forecast data, J. Geophys. Res., 111, D03 301, doi:10.1029/2005JD006081, 2006.

Veryard, R. and Ebdon, R. A.: Fluctuations in tropical stratospheric winds, Meteor. Mag., 90, 125–143, 1961.

Waugh, D. and Hall, T.: AGE OF STRATOSPHERIC AIR: THEORY, OBSERVATIONS, AND MODELS, Rev. of Geophysics, 40, 1–1, doi:10.1029/2000RG000101, 2002.

Waugh, D. W.: Seasonal variation of isentropic transport out of the tropical stratosphere, J. Geophys. Res., 101, 4007–4024, 1996.

Witte, J. C., Schoeberl, M. R., Douglass, A. R., and Thompson, A. M.: The Quasi-biennial Oscillation and annual variations in tropical ozone from SHADOZ and HALOE, Atmos. Chem. Phys. Diss., 8, 6355–6378, 2008.

WMO: Scientific Assessment of Ozone Depletion: 2002, Global Ozone Research and Monitoring Project - Report No. 47, Geneva, p. 498, 2003.

Zawodny, J. M. and McCormick, M. P.: Stratospheric Aerosol and Gas Experiment II measurements of the quasi-biennial oscillations in ozone and nitrogen dioxide, J. Geophys. Res., 96, 9371–9377, 1991.

Acknowledgements

First of all I have to thank Marco Giorgetta for being the best PhD advisor a student could wish for, which became manifest in patient attention to my work, constant advise and motivation, and many brilliant ideas that entered this work.

Secondly, I am grateful to Jochem Marotzke and Erich Roeckner for always constructive and helpful discussions in the meetings of the advisory panel of the IMPRS-ESM, which helped a lot to complete this work in a reasonable time in not always favorable conditions.

I thank Paul Konopka, Rolf Müller and Nicole Thomas for their part in establishing what become a fruitful cooperation with the ICG-1 theory group at Forschungszentrum Jülich. Hauke Schmidt, Claudia Timmreck, Sebastian Rast, and many others contributed to my work with valuable comments, discussions, and ideas.

I thank Antje Weitz and Conni Kampmann of the IMPRS office for their assistance and motivation, and all students of the IMPRS which constitute the international atmosphere I enjoy a lot, in particular Rita Seiffert, Claas Teichmann, Hui Wan and Malte Heinemann for their long-lasting company in the struggle of doing a PhD. Adetutu Mary Aghedo provided a great template for this thesis.

Further thanks go to CIS, BIS and the other service groups at and around the MPI for Meteorology for providing exemplary service and a great working environment.

I thank my parents and sister for their permanent support, confidence in my success, and providing a refuge from all this.

Publikationsreihe des MPI-M
„Berichte zur Erdsystemforschung“ , „*Reports on Earth System Science*“, ISSN 1614-1199
Sie enthält wissenschaftliche und technische Beiträge, inklusive Dissertationen.

Publikationsreihe des MPI-M
„Berichte zur Erdsystemforschung“ , „*Reports on Earth System Science*“, ISSN 1614-1199
Sie enthält wissenschaftliche und technische Beiträge, inklusive Dissertationen.

Publikationsreihe des MPI-M
„Berichte zur Erdsystemforschung“ , „*Reports on Earth System Science*“, ISSN 1614-1199
Sie enthält wissenschaftliche und technische Beiträge, inklusive Dissertationen.

Berichte zur Erdsystemforschung Nr.30 November 2006	**Long-term interactions between ice sheets and climate under anthropogenic greenhouse forcing Simulations with two complex Earth System Models** Miren Vizcaino
Berichte zur Erdsystemforschung Nr.31 November 2006	**Effect of Daily Surface Flux Anomalies on the Time-Mean Oceanic Circulation** Balan Sarojini Beena
Berichte zur Erdsystemforschung Nr.32 November 2006	**Managing the Transition to Hydrogen and Fuel Cell Vehicles – Insights from Agent-based and Evolutionary Models –** Malte Schwoon
Berichte zur Erdsystemforschung Nr.33 November 2006	**Modeling the economic impacts of changes in thermohaline circulation with an emphasis on the Barents Sea fisheries** Peter Michael Link
Berichte zur Erdsystemforschung Nr.34 November 2006	**Indirect Aerosol Effects Observed from Space** Olaf Krüger
Berichte zur Erdsystemforschung Nr.35 Dezember 2006	**Climatological analysis of planetary wave propagation in Northern Hemisphere winter** Qian Li
Berichte zur Erdsystemforschung Nr.36 Dezember 2006	**Ocean Tides and the Earth’s Rotation - Results of a High-Resolving Ocean Model forced by the Lunisolar Tidal Potential** Philipp Weis
Berichte zur Erdsystemforschung Nr.37 Dezember 2006	**Modelling the Global Dynamics of Rain-fed and Irrigated Croplands** Maik Heistermann
Berichte zur Erdsystemforschung Nr.38 Dezember 2006	**Monitoring and detecting changes in the meridional overturning circulation at 26°N in the Atlantic Ocean- The simulation of an observing array in numerical models** Johanna Baehr
Berichte zur Erdsystemforschung Nr.39 Februar 2007	**Low Frequency Variability of the Meridional Overturning Circulation** Xiuhua Zhu
Berichte zur Erdsystemforschung Nr.40 März 2007	**Aggregated Carbon Cycle, Atmospheric Chemistry, and Climate Model (ACC2) – Description of the forward and inverse modes –** Katsumasa Tanaka, Elmar Kriegler
Berichte zur Erdsystemforschung Nr.41 März 2007	**Climate Change and Global Land-Use Patterns — Quantifying the Human Impact on the Terrestrial Biosphere** Christoph Müller
Berichte zur Erdsystemforschung Nr.42 April 2007	**A Subgrid Glacier Parameterisation for Use in Regional Climate Modelling** Sven Kotlarski

Publikationsreihe des MPI-M
„Berichte zur Erdsystemforschung“ , „*Reports on Earth System Science*“, ISSN 1614-1199
Sie enthält wissenschaftliche und technische Beiträge, inklusive Dissertationen.



ISSN 1614-1199